PhD THESIS

COMBINATION OF OPTICAL AND MICROWAVE DATA OF ALOS FOR TROPICAL FOREST MAPPING

January 2010

NGUYEN THANH HOAN

Graduate School of Science

CHIBA UNIVERSITY

（千葉大学学位申請論文）

熱帯林マッピングのためのALOS光学データとマイクロ波データの結合

2010 年 **1** 月

千葉大学大学院理学研究科
地球生命圏科学専攻地球科学コース

NGUYEN THANH HOAN
グエン　タン　ホアン

COMBINATION OF OPTICAL AND MICROWAVE DATA OF ALOS FOR TROPICAL FOREST MAPPING

January 2010

Thesis by

NGUYEN THANH HOAN

For the degree of

Doctor of Philosophy

In

Remote Sensing and GIS

Approved by: **Supervisor**

Prof. Ryutaro Tateishi

Members of dissertation committee:

1. Prof. Hiroaki Kuze
2. Prof. Akihiko Kondoh
3. Prof. Susumu Okitsu

Graduate School of Science

CHIBA UNIVERSITY, JAPAN

ACKNOWLEDGEMENTS

This study is my PhD thesis, and at the same time, it also is a study in the frame work of ALOS program of JAXA as a Principal Investigator (PI) member. I warmly give thanks to JAXA provided ALOS data for this study.

This PhD graduation is an important milestone of my life. The first of all, I would like to express my deepest sincere appreciation and thanks to my supervisor Prof. Ryutaro Tateishi for his guidance, valuable suggestions during this study course and for his helps during my stay in Japan.

I also would like to express my gratefulness to dissertation committee: Prof. Hiroaki Kuze, Prof. Akihiko Kondoh and Prof. Susumu Okitsu for their valuable comments and suggestions, special thanks to Prof. Hiroaki Kuze for his useful, careful and very kind advices in improving the manuscript.

I wish to express my gratitude to SAGAWA Scholarship Foundation for awarding me SAGAWA scholarship in the last two years of this study course. My life in Japan should have been harder so much if I did not have this support.

I would like to thank my colleagues in Tateishi laboratory for their co-operation in study, for their comments and suggestions in discussions and seminars, for their helps in Japanese translation, specially to Kobayashi Toshiyuki who helped me so much for finishing necessary papers and procedures in Japanese.

I wish to give my thanks to my Vietnamese friends in Chiba for funny, happy times, special thanks to Ho Van Ngoc and Dinh Ngoc Linh who helped me very much during my stay in Japan.

I would like to express my gratitude to my boss, Prof. Nguyen Dinh Duong, and to my office in Vietnam, Institute of Geography, Vietnamese Academy of Science and Technology (VAST) for giving me a chance to carry out this PhD course. I also thank

my colleagues in Vietnam, who helped me collect the concerned data for this study.

As the final, I warmly give my extreme gratitude to my family, wherever they are my Mum, Dad, my siblings; the thanks from my heart go to my lovely daughter, Nguyen Nhat Linh, and to my wife, Nguyen Thi Huong. Their encourages and love give me have more forces to finish this study.

ABSTRACT

Tropical forests cover large parts of the Earth's land surface. These forests hold an enormous biodiversity, and they are disappearing at an alarming rate. Tropical forest mapping frequently is very necessary, especially in developing countries, the main located regions of tropical forests.

Surveying and monitoring tropical forest frequently on the ground is very difficult related to its existence in the complex terrains, large areas; therefore remote sensing images have been widely applied as an important tool for mapping and monitoring tropical forest. For the local high detail studies, high resolution images are required, but collecting good multi-temporal optical images of high resolution satellites for tropical regions in one year cycle to describe phenology of objects for forest mapping is very difficult or impossible because of the presence of the cloud and long repeat cycle of satellites. Microwave data can observe objects in every weather condition and it can be used to analyze structure of forest to complement information for optical data.

ALOS satellite of Japan was launched successfully on 24 January 2006. It has both microwave and optical sensors. With high resolution (~10m), this data will be very useful for land studies including forest studies in local scale. The study of combination between optical and microwave data also becomes more feasible. Therefore, this study presents a possibility to improve accuracy of tropical forest mapping by combination of optical and microwave images of ALOS. Study area is located in the southern part of Vietnam.

Cloud is always problem of optical remote sensing data. And of course, ALOS/AVNIR-2 images are also affected. Microwave images are not affected by cloud. One of the main purposes of this study is to develop a method to remove cloud in optical images based on interpolation from SAR data. This method was developed based on interpolating under cloud pixel values for optical images. A combination

method of Total Reflectance Radiance Index (TRRI) and Cloud-Soil Index (CSI) is used to define cloud. Because around-cloud pixels are mixture of cloud and other objects, those are very difficult to define. Therefore, the around-cloud pixels are extended from cloud. Cloud shadow problem is also discussed in this study. Condition to apply this method is satisfied when objects in optical image and radar image change not very much. This method is experimented on simulated ALOS data from Landsat/TM and JERS-1/SAR images. A cloud free and shadow free image is obtained by the interpolation. Original and interpolated images are almost similar together. This method also can be applied for combination of two optical images to remove cloud if spatial change of objects in cloud cover area is not so much. The developed cloud removal program includes many functions like: define cloud, extend cloud, get shadow, remove cloud and so on. This is free software for every one.

Another main purpose of this study is to improve accuracy of tropical forest mapping. The first, ALOS/AVNIR-2 images are used to classify the forest map, then, ALOS/PALSAR single-polarized and dual-polarized images are used to improve accuracy of the classification result by a combination model. ALOS/PRISM images are used to make Pan-sharpen images for collecting training data and validation data. Tropical natural forests, the most biodiverse form of forest, are disappearing very quickly and they are very necessary to be protected. Therefore, discrimination of Planted Forest and Natural Forest is also one of the most important purposes of this study.

Accuracy assessment was done by selecting 330 random points to validate for 11 classes. The overall accuracy of ALOS/AVNIR-2 classification result is 77.0%, while after combining with ALOS/PALSAR, it is increased up to 88.2%. The accuracy is higher than 90% for main forest classes.

Table of Contents

List of Figures

List of Tables

CHAPTER 1

INTRODUCTION

1.1. Background

Tropical forests cover large parts of the Earth's land surface. These forests hold an enormous biodiversity, and they are disappearing at an alarming rate (Muljanto Nugroho 2006), so tropical forest mapping is very necessary, especially in developing countries, the main located regions of tropical forests and in these countries many problems of forest management are existing.

Surveying and monitoring tropical forest frequently on the ground is very difficult related to its existence in the complex terrains, large areas. Therefore, remote sensing images have been widely applied as an important tool for mapping and monitoring tropical forest. Forest mapping by remote sensing data already has been known by many programs like FRA 2000 by FAO using SPOT Vegetation data, Global Forest Mapping (GRFM/GBFM) Program by JAXA using JERS-1 SAR data and so on. These programs cover global scale. Therefore, the broad categories mapped by these programs fail to deliver valuable and useful information on the variation within the tropical forest environment (Tottrup 2004). Many other studies of forest mapping using high resolution images have been presented in several works, e.g. of using optical images for forest mapping (Rahman et al. 2005, Tottrup 2004, Giles M. Foody et al. 2003, Helmer et al. 2000). These studies used multi-temporal images. But, collecting good multi-temporal images of high resolution satellites for tropical regions in one year cycle is very difficult or impossible because of the presence of the cloud and long repeat cycle of satellites. E.g. of using microwave data for forest mapping (Almeida-Filho et al. 2009, Feilong Ling et al. 2008, Shane Cloude et al. 2007, Fransson et al. 2007, Sgrenzaroli et al. 2002,

Takeuchi et al. 2000), microwave data can be used to analyze some characters of forest. Specially, microwave data is very useful for studies about forest cover change detection, forest fire and so on, because it can observe objects in every weather condition and it also can observe the objects that lie under surface. According to Thuy Le Toan (Thuy Le Toan et al. 2001), the interest in using radar remote sensing for monitoring forest cover raises from the two following assets of radar data. The first is that radars can provide information related to the canopy volume, which cannot be collected by other means. These have been identified as: above ground biomass, annual increment of stand biomass, and vertical distribution of biomass. The other advantage of radars is the possibility of acquire data over areas with frequent cloud or haze coverage, and the possibility to acquire data during and rapidly after events such as fires or storms. According to Dobson and M. Craig (Dobson and Craig 2000), the principal uses of radar will be to map forest structure and moisture, this information is largely complementary to that obtained by optical techniques. However, the studies about combination of optical and radar images for forest mapping is not so many, some of them about using synergism of SAR and optical data for land use classification (Kuplich 2000, Juha Hyyppa et al. 2000), including some forest types in categories table with limited number of forest classes. In short, there are some contradictions between spatial resolution and repeat cycle of optical remote sensing data: Optical Moderate Resolution Images (like MODIS, MERIS) have a good repeat cycle, but resolution is too coarse for local studies. On the other hand, Optical High Resolution Images have good resolution, but repeat cycle is too long. Therefore, it is very difficult to separate between Forest and growing Paddy/Cropland because it is not so easy to collect multi-temporal data for one year cycle to describe phenology of objects. Microwave data can separate Forest from Paddy/Crop types and it can be used to analyze structure of forest to complement information for optical data.

ALOS satellite of Japan was launched successfully on January 24 2006. It has both microwave and optical sensor. With high resolution (~10m), this data will be very useful

for land studies including forest studies in local scale. The study of combination between optical and microwave data also becomes more feasible. Therefore, this study presents a possibility to improve accuracy of tropical forest mapping by combination of optical and microwave images of ALOS. To support for managing reforestation activities and preserving existing natural forest, discrimination of Planted Forest and Natural Forest is one of the most important purposes of this study. This study will not discuss biomass estimation and wood volume estimation, due to the lack of ground truth measurement data.

Cloud is always problem of optical remote sensing data. Microwave images are not affected by cloud. Developing a method to remove cloud in optical images based on SAR data is also one of the important purposes of this study.

1.2. Deforestation in Vietnam

In the recent years, deforestation occurs very quickly in developing countries, the main distribution locations of tropical forests. An example in Vietnam, according to 2005 report conducted by the Food and Agriculture Organization of the United Nations (FAO), Vietnam has the second highest rate of deforestation of primary forests in the world, second only to Nigeria (Butler and Rhett 2005). As of 2005, 12,931,000 hectares (the equivalent of 39.7% of Vietnam's land cover) was forested, although only 85,000 hectares (0.7% of the land cover) was primary forest, the most biodiverse form of forest (Patrick Meyfroidt and Eric F. Lambin 2008).

A real situation of deforestation of natural forest in Vietnam was shown in Figure 1.1 by remote sensing images.

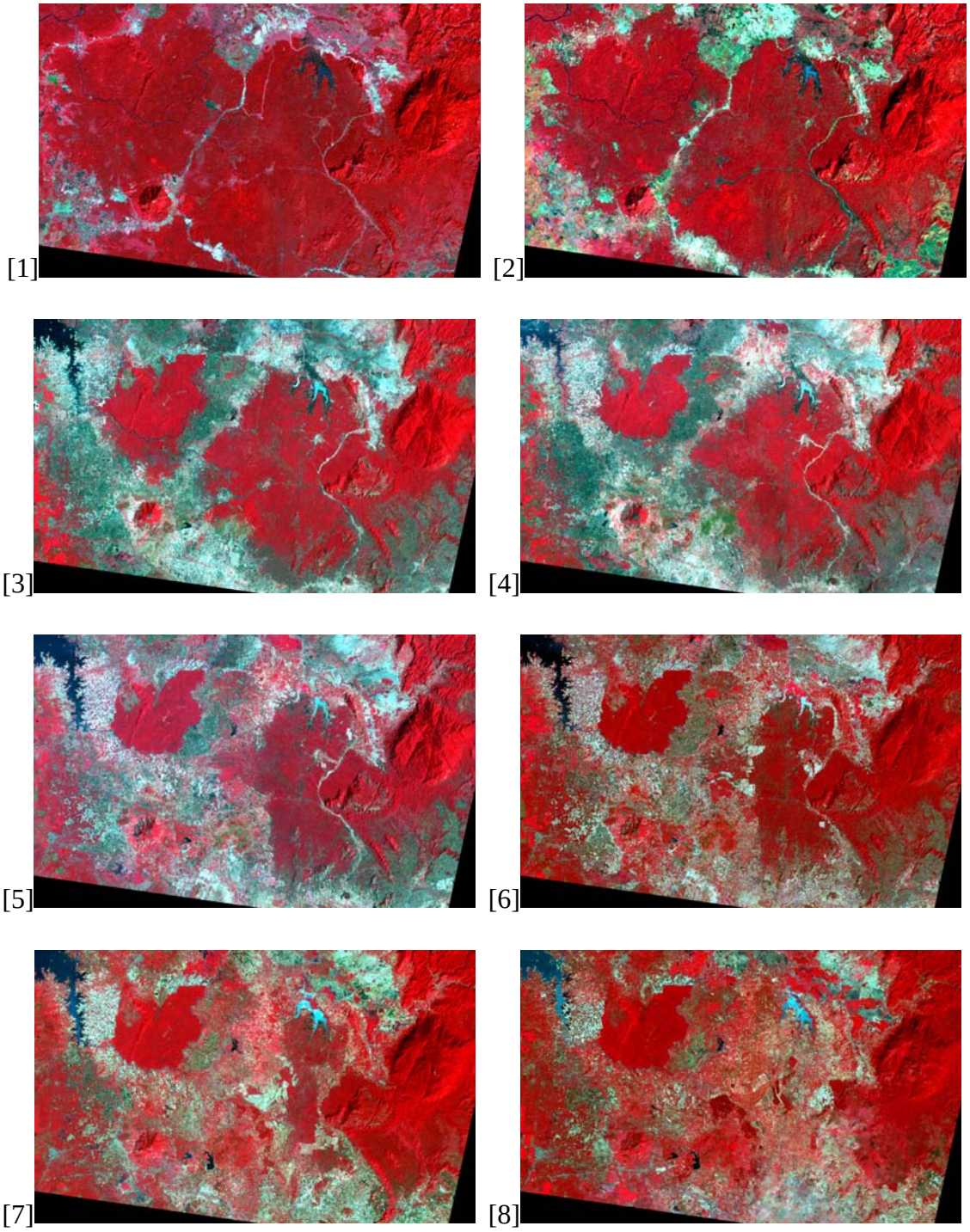

Figure 1.1: Deforestation of natural forest in one part of the study area from 1973 to 2007 (Color composite: R - NIR, G - Red, B - Green)

[1]: Landsat/MSS 1973; [2]: Landsat/MSS 1976; [3]: Landsat/TM 1989; [4]: Landsat/ TM 1992; [5]: Landsat/TM 1996; [6]: Landsat/TM 1998; [7]: Landsat/ETM 2002; [8]:

ALOS/AVNIR-2 2007.

Figure 1.1 is one part of the study area of this study (It will be presented in the section 1.6), covering approximately 64 kilometers of length and 40 kilometers of width (greater than Tokyo capital of Japan).

- In the year 1973, almost the image was covered by natural forest.
- To the year 1976 (after 3 years), some forest areas were already lost, but speed of deforestation is not very high. The forest was cut by farmers to get cultivated land.
- 13 years later, to the year 1989, a large area of forest was already lost, but speed is also not very high, and main purpose was still for cultivated land.
- After 1989, opening economy in Vietnam (from 1986), affected by the pressure of economy development, many forests were cut to get wood for making furniture and export.
- To 1996, rubber for export became a valuable product. A large forest area was cut to get land for rubber plantation. Forest areas were cut very clearly by machine. The white fields can be seen clearly in the remote sensing images from the year 1998 to 2007 in Figure 1.1.
- Around the year 1997-1998, a big event occurred in this area. It was discovered that many forests had been destroyed by forest protectors from the offices of province to community and afforestation yards. Many people were arrested. But after that, every thing became silent again. And deforestation was still continued faster and faster. To the year 2007, almost forests in flat areas were already destroyed (Figure 1.1 [8]).

1.3. Forest mapping in Vietnam

Although deforestation is occurring very quickly, but forest mapping in the developing

countries like Vietnam has many problems. The Environmental Atlas of Vietnam published in 1999 by Ministry of Natural Resource and Environment of Vietnam includes only forest maps of 1993 and 1983, six year after the atlas published. Figure 2.4 is a example of Vietnam Forest map 1993 in the study area. Both of the two maps were drawn by manually in field works. This work spent so much time, labor and money, in normal, it needs many years to finish a forest map for whole country. Accuracy of these maps is depended on local surveyors, and of course, it is not the same in the different locations.

In currently, the newest official forest map of Vietnam is Vietnam Forest map 2005. This map was produced for Ministry of Resource and Environment by Forest Inventory and Planning Institute (FIPI) of Vietnam in 2008 using Landsat/ETM images 2005. Legend of this map includes 17 classes, among them, 13 classes of forest including: (1) rich evergreen broadleaf forest, (2) medium evergreen broadleaf forest, (3) poor evergreen broadleaf forest, (4) young forest has a wood volume, (5) young forest has no wood volume, (6) semi-deciduous forest 1 (rừng khộp), (7) semi-deciduous forest 2, (8) bamboo forest, (9) mixed forest, (10) mangrove forest, (11) planted forest, (12) bare land, (13) rocky mountain, (14) agricultural land, other lands, (15) water bodies, (16) needle-leaf forest, (17) rubber forest, (null) no data. This map was shown by random color as in Figure 2.5. Some of the classes are impossible to estimate if using only Landsat/ETM images. Accuracy of this map also needs to be discussed. Figures 1.2 and 1.3 are examples to illustrate some of mistakes that are existing in Vietnam forest map 2005. Forest as shown in Figure 1.2 (*a* and *b*), is existing in Landsat/ETM image 2002 and ALOS/AVNIR-2 image 2007, respectively, however in Vietnam Forest map 2005 (*c*) it does not appear at all.

Figure 1.3 (*a* and *b*) shows, a homogeneous forest area in Landsat/ETM image 2002 and in ALOS/AVNIR-2 image 2007, while in the Vietnam forest map 2005 (Figure 1.3(*c*)), it has a very clear boundary. Here are only some of many mistakes that are easy to find

in the Vietnam forest map 2005. The color composites of Landsat/ETM in Figures 1.2 and 1.3 are R-SWIR, G-NIR, B-Red and that of ALOS/AVNIR-2 are R-Red, G-NIR, B-Green.

(*a*) (*b*) (*c*)

Figure 1.2: Mistakes of Vietnam Forest map 2005: Forest in Landsat/ETM image 2002 (*a*), forest in ALOS/AVNIR-2 image 2007 (*b*), but non-forest in Vietnam forest map 2005 (*c*)

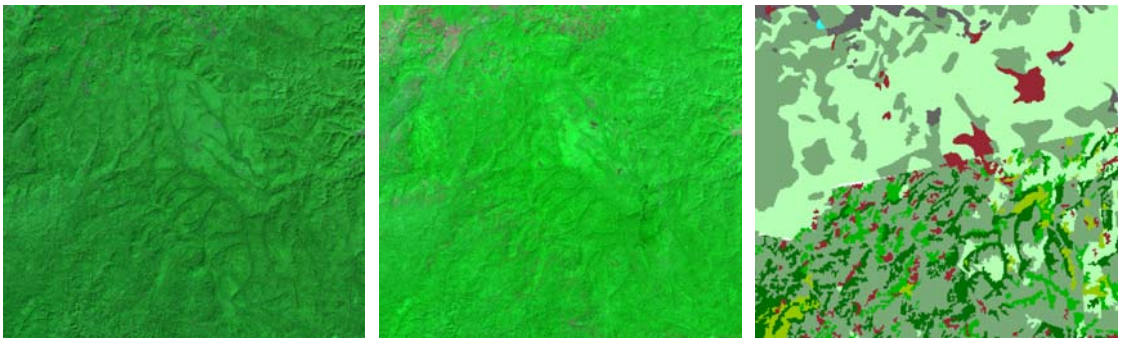

(*a*) (*b*) (*c*)

Figure 1.3: Mistakes of Vietnam Forest map 2005: Homogeneous forest in Landsat/ETM image 2002 (*a*) and in ALOS/AVNIR-2 image 2007 (*b*), but existing a clear boundary in Vietnam forest map 2005 (*c*)

Since the early 1990s, Vietnam government has spent so much money for reforestation programs (Patrick Meyfroidt and Eric F. Lambin 2008). One of the biggest programs is the “Five Million Hectares Reforestation Program”. Japan International Cooperation Agency (JICA) is also supporting this national program by developing sets of measures

to rehabilitate natural forest in degraded watershed area of Northern Vietnam for forest management organizations and local people through conducting studies on establishment of sets of techniques for rehabilitation of natural forest and on demonstration of livelihood improvement activities with utilization of forest resources (JICA 2008). However, because of insufficient information, Forest Protection Department (FPD), Ministry of Agriculture and Rural Development of Vietnam (the biggest office of Vietnam for forest protection, on behalf of government to control forest) can not control reforestation activities and deforestation also. One of the main causes is poor quality of current forest maps as presented above. One of the other evidences is a cooperation program of FPD with Space Technology Institute (STI) of Vietnam and Tokyo University of Japan. In this program, according to requirements from FPD, they wants to know the current forest area in Vietnam, especially central high land area supported by STI, Vietnamese Academy of Science and Technology (VAST) and Tokyo University, but still now, this program is in starting steps, it has not any products yet (Takeuchi 2008). The offices of provinces, districts and afforestation yards have spent so much money for reforestation from government, but government can not control that how many hectares of forest already have been planted newly. Government has not enough information to check the truth of reports from province, district and afforestation yard offices. Therefore, developing a method for surveying and monitoring tropical forest frequently is very necessary.

1.4. ALOS data

ALOS stands for Advanced Land Observing Satellite, which was launched by Japan Aerospace Exploration Agency in January 2006. Its Japanese name is "DAICHI". The size of DAICHI is 3.5m wide x 4.5m long x 6.5m high, with its Solar Battery Paddle is 22m x 3m wide, gross weight is approximately 4 tons, which is one of the largest among

Land Observing Satellites. The main characteristics of the ALOS satellite are shown in Table 1.1.

Table 1.1: ALOS major specifications

Launch Date	January 24, 2006
Launching Vehicle	H - IIA
Launch Site	Tanegashima Space Center, Japan
Spacecraft Mass	Approx. 4 tons
Generated Power (Solar paddle)	Approx. 7kw (at End Of Life)
Designed EOL	3-5 years
Orbit	Sun Synchronous, Sub recurrent Repeat Cycle: 46 days Sub-Cycle : 2 days Altitude : 691.65km (Above the equator) Inclination : 98.16 deg.
Attitude Determination Accuracy	2.0 x 10-4 deg. (off-line, with GCP)
Position Determination Accuracy	1m (off-line)
Data Rate	240Mbps (Via Data Relay Test Satellite) 120Mbps (Direct Transmission)
On-board Data Recorder	Solid-state Data Recorder (90Gbytes)

ALOS has three remote-sensing instruments. PRISM is a panchromatic radiometer with spatial resolution in order to obtain terrain data including elevation. AVNIR-2 is a visible and near-infrared radiometer for observing land and coastal zones and provides better spatial resolution. PALSAR is a phased array type L-band Synthetic Aperture

Radar, an active microwave sensor for cloud free and day and night land observation. The general concepts of the "Three Sensors" are shown in Table 1.2.

Table 1.2: General Concepts of the "Three Sensors"

Sensor	Spatial Resolution / Swath Width	Characteristics	Utilization
PRISM	Spatial Resolution : 2.5m Swath Width : 35km(Triplet mode) 70km(Nadir Only)	It has three independent optical systems for viewing nadir, forward and backward producing a stereoscopic image along the satellite's track.	Cartography, making DSM for mapping, urban planning, agriculture, forest monitoring, coastal monitoring, monitoring illegal dumping, flood monitoring etc.
AVNIR-2	Spatial Resolution : 10m Swath Width : 70km	The Advanced Visible and Near Infrared Radiometer type 2 (AVNIR-2) is a visible and near infrared radiometer for observing land and coastal zones.	It provides better spatial land-coverage maps, wide range of urban planning, agriculture(vegetation research), forest monitoring, coastal monitoring, pollution monitoring on ports and harbors, plants monitoring, flood monitoring etc.
PALSAR	Spatial Resolution : 10m(fine resolution mode)	The Phased Array Type L-band Synthetic Aperture Radar	It enables to make DEM, extract topography data by interferometry, estimate

	100m(Scan Sar mode) Observation Swath : 70km (fine mode) 250-350km (Scan SAR)	(PALSAR) is an active microwave sensor using L-band frequency, which can observe with fine resolution in a conventional mode as well as wider swath with a SAR images.	biomass, forest monitoring, agriculture, monitoring oil spill, moisture of soil, shipping inspection etc.

The characteristics of ALOS/AVNIR-2 are shown in Table 1.3.

Table 1.3: Characteristics of ALOS/AVNIR-2

Bands	Wavelengths (nm)
1	420 – 500
2	520 – 600
3	610 – 690
4	760 – 890

Major mission of ALOS includes cartography, regional observation, disaster monitoring and resource surveying. As examples of an exploration study, JAXA sets 12 categories as "major categories of research". They are, "Land Use and Land Cover Research", "Disaster Prevention and Disaster Monitoring", "Land and Mineral Resources", "Biological Resources", "Oceanography", "Agriculture" and so forth, and to promote the study that encourage to use Satellite data (ALOS 2009).

1.5. Objectives of this study

As presented in the above sections, with available data of ALOS satellite, the study of combination between optical and microwave data becomes more feasible. This study presents a possibility to improve accuracy of tropical forest mapping by combination of optical and microwave images of ALOS. Main objectives of this study include:

- Developing a model to remove cloud in optical data based on microwave data
- Separating planted forest and natural forest, bamboo and others based on analyzing structure of forest (using microwave data)
- Establishing a forest map in high scale, high accuracy with a cheap cost and in a short time. Ultimate is to develop a method for producing forest map annually by high resolution remote sensing image.

1.6. Study area

The study area, as shown in Figure 1.4, is located in the southern part of Vietnam, between the range $11^{o}00'N$ - $11^{o}45'N$ and $106^{o}45'E$ - $107^{o}30'E$, approximately 50km north of Ho Chi Minh city. This area lies in tropical zone, covering about $6000km^2$. It includes a main part of Cat Tien national park (one of the biggest natural reserves of Vietnam) and surrounding areas. This area is covered mainly by rainforests. The dominant forest formation is the broadleaf evergreen forest.

Cat Tien National Park is estimated as the reserve of natural resources in Vietnam with lots of rare, specious and endemic genes of fauna and flora, as plentiful site for scientists, domestic and foreign tourists. Cat Tien National Park is part of the wet tropical forest complex and one of the specious natural forests remaining in Vietnam.

The diversity of the Park has been recognized by WWF when this international organization selected the Park as one of 200 global ecological zones including the land and its water area with its well-known biological diversity. In 2001, Cat Tien National Park has been listed by UNESCO as the 411th biosphere Reserve Zone in the world (UNESCO 2009).

Figure 1.4: Location map of the study area (hatching)

1.7. Structure of the thesis

Structure of this thesis was developed based on methodology of whole study. A flow

chat of the methodology is shown in Figure 1.5.

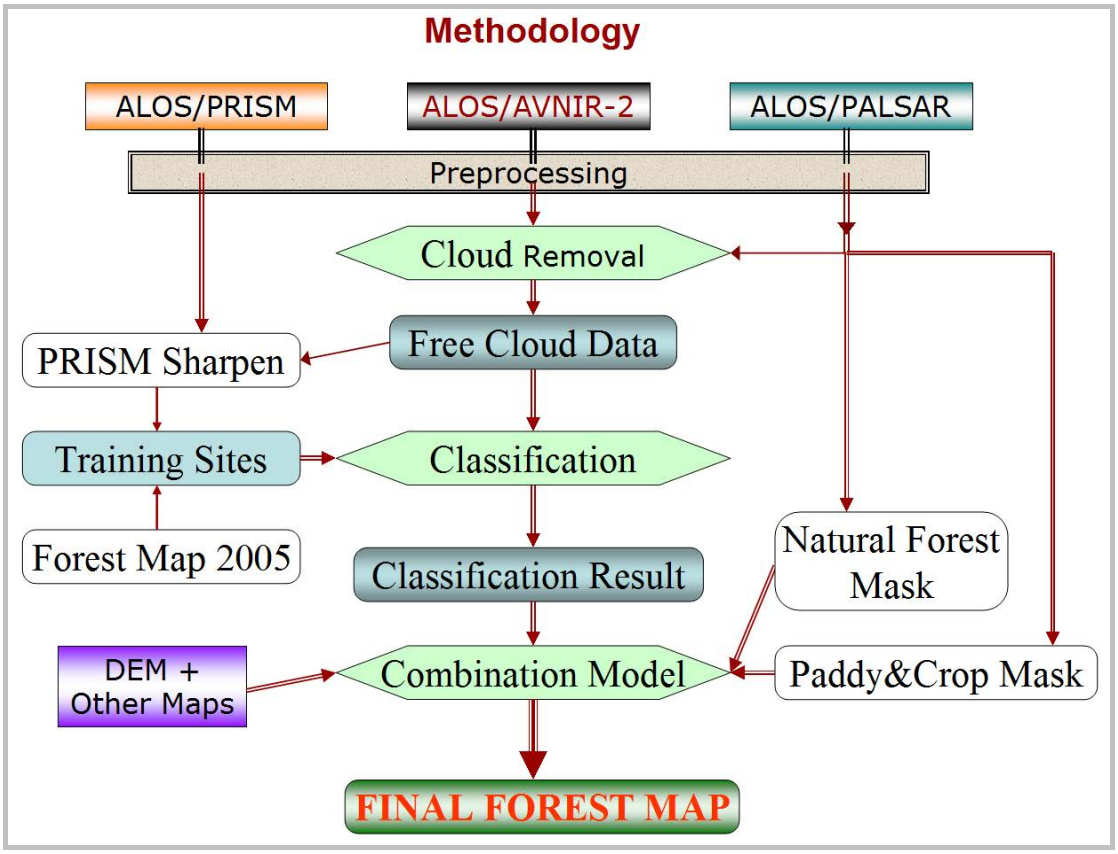

Figure 1.5: A flow chat of methodology

This thesis is presented in five chapters and conclusion section.

Chapter 1 introduces overview about existing studies of using remote sensing images for forest mapping. This chapter also explains motivations for choosing this study including situations of deforestation in tropical region, realities of tropical forest mapping in Vietnam and so on. In addition, this chapter presents about ALOS data, study area, objectives of this study and structure of this thesis.

Chapter 2 presents data acquisition and some preprocessing steps of ALOS data including: geometric correction of ALOS/AVNIR-2, ALOS/PALSAR and ALOS/PRISM images; problems of different digital number (DN) levels when making mosaic images. PRISM-sharpening and some other techniques

are also presented in this chapter.

Chapter 3 presents a new method for cloud removal of optical data based on SAR data. This method were also applied successfully in some other extension applications like for Landsat/ETM images and for ASTER images. This section provides a free software of the cloud removal method for every one.

Chapter 4 shows methodology to extract information from ALOS/AVNIR-2 images and ALOS/PALSAR images for tropical forest mapping. Combination model to combine the two types of data is also presented in this chapter. This chapter is another new point and also one of the most important sections of this study.

Chapter 5 presents validation method and its result. Some discussions about combination of optical images and SAR images for tropical forest mapping are also presented in this chapter.

Conclusion section sums up all results of this study. Limitations of this study are also discussed in this section.

CHAPTER 2

DATA ACQUISITION AND SOME TECHNIQUES FOR PREPROCESSING OF ALOS DATA

2.1. Data acquisition

The study area is covered fully by four scenes of ALOS/AVNIR-2 or six scenes of ALOS/PALSAR. The data was collected for this study including:

- The Vietnam forest map of 1993 derived from the Environmental Atlas of Vietnam published in 1999 by Ministry of Natural Resource and Environment of Vietnam. This map was in vector format and drawn by manually as shown in Figure 2.1.
- The Vietnam Forest map of 2005 produced in 2008 by Forest Inventory and Planning Institute (FIPI) of Vietnam using Landsat/ETM images in 2005 as shown in Figure 2.2. This map was ordered by Ministry of Resource and Environment of Vietnam. It is in raster format, 50m resolution. This map is the newest official forest map of Vietnam in current.
- Four ALOS/AVNIR-2 images, 10m resolution, in date 2007/01/19, 2007/01/19, 2007/02/05, 2007/02/05 as shown in Figure 2.3. In whole the year 2007, only the four images that were found in the study area are good quality (few cloud).
- Three ALOS/PRISM images, 2.5m resolution, in date 2009/03/28, 2009/03/31, 2009/03/31 as shown in Figure 2.4.
- Six ALOS/PALSAR single-polarized images, 6.25m resolution, three of them in date 2007/02/02 and other three images in date 2007/02/19 as shown in Figure 2.5.
- Six ALOS/PALSAR dual-polarized images, 12.5m resolution, three images in date 2007/06/20 and three others in date 2007/07/07 as shown in Figure 2.6.

- Four ALOS/PALSAR multi-polarized images, 12.5m resolution, two of them in date 2006/10/28 and two others in date 2007/03/15 as shown in Figure 2.7. From the launched time of the ALOS satellite (2006) to May 2009, only the four multi-polarized images have been found in the study area. Observed times of them are very far together and they cover only small part of study area. In addition, DN levels of them are not the same. Boundary of them looks clear in mosaic image.

- The 9 pieces of local topographic map 2005 gotten from Map Department, Ministry of Natural Resources and Environment of Vietnam as shown in Figure 2.8. This map includes 3 layers: elevation contour lines, traffic roads and hydrology network. The elevation contour lines layer will be used to develop high quality DEM for ALOS/PALSAR ortho-rectification and in combination model (Chapter 4). The traffic roads and hydrology network layers will be used to check geometric problems of remote sensing images and to collect ground control points (GCPs) for geometric correction.

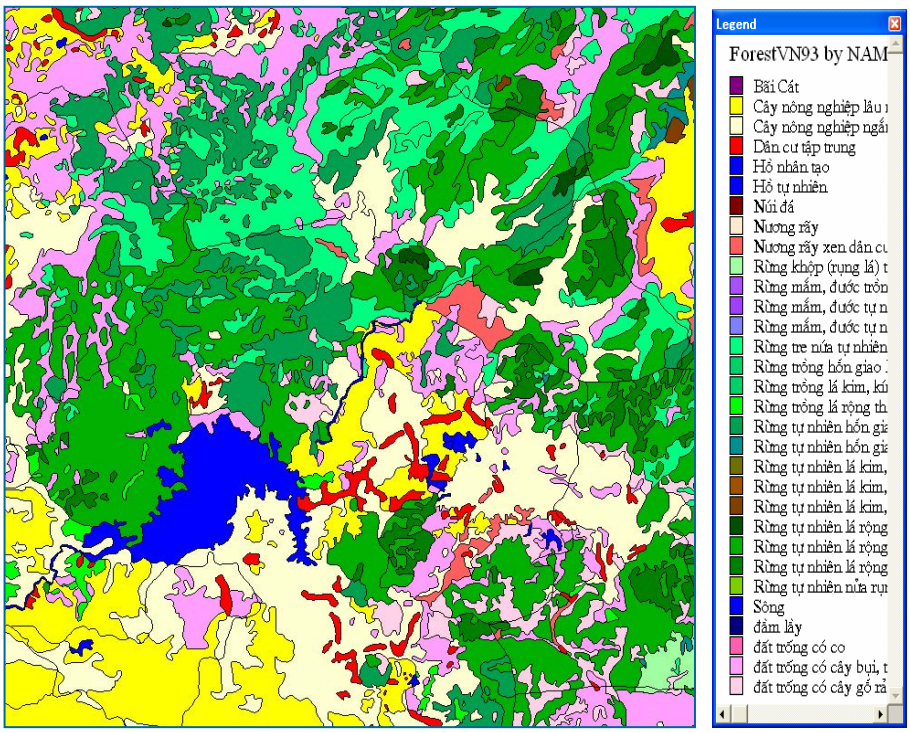

Figure 2.1: Vietnam Forest map 1993 was drawn by manually (random color)

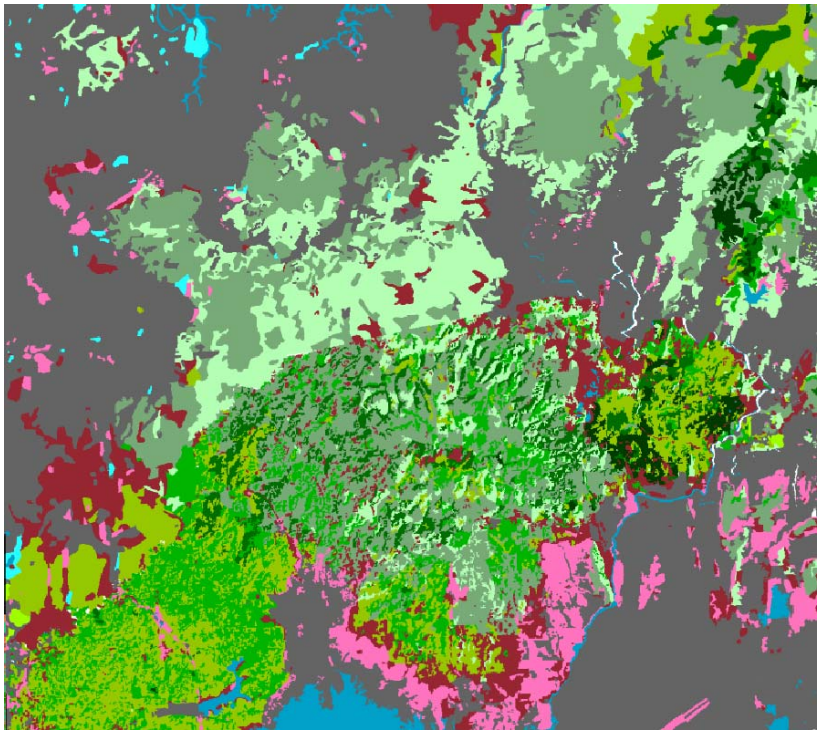

Figure 2.2: Vietnam Forest map 2005 (random color)

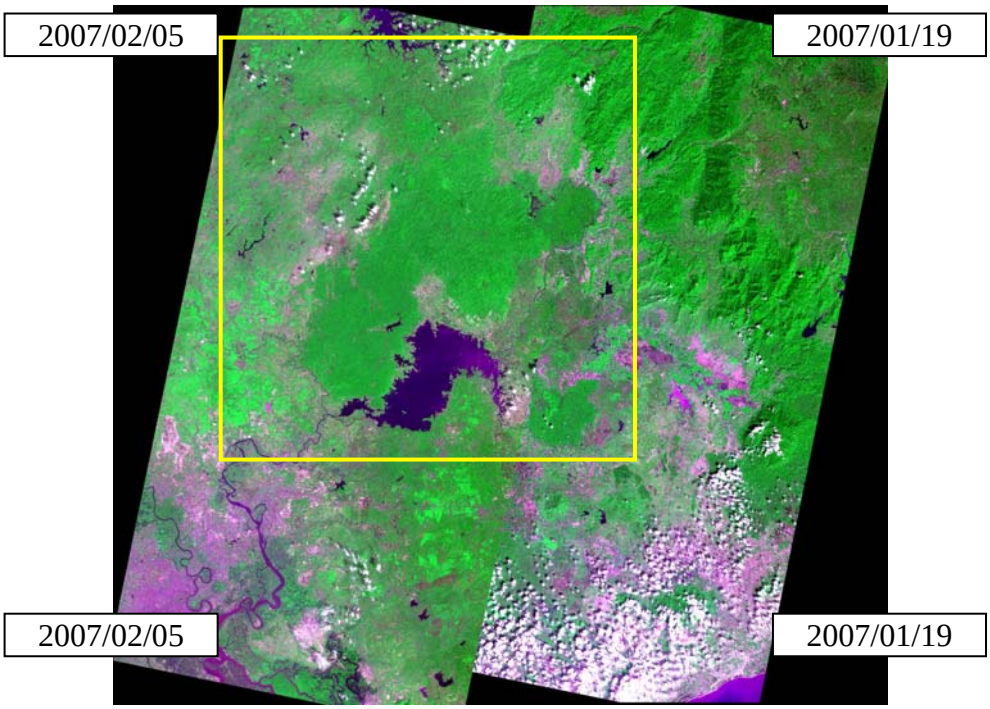

Figure 2.3: The four images of ALOS/AVNIR-2 10m resolution and observed dates (color composite: R-Red, G-NIR, B-Green)

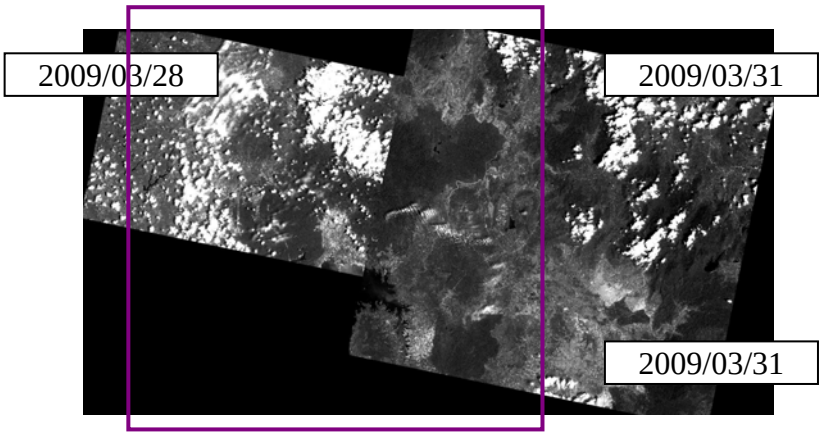

Figure 2.4: The three images of ALOS/PRISM 2.5m resolution and observed dates

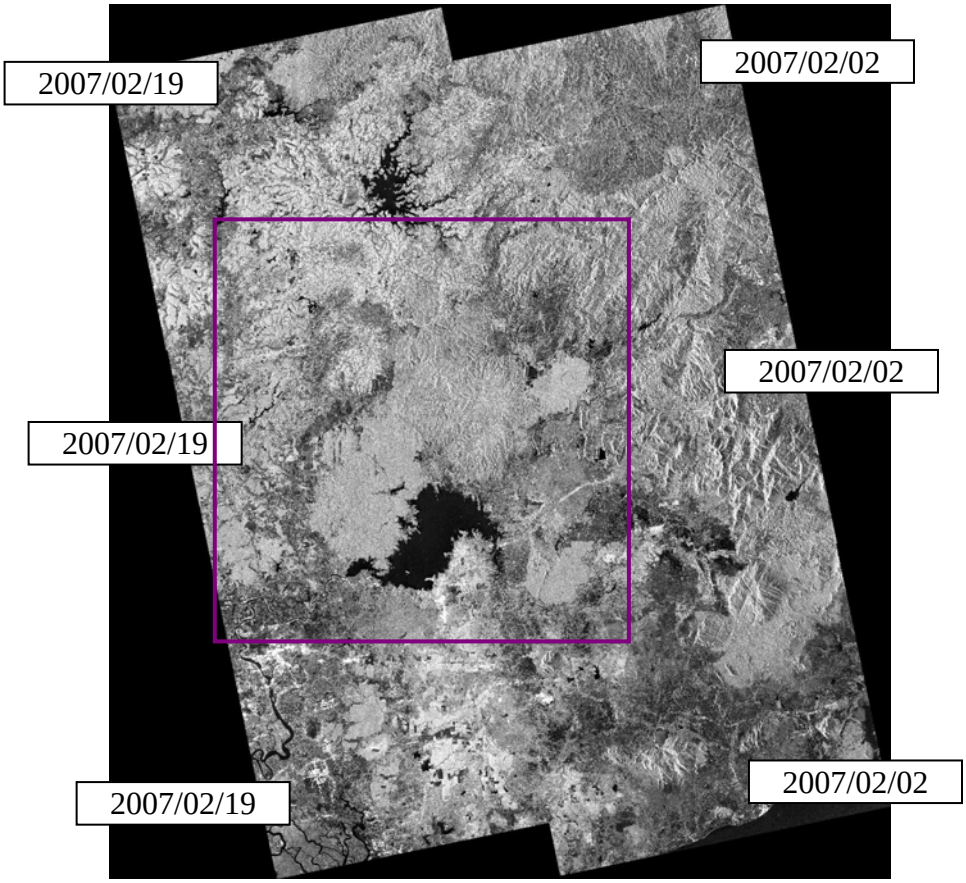

Figure 2.5: The six images of ALOS/PALSAR single-polarization and observed dates

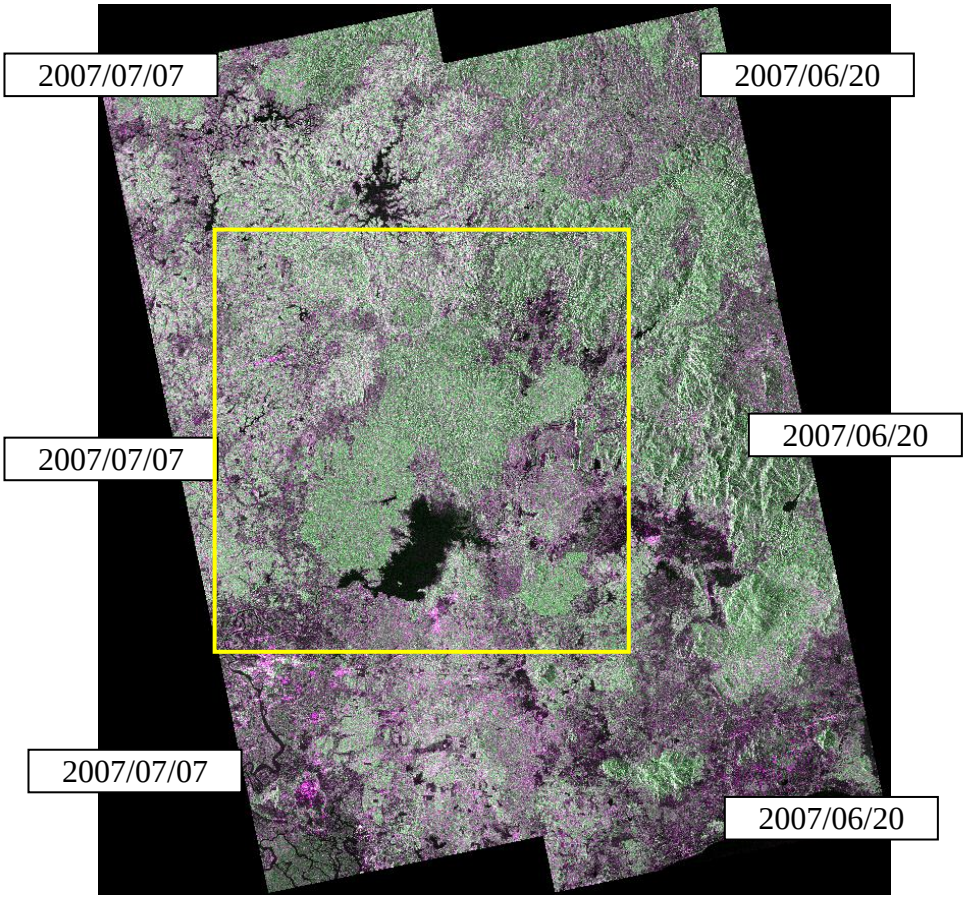

Figure 2.6: The six images of ALOS/PALSAR dual-polarization and observed dates (color composite: R-HH, G-HV, B-HH)

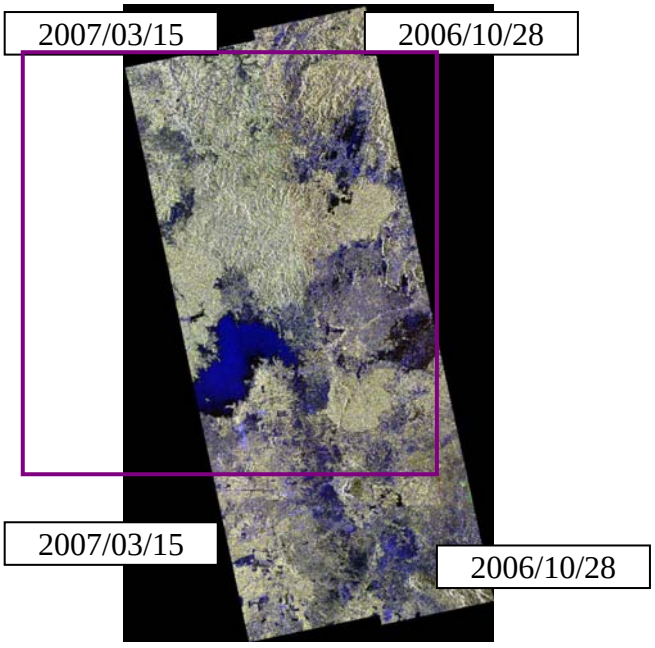

Figure 2.7: The four images of ALOS/PALSAR multi-polarization and observed dates (color composite: R-HH, G-HV, B-VH)

The rectangles in the above Figures are the study area of this study.

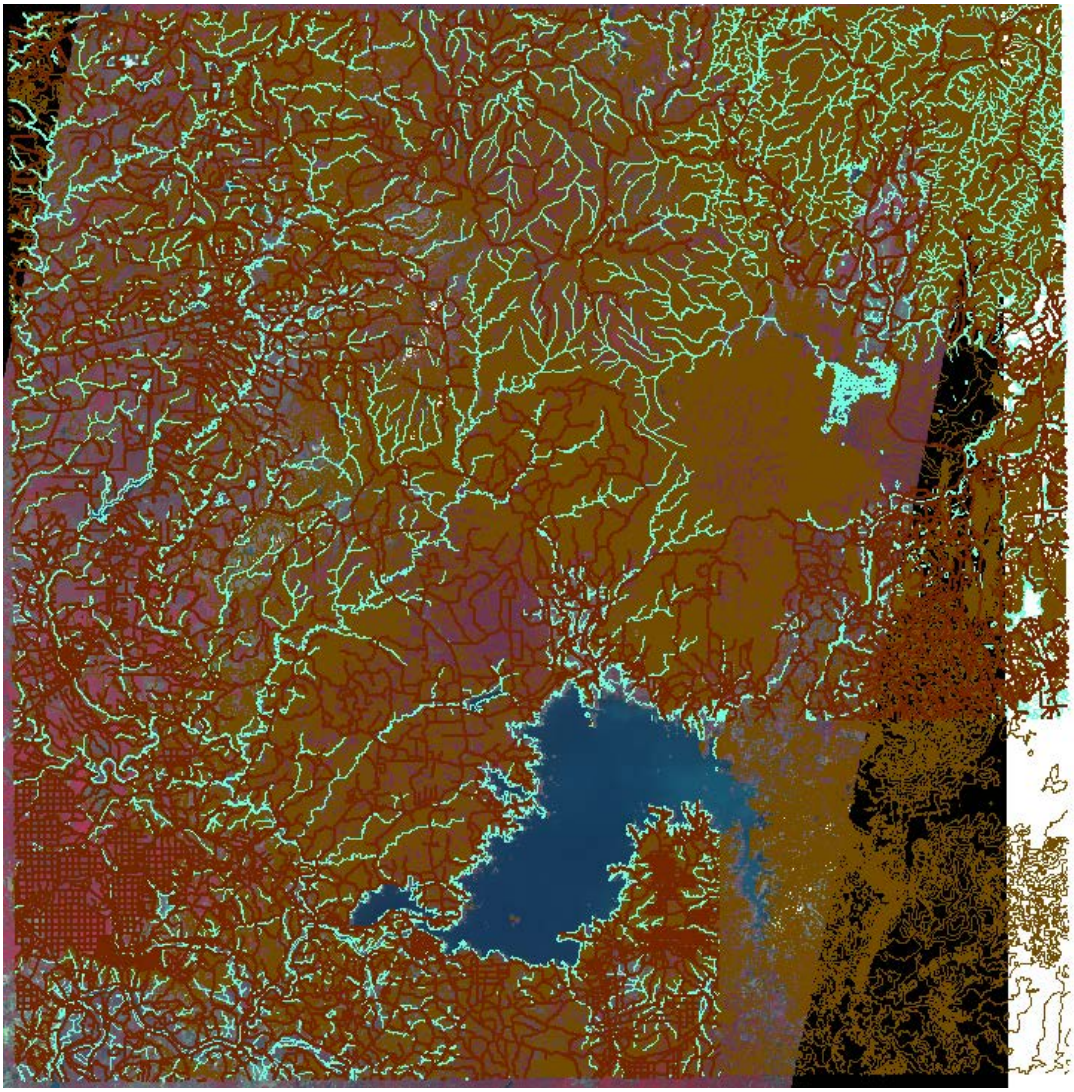

Figure 2.8: The 9 pieces of topographic map from Map Department, Ministry of Natural Resources and Environment of Vietnam - 2005. The dark-yellow color is elevation contour lines, the dark-brown color is traffic roads, and the yellow-blue color is hydrology network

In addition, some images of Landsat/MSS, Landsat/TM, Landsat/ETM sensors covering one part of the study area in the year 1973, 1976, 1989, 1992, 1996, 1998, 2002 were also collected to illustrate for deforestation in Vietnam as shown in Figure 1.1. ASTER GDEM developed from ASTER data (GDEM 2009) and SRTM DEM developed from radar interferometer - the Shuttle Radar Topography Mission 2000 - (SRTM 2006) were also collected for reference data.

ALOS/PALSAR single-polarized images were selected closest to ALOS/AVNIR-2 images as possible about time (there are no dual-polarized images and multi-polarized images around that time). This selection can reduce effects of land cover change when combine them together to remove clouds (Hoan and Tateishi 2009) and to separate between forests and growing paddy/croplands.

The received ALOS data and the local maps arise some problems when combine them together. The next sections in this chapter will present these problems including:

- Geometric correction for ALOS/AVNIR-2, ALOS/PRISM and ALOS/PALSAR data
- DN value normalization for ALOS/AVNIR-2 images.

In addition, ALOS/PALSAR filtering, PRISM sharpening and some others also will be mentioned in this chapter. About cloud problem, cloud removal of ALOS/AVNIR-2 images will be presented in the next chapter.

2.2. Geometric problems

Processing level of the received ALOS/AVNIR-2, ALOS/PRISM images is 1B2 and ALOS/PALSAR images is 1.5. All of them are Geo-coded images (CEOS format) and in a same coordinate system. However, when overlay together, objects in these images have not same position. Figure 2.9 illustrates this problem.

Figure 2.9: Different position of objects between ALOS/AVNIR-2 and ALOS/PALSAR data (Red layer is ALOS/AVNIR-2 image. White layer is ALOS/PALSAR image)

When overlay local maps to the images of ALOS/AVNIR-2 and ALOS/PALSAR, they do not match together also. These problems are shown in Figure 2.10.

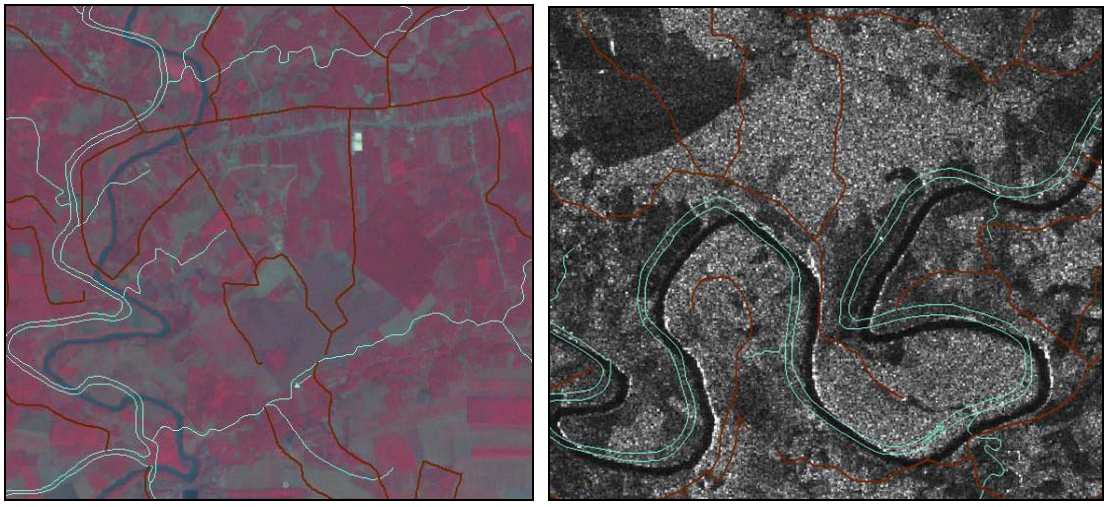

(*a*) (*b*)

Figure 2.10: Shifting problems of existing local maps and images; (*a*) ALOS/AVNIR-2 and (*b*) ALOS/PALSAR

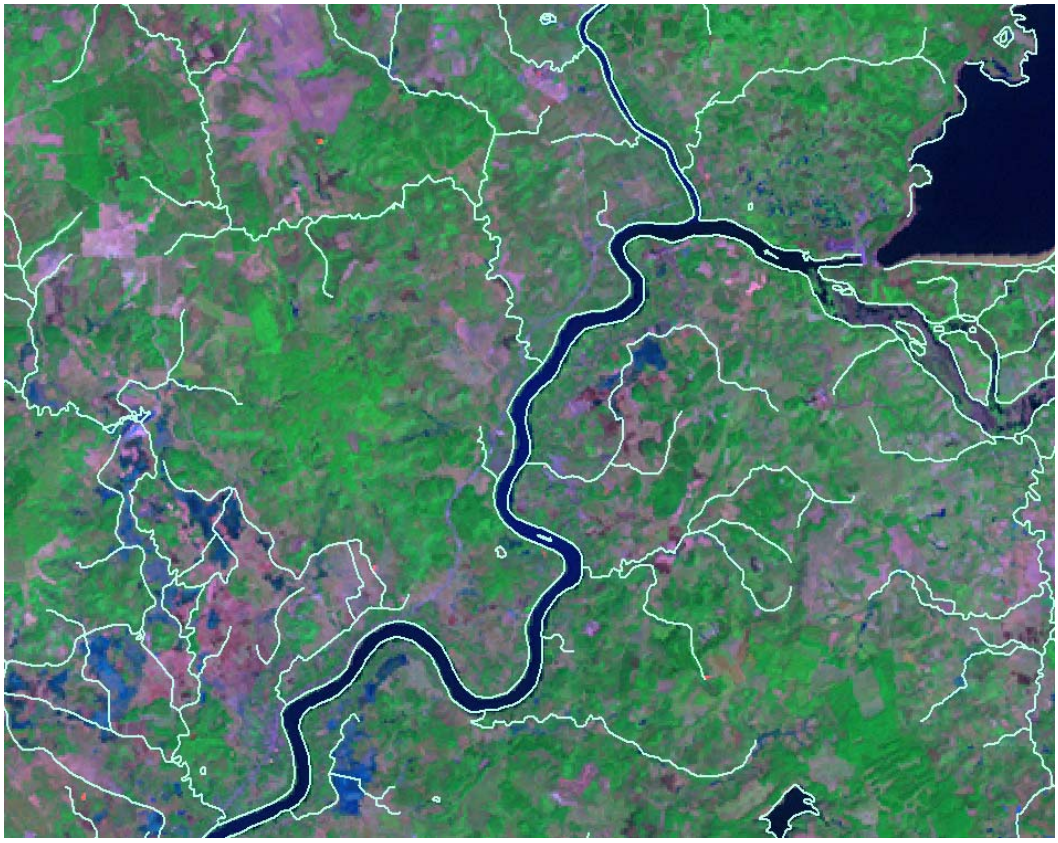

Figure 2.11: Landsat/ETM image and local maps overlay well together

While, Geo-coded Landsat/ETM images downloaded from website of Maryland University and local maps can overlay together very well (Figure 2.11). Therefore, the Landsat/ETM image 2002 was used as reference image to collect ground control points (GCPs) for geometric correction of ALOS/AVNIR-2 image.

To find the best way for geometric correction, analyzing geometric structure of images is necessary. Maximum height of mountains in the study area is 639m. Maximum error of position affected by terrain is calculated based on the Eq. (2.1).

$$L_{\max} = H_{\max} * \tan(\frac{\pi * \xi}{180}) \qquad (2.1)$$

Where, $L_{\max}$ is maximum error of position; $H_{\max}$ is maximum height of mountains; ξ is off-nadir angle in degree.

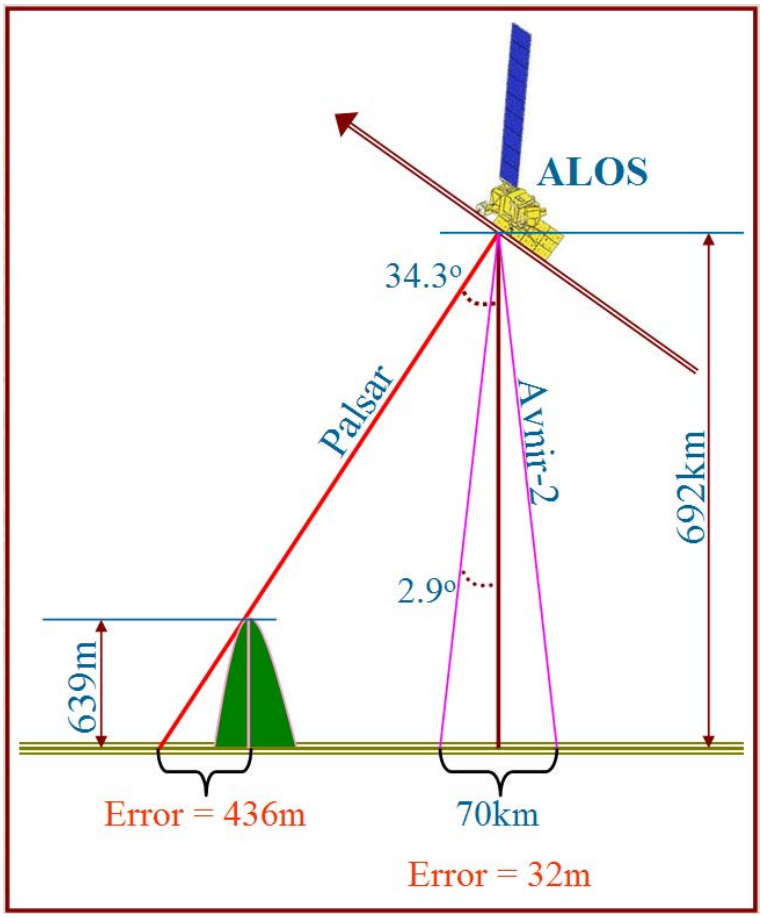

Figure 2.12: Schematic image of position errors affected by terrain in ALOS data

According to information from headers of ALOS images, off-nadir angle of ALOS/PALSAR single-polarized and dual-polarized images is 34.3°. That of ALOS/PALSAR multi-polarized images is 23.1°. So, maximum error of position affected by terrain in ALOS/PALSAR images is 436m (calculated for ξ=34.3°) in the study area. The schematic image of the position errors is described in Figure 2.12.

With similar calculation, based on altitude of ALOS satellite is 692km and swath width of ALOS/AVNIR-2 is 70km, maximum off-nadir angle (boundary pixels) of ALOS/AVNIR-2 is also calculated, it is 2.9°. So maximum error of position affected by terrain in ALOS/AVNIR-2 images is 32m in theory (if the highest mountain is in margin of image). However, the highest mountains in the study area are located nearly the central path of ALOS/AVNIR-2 and ALOS/PRISM images, so effects of terrain in the

ALOS/AVNIR-2 images are not much. Maximum error of position affected by terrain in ALOS/PRISM images is similar to ALOS/AVNIR-2 images. Therefore, normal geometric correction (plane geometric correction or two dimensions) is acceptable for ALOS/AVNIR-2 images and ALOS/PRISM images. Orthogonal geometric correction is necessary for ALOS/PALSAR images. A flow chart of geometric correction methodology is shown in Figure 2.13.

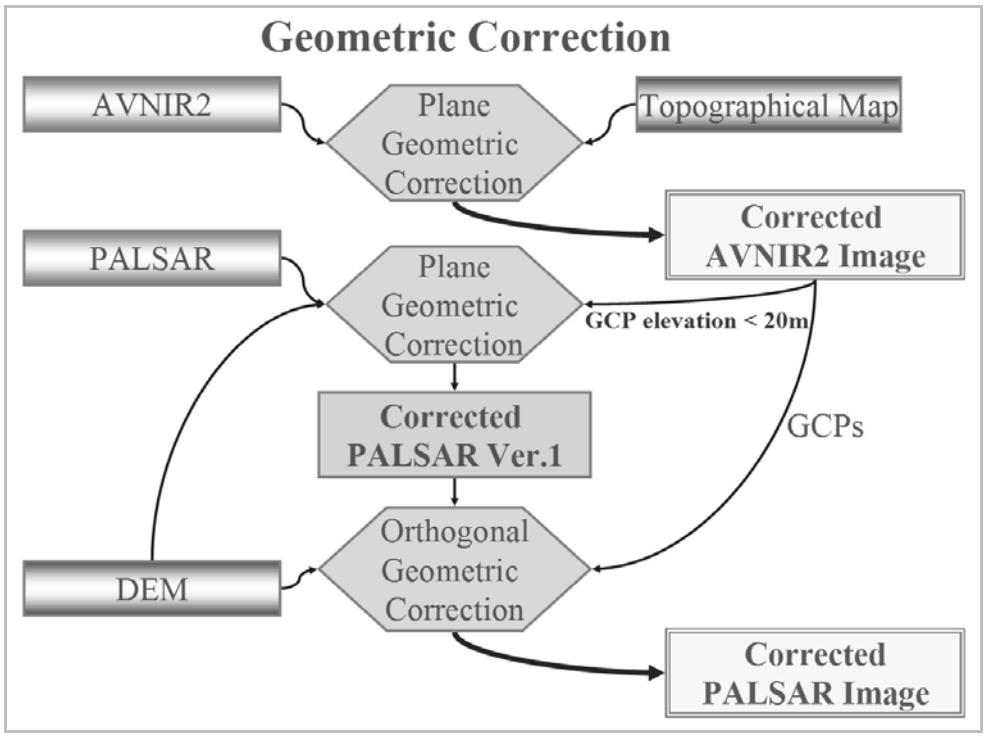

Figure 2.13: A flow chart of Geometric Correction Methodology

DEM for geometric correction 10m resolution was developed from elevation contour lines that were derived from local topographic maps.

A plane geometric correction method was applied for ALOS/AVNIR-2 images. Whereas for ALOS/PALSAR data, it was divided into 2 steps:

- The first step, plane geometric correction was used to correct the parts that have elevation less than 20m. Based on DEM, the ALOS/AVNIR-2 image was cut to get under 20m parts as shown in Figure 2.14. GCPs for the plane geometric correction were collected in this part only based on the corrected ALOS/AVNIR-2 image.

Corrected ALOS/PALSAR Ver.1 as shown in Figure 2.13 (already corrected in the first step) is correct in the low terrain part, but it is not correct in high mountain part as shown in Figure 2.15. In Figure 2.15 (*a*), rivers in local map and in image are matching well together, but in Figure 2.15(*b*), streams in local map and in image are shifted together.

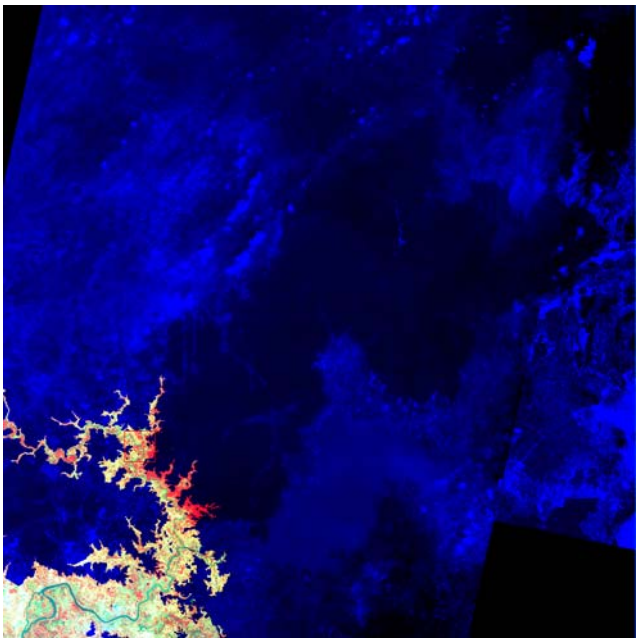

Figure 2.14: The part of ALOS/AVNIR-2 image has elevation less than 20m

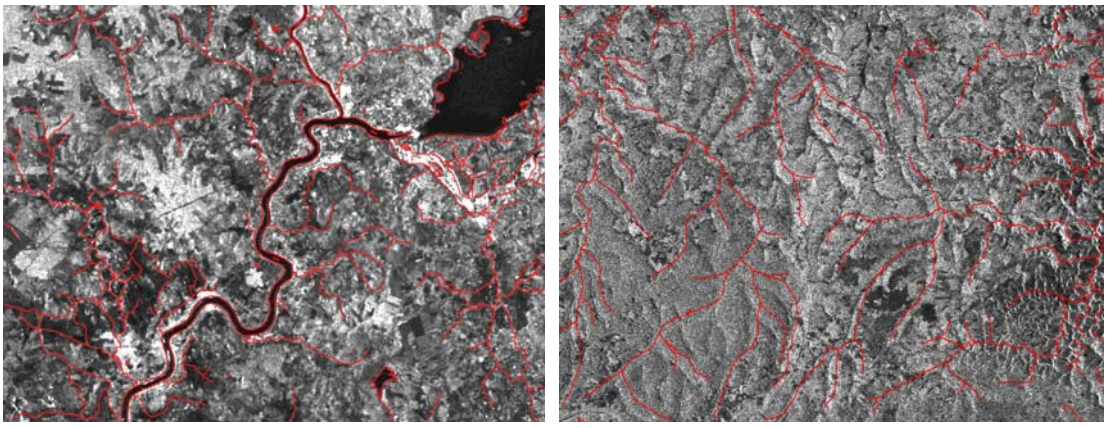

(*a*) (*b*)

Figure 2.15: Comparison of the corrected ALOS/PALSAR version 1 and local maps: (*a*) in low terrain part, (*b*) in high mountain part

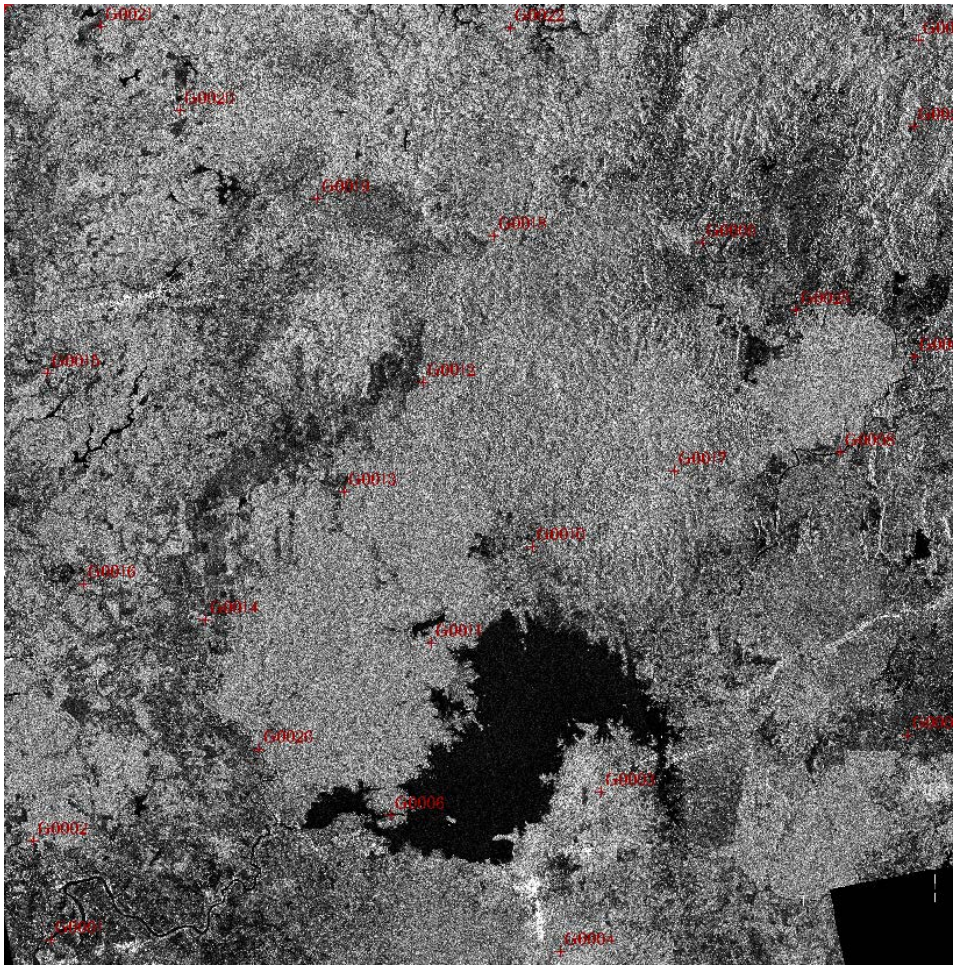

Figure 2.16: Distribution of 27 GCPs for ALOS/PALSAR orthogonal geometric correction

- The second step, the corrected ALOS/PALSAR Ver.1 was corrected again to reduce effects of terrain by Orthogonal Geometric Correction method. 27 GCPs were collected very carefully based on the corrected ALOS/AVNIR-2 image and the DEM developed from contour lines of local topographic map. These 27 GCPs are distributed in whole the study area as shown in Figure 2.16. Coordinates and elevations of them are shown in Table 2.1. Rational Function Math Model of PCI software was used and parameters of the model were computed based on GCPs.

Used coordinate system is UTM, zone 48, ellipsoid WGS84. Mean errors were constrained less than 1 pixel (10m).

Table 2.1: Coordinates and elevations of 27 GCPs for orthogonal geometric correction of ALOS/PALSAR images

ID	Column	Line	X axis (m)	Y axis (m)	Elevation (m)
G01	1719	8503.5	695375	1218535	10
G02	1566.5	7650.5	693855	1227090	41
G03	6432.5	7172	742800	1231825	152
G04	6113	8581.75	739500	1217820	127
G05	9073.5	6637	769310	1237070	105.25
G06	4627.75	7395.25	724577.5	1229633	67
G07	9062.5	3285	769600	1270210	138
G08	8442.5	4138.25	763230	1261815	120
G09	7225	2308.5	751105	1280055	140
G10	5814.25	5017	736585	1253260	72
G11	4960.5	5884	727965	1244673	76
G12	4863.75	3585	727065	1267580	90
G13	4207.5	4554.5	720450	1257970	100
G14	3033.5	5696.5	708572.5	1246630	60
G15	1674.25	3564.5	694802.5	1268053	64
G16	1989.5	5402.5	698030	1249625	50
G17	7027.5	4328.75	749100	1260060	264.5
G18	5456	2280.25	733365	1280580	307
G19	3960	1981	718020	1283680	150
G20	2793	1231	706085	1291315	80
G21	2113	515.5	699202.5	1298565	123
G22	5570	445.5	734555	1298815	273
G23	9025.5	477	770035	1298080	530
G24	8996.5	1237.5	769710	1290585	560

G25	8036.5	2896	759262.5	1274145	140
G26	3499	6832.5	713190	1235255	13
G27	8332.5	8111	761680	1222485	80

Geometric correction was also applied to ALOS/PRISM data by the same way as ALOS/AVNIR-2 data.

Hence, all ALOS images and local existing maps are identical overlay together.

2.3. DN value normalization

Four ALOS/AVNIR-2 images were used to cover whole study area as mentioned before, although the observed time of the images are close together (2007/01/19 and 2007/02/05), but DN value levels of them are not the same. It is clearly observed the boundary between images after making mosaic (Figure 2.18(*a*)). Therefore the mosaic image cannot be used directly for forest classification. Converting DN value to reflectance value is a perfect way to solve that problem, however information to convert from DN value of ALOS/AVNIR-2 image to reflectance value is not enough. For the reflectance conversion from ALOS data, Eq. (2.2) is usually used (Yuji Sakuno et al. 2007).

$$R_\lambda = (\pi[L_\lambda - Lp_\lambda]d^2)/(ESUN_\lambda \cos\theta_z) \qquad (2.2)$$

Where, R is the effective at-satellite reflectance (unit less); L_λ is spectral radiance ($Wm^{-2}sr^{-1}\mu m^{-1}$); Lp_λ is pathradiance ($Wm^{-2}sr^{-1}\mu m^{-1}$); d is the Earth-Sun distance in astronomical, $ESUN_\lambda$ is the mean solar exoatmospheric irradiance in $Wm^{-2}\mu m^{-1}$ at wave length λ; and θ_z is the solar zenith angle in degrees. Almost parameters in the Eq. (2.2) can be collected except *ESUN*. Therefore, the Eq. (2.2) was not used in this

study.

Convert DN value to radiance value is also another choice. The radiance conversion from DN value of ALOS/AVNIR-2 data was calculated based on Eq. (2.3).

$$L_\lambda = a_\lambda DN_\lambda + b_\lambda \quad (2.3)$$

Where, *a* and *b* show the gain and offset of the radiance conversion coefficient respectively written by the header of ALOS/AVNIR-2 data. But, the gain and offset values of all the four received ALOS/AVNIR-2 images are the same together as shown in Table 2.2.

Table 2.2: Radiance conversion parameters of the four ALOS/AVNIR-2 images

Bands	Gain	Offset
1	0.5880	0
2	0.5730	0
3	0.5020	0
4	0.5570	0

Consequently, converting to radiance value will have no meaning in this case. Therefore, in this study, normalization method was chosen. In normalization, mean and standard deviation values of a common area were used. To get a good result, a common part of two images that has no cloud and includes many types of land cover objects was cut (Figure 2.17). Then, mean and standard deviation values were calculated for the part that already cut it. These mean and standard deviation values will be used to normalize for whole image (Hoan and Tateishi 2008).

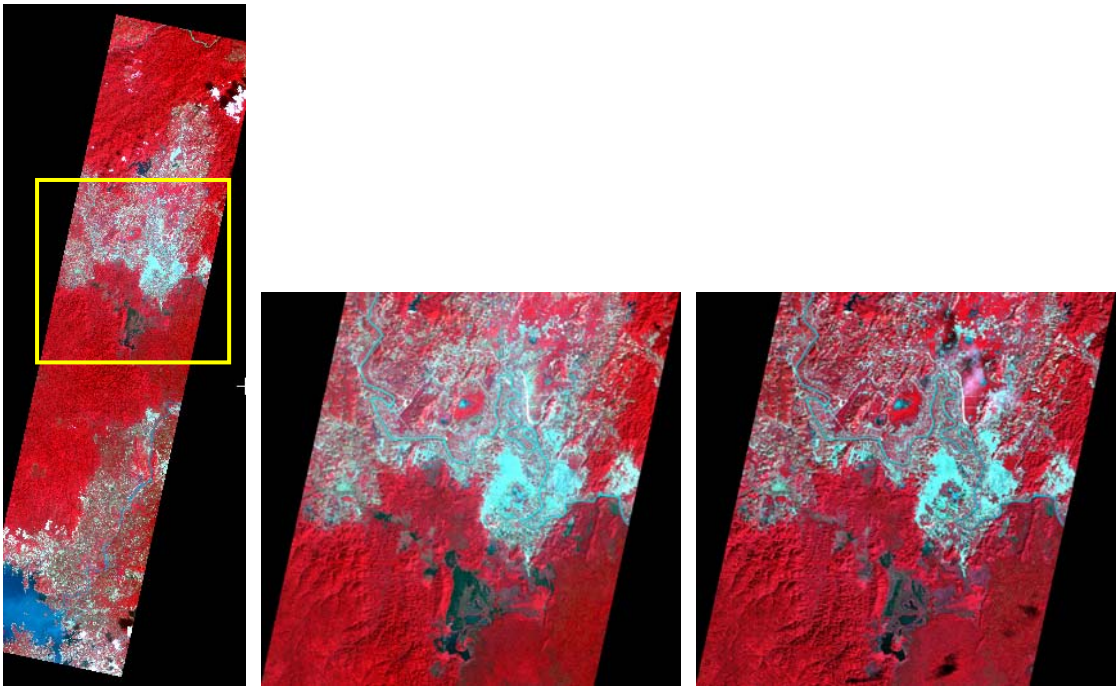

(*a*) (*b*) (*c*)

Figure 2.17: Common area was used for normalization, (*a*) common area of two images, (*b*) the cut part of image1, (*c*) the cut part of image2, the yellow rectangle in (*a*) is the part that was cut to become (*b*) and (*c*).

Mean and standard deviation values derived from the cut parts of the image1 and image2 are shown in Tables 2.3 and 2.4.

Table 2.3: Mean and standard deviation values in the common area of background image (Image1)

Basic Stats	Min	Max	Mean	Stdev
Band 1	0	179	92	48
Band 2	0	209	73	40
Band 3	0	248	60	36
Band 4	0	198	88	48

Table 2.4: Mean and standard deviation values in the common area of the image that will be normalized (Image2)

Basic Stats	Min	Max	Mean	Stdev
Band 1	0	255	69	37
Band 2	0	255	56	33
Band 3	0	255	44	33
Band 4	0	253	89	52

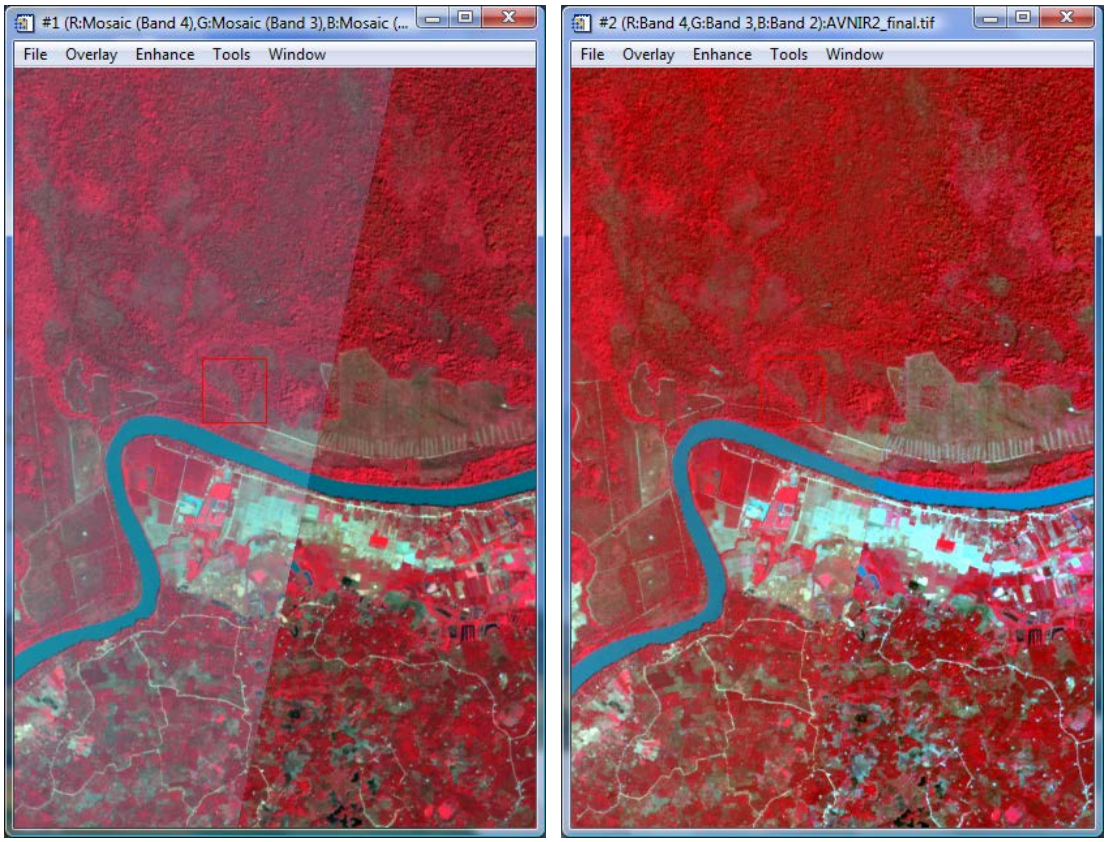

(*a*) (*b*)

Figure 2.18: ALOS/AVNIR-2 mosaic image: (*a*) before normalization, (*b*) after normalization (Color composite: R-NIR; G-Red; B-Green)

It is assumed that there are no change in the common part of the two images. In this

case, linear model was used as the Eq. (2.4) (Duong et al. 1999).

$$\frac{DN_1[i,j]-M_1}{\sigma_1}=\frac{DN_2[i,j]-M_2}{\sigma_2} \quad (2.4)$$

The Eq. (2.5) is changed from the Eq. (2.4). The Eq. (2.5) was used to normalize the ALOS/AVNIR-2 images.

$$a[i,j]=(b[i,j]-M_2)*\frac{\sigma_1}{\sigma_2}+M_1 \quad (2.5)$$

Where,

M_1, M_2	Mean value in the cut part of image1 and image2
DN_1, DN_2	Digital number in image1 and image2
σ_1, σ_2	Standard deviation in the cut part of image1 and image2
$a[i,j]$	DN value after normalization
$b[i,j]$	DN value before normalization

* Please note that Image1 is background image and image2 is the image that will be normalized following the image1.

After successfully performed normalization, the boundary of images cannot be determined visually as shown in Figure 2.18(*b*).

2.4. Some other processing

Some other processing was also done including:

- To choose a suitable filter method for ALOS/PALSAR images, many existing SAR filter methods were used to compare together including: Lee, Enh.Lee, Kuan, Gamma, Enh.Frost and Frost. Also many sizes of window filter were tried to apply,

from 3x3 to 11x11. The criteria to choose a good filter method are almost how much can keep structures of forest as well as reduce noises. The comparison was carried out visually. Finally, Frost filter method and window size 5x5 were chosen for ALOS/PALSAR filtering.

- The ALOS/PRISM mosaic image were combined with the ALOS/AVNIR-2 mosaic image to make pan-sharpen images 2.5m resolution for collecting training data and validation data. All the five available methods for sharpening of ENVI software version 4.2 were applied including: HSV, Color Normalized (Brovey), Gram-Schmidt Spectral Sharpening, PC Spectral Sharpening, and CN Spectral Sharpening. Subsequently, HSV sharpening method was selected based on visual comparison. In this PRISM-sharpen image, canopies of forest trees can be seen clearly as shown in Figure 2.19. Therefore, collecting training data and validation data can get a good accuracy based on this sharpen image.

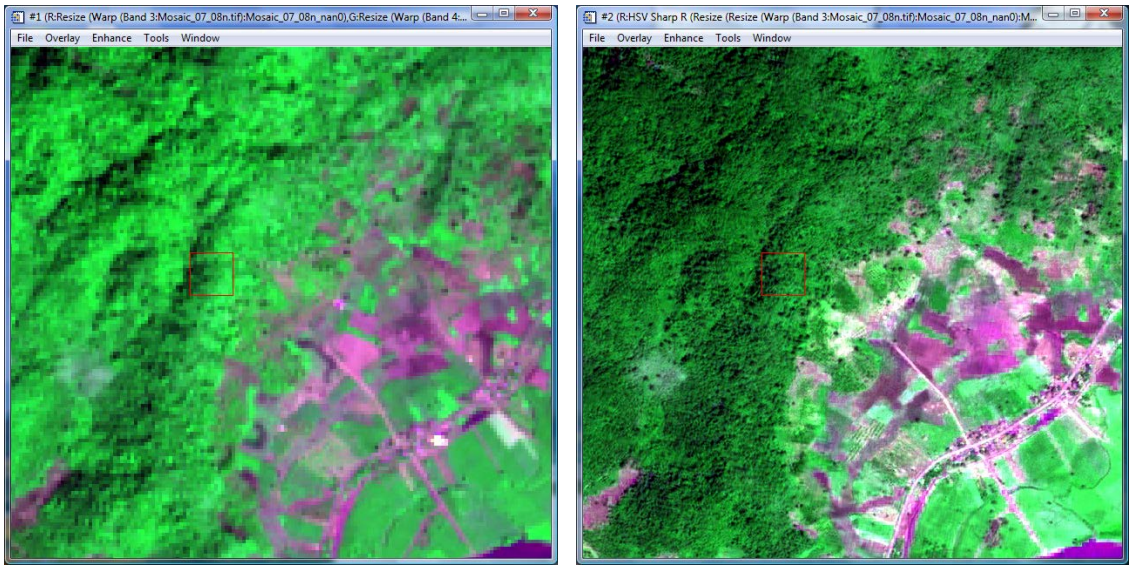

(*a*) (*b*)

Figure 2.19: Comparison of (*a*) ALOS/AVNIR-2 image (Color composite: R-NIR; G-Red; B-Green) and (*b*) PRISM-sharpen image by HSV method

- High quality DEM, 10m resolution was developed from elevation contour lines of topographic maps (Map-DEM). This DEM was already used for orthogonal

geometric correction of ALOS/PALSAR images. In addition, it also will be used to produce Tree-Height map and high slope map. The high slope map will be used in the combination model that will be presented in Chapter 4.

- Tree-Height map were developed based on comparison of SRTM-DEM and the Map-DEM. The comparison of the two DEM data is shown in Table 2.5.

Table 2.5: Comparison of SRTM-DEM and Map-DEM

SRTM - DEM	Map-DEM
Developed from radar interferometer (the Shuttle Radar Topography Mission - 2000)	Developed from elevation contour lines of local topographic maps
Used radar is in C-band (5.6cm), Incidence angle (θ): 30^o – 60^o.	Topographic maps are produced by surveying on ground and airborne images.
So, elevation value is top of forest canopy	**So, elevation value is height of ground**

Therefore, height of trees can be calculated as following:

[Tree-Height] = [SRTM-DEM] - [Map-DEM]

Although accuracy of SRTM-DEM is not very good in some parts of the world (Iwaoa et al. 2008), but to separate heights of the objects that is near together is possible. In this study, some clear no-change elevation points of SRTM-DEM and Map-DEM were selected to compare. Then, elevation level of SRTM-DEM was corrected again based on Map-DEM by average value of different elevations between the two DEM data.

The Tree-Height map is shown in Figure 2.19. It will be used as a reference data for collecting training data and validation data.

- There are some clouds in the received ALOS/AVNIR-2 images. Cloud removal program was used to solve this problem. The Cloud Removal program was developed by the author as one part of this study (Hoan and Tateishi 2009). This problem will be presented clearly in Chapter 3.

Finally, all images and maps were cut following the study area boundary and resampled to 10 meter resolution. The data was prepared successfully for the next steps including (Figure 2.19):

- One mosaic image of ALOS/AVNIR-2 around February 2007.
- One mosaic image of ALOS/PALSAR single-polarization around February 2007.
- One mosaic image of ALOS/PALSAR dual-polarization around June 2007.
- One mosaic image of ALOS/PRISM around March 2009.
- Existing local forest map 2005
- STRM-DEM
- Map-DEM
- Tree-Height map

ALOS/PALSAR multi-polarized images have some problems, so they were not used for forest mapping. These problems will be presented more in Chapter 4.

In addition, Vietnam forest map 1993 and ASTER-GDEM were also collected. But they were used to illustrate some problems only as presented in the above sections. They were not used for forest mapping. Therefore, they are not listed in Figure 2.20.

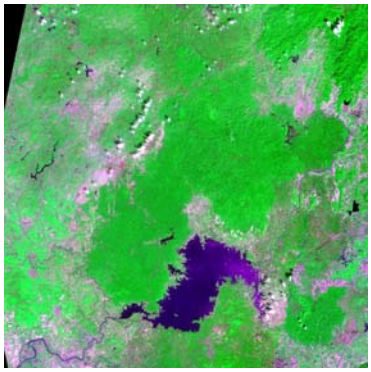

AVNIR-2

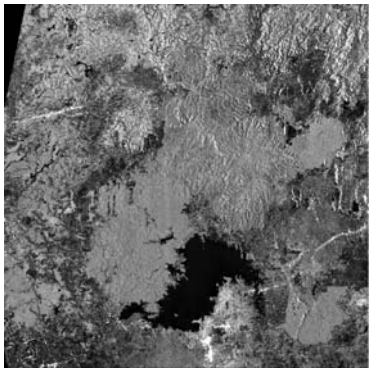

PALSAR single-polarization

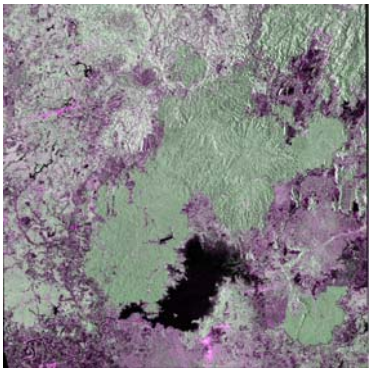

PALSAR dual-polarization

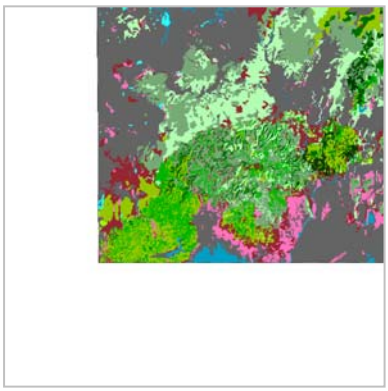

Existing forest map 2005

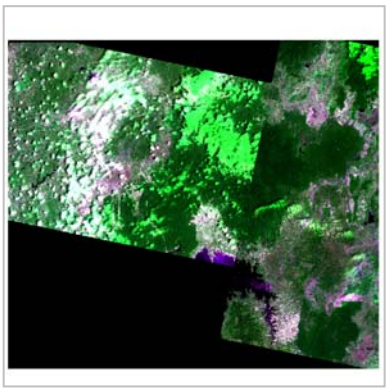

PRISM-sharpen

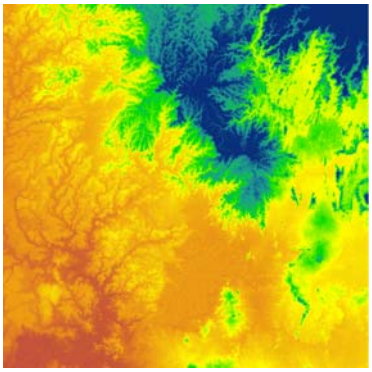

SRTM-DEM

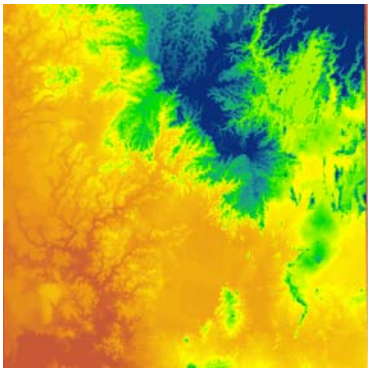

Map-DEM

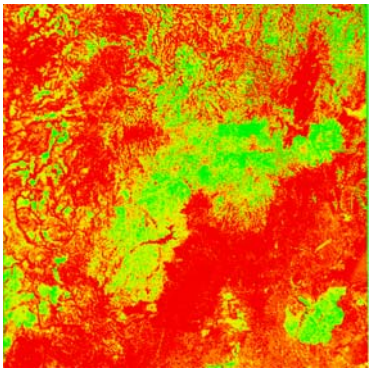

Height of trees

Figure 2.20: The data prepared for the next processing steps

CHAPTER 3

CLOUD REMOVAL OF OPTICAL IMAGE USING SAR DATA FOR ALOS APPLICATIONS

3.1. Introduction

Cloud is always problem of optical remote sensing data, and of course, ALOS/AVNIR-2 images are also affected. Microwave images are not affected by cloud. ALOS satellite has both optical and microwave sensors, similar resolution (~10m). Therefore, this study proposed a method to remove cloud in optical images based on interpolation from SAR data. This method was developed based on interpolating under cloud pixel values for ALOS/AVNIR-2 images.

To remove cloud, it needs to be defined. A combination method of Total Reflectance Radiance Index (TRRI) and Cloud-Soil Index (CSI) is used to define cloud. TRRI is an index developed by Prof. Nguyen Dinh Duong, Vietnamese Academy of Science and Technology (VAST), Vietnam (Duong 1998) and CSI is an index developed by the author for this study based on some studies before (Hoan and Duong 2004, Hoan et al. 2005). Because around-cloud pixels are mixture of cloud and other objects, that is very difficult to define. Therefore, the around-cloud pixels are extended from cloud. Cloud shadow problem is also discussed in this section.

Requirement of this method is suited when objects in ALOS/AVNIR-2 and ALOS/PALSAR data are not different very much. That means, this method can apply for the data in which optical image and microwave image in the same geographic place are not very far together about time. With ALOS satellite, it was hoped that this requirement will be satisfied.

When this study was started, ALOS data had not been available yet, therefore this study was experimented on simulated ALOS data from Landsat/TM and JERS-1/SAR images. This simulated way will be presented in the next section.

This method also can be applied for removing cloud in optical images based on other optical images. In this study, some examples of removing cloud in ASTER image based on Landsat/ETM image, removing cloud in Landsat/TM image based on Landsat/TM image are also shown. This method is suitable to make a series of cloud free multi-temporal images for change detection studies, natural resource and environment monitoring studies and so on.

3.2. Simulated ALOS data

This study was experimented on simulated ALOS data. The ALOS/AVNIR-2 includes 4 spectral channels. Wavelengths of them are close to Landsat/TM images. The comparison of both data is shown in Table 3.1.

Table 3.1: Comparison of characteristics between ALOS/AVNIR-2 and Landsat/TM

Bands	ALOS/AVNIR-2 (nm)	Landsat/TM (nm)
1	420 – 500	450 – 520
2	520 – 600	530 – 610
3	610 – 690	630 – 690
4	760 – 890	750 – 900

Therefore, the first 4 bands of Landsat/TM image were used instead of ALOS/AVNIR-2 image.

The frequency of ALOS/PALSAR is close to JERS-1/SAR data as shown in Table 3.2.

Table 3.2: Comparison of characteristics between ALOS/PALSAR and JERS-1/SAR

	ALOS/PALSAR	JERS-1/SAR
Frequency (MHz)	1270 L-band	1300 L-band

So, JERS-1/SAR data was used instead of ALOS/PALSAR data.

In this study, Landsat/TM image date 1992/10/21 and JERS-1/SAR image date 1992/10/27 of Hanoi, Vietnam were used.

JERS-1/SAR image was resampled to 30 meter spatial resolution to correspond with Landsat/TM image. It was also applied GAMMA 3X3 FILTER (Lopes et al. 1993, Zhenghao and Fung 1994) to reduce noises. And it was corrected about geometry by orthogonal geometric correction before using for interpolation to remove cloud in optical image. The DEM developed from local topographic map 1:50,000 was used for orthogonal geometric correction. Rational Function Math Model of PCI software was used and parameters were computed based on GCPs. Figure 3.1 is an illustration of JERS-1/SAR image after these processing.

Figure 3.1: JERS-1/SAR image 30 m resolution after processing of GAMMA 3X3 FILTER and Orthogonal Geometric Correction

In the Landsat/TM image, there was no cloud. Cloud was gotten from another Landsat/TM image and overlay to the Landsat/TM image date 1992/10/21 as shown in Figure 3.2.

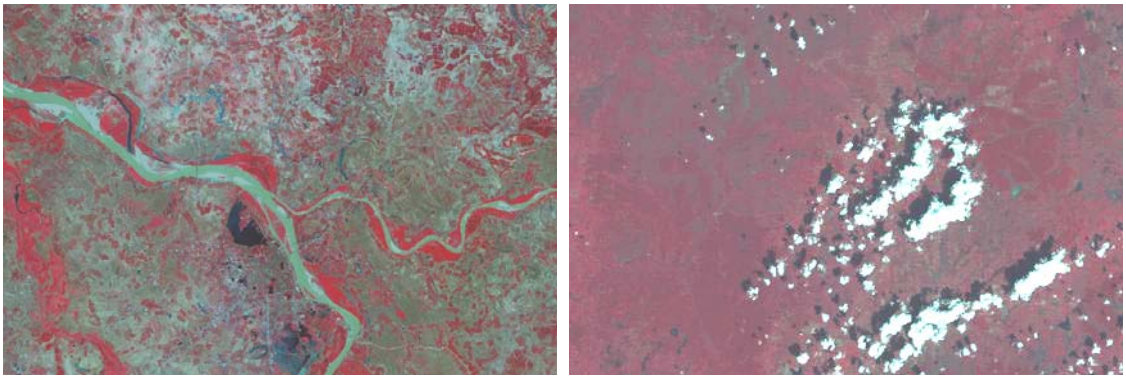

Figure 3.2: Landsat/TM image date 1992/10/21 (left) and Landsat/TM image used to get cloud (right)

By this way, we have perfect data for experimenting the cloud removal program85 including: cloud image to test the cloud defining method, to test the interpolation method and we also have original data (under cloud data – before overlay cloud) to compare with interpolated result for validation. Figure 3.3 shows the Landsat/TM image after overlaying cloud

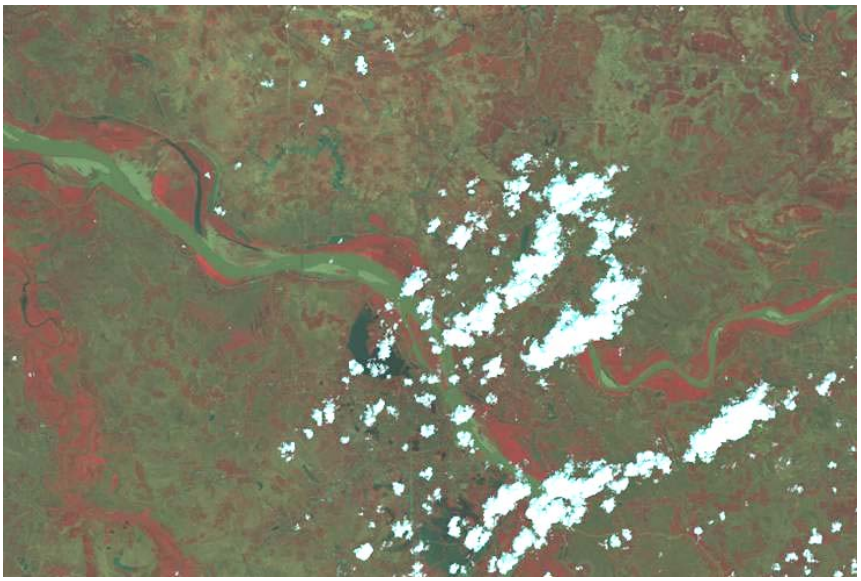

Figure 3.3: Landsat/TM image date 1992/10/21 after overlaying cloud

3.3. Methodology

Outline of cloud removal methodology is illustrated in Figure 3.4 .

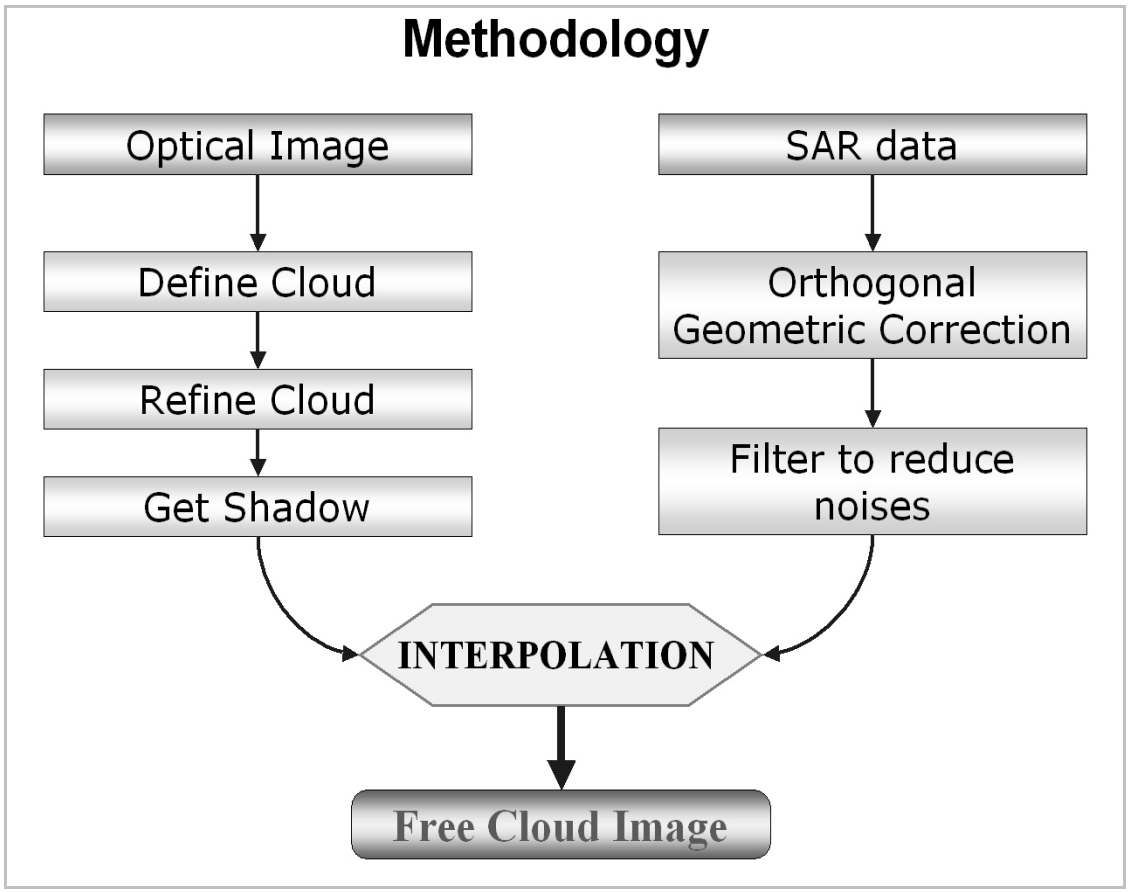

Figure 3.4: A flow chart of cloud removal methodology

3.3.1. Defining Cloud

Reflectance of cloud is always high from visible wave to near infrared wave. So, values of cloud will be high in the all 4 bands of ALOS/AVNIR-2 data. Therefore, with thick

clouds, it is very easy to define them by TRRI index. This index is defined by the Eq. (3.1) (Duong 1998):

$$TRRI = \frac{\int_{1}^{n} I_i \Delta}{\int_{1}^{n} I_{\max} \Delta} * 100 \qquad (3.1)$$

Where,

TRRI	Value of index
I_i	Digital count of channel i
n	Number of spectral channels
I_{max}	Maximal digital count for given quantization level
Δ	Spectral channel difference

With thin clouds, they are more difficult. Usually, they are mixed by some dry objects like dry sand or dry bare land. As we know, in the wavelengths from visible to infrared, reflectance of dry bare land is always going up according to growing of wavelength. And reflectance of clear water is always going down (Murai 1996, Liew 2001). Because cloud includes water, so reflectance curve of cloud will be going down and reflectance values will be lower in the last bands of ALOS/AVNIR-2 image. The difference of thin cloud reflectance and dry soil reflectance is shown in Figure 3.5 (pixel values were gotten from Landsat/TM image).

To define cloud, the TRRI index is used to divide image into 3 parts: thick cloud, non-cloud and mixture by 2 level values (as shown in Figure 3.5).

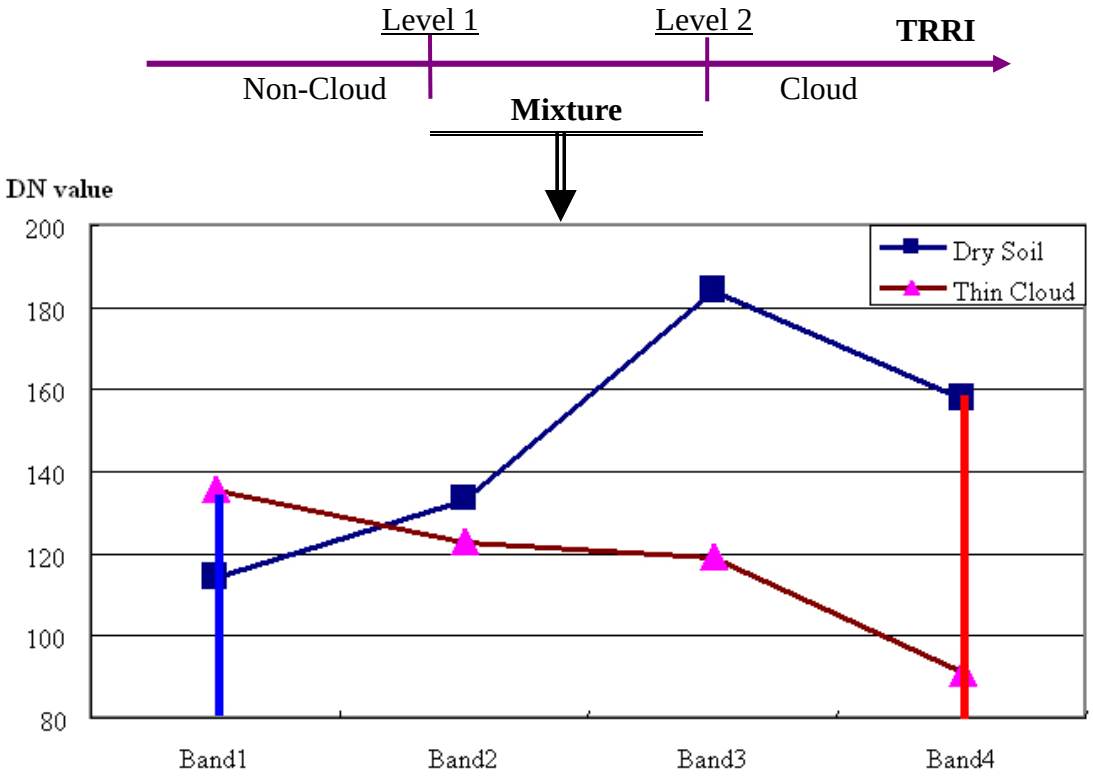

Figure 3.5: Model for defining cloud

In the mixture part, reflectance of thin cloud in blue band (band 1) is higher than that of dry soil and reflectance of thin cloud in band 4 is lower than that of dry soil. Therefore, thin cloud and other dry objects can be separated by Cloud-Soil Index (CSI). This index is calculated as the Eq. (3.2).

$$CSI = \frac{Band1 - Band4}{Band1 + Band4} \qquad (3.2)$$

Based on the model for defining cloud, a program was developed to define cloud by Visual C language. It is called Define Cloud function in a package of programs called Cloud Removal Program. The window and parameters of this function are shown in Figure 3.6.

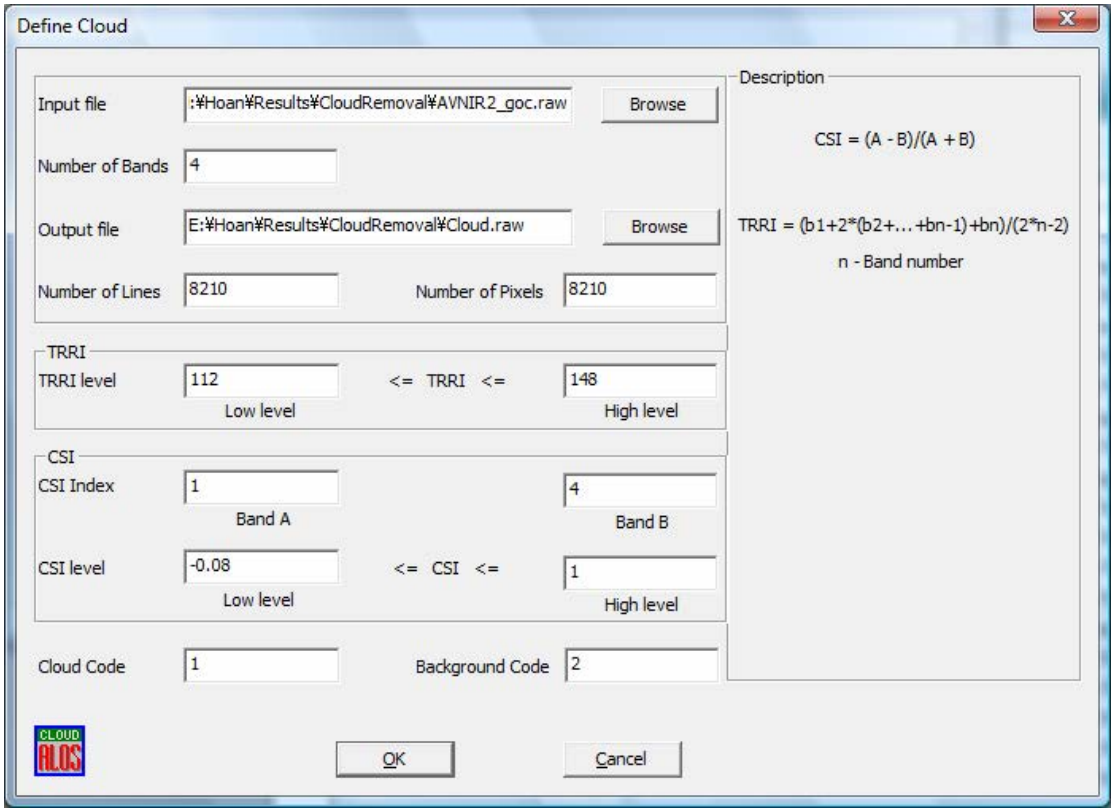

Figure 3.6: Window and parameters of the Define Cloud function

Result of cloud definition is shown in Figure 3.7.

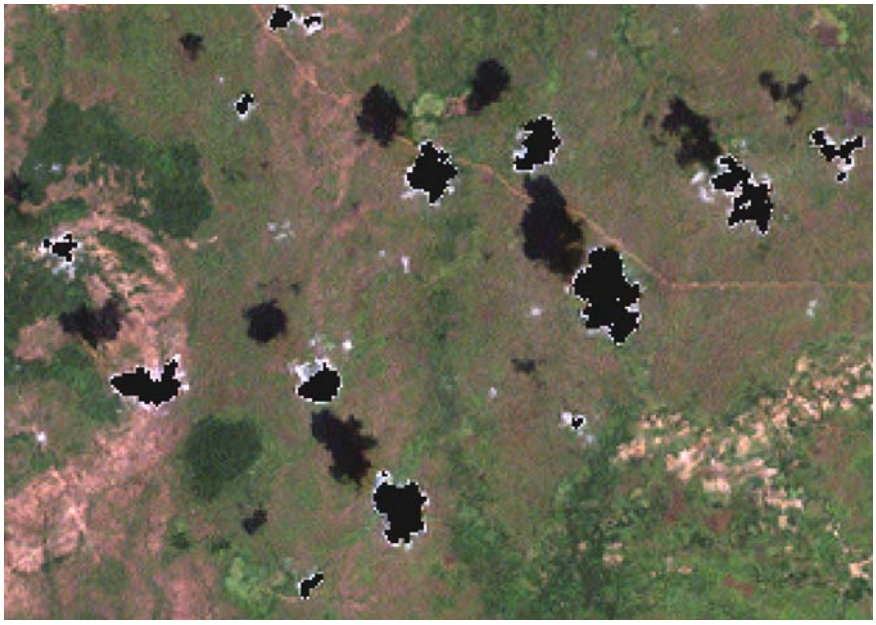

Figure 3.7: Cloud obtained by the cloud defining method (black areas)

In this result, boundary of cloud is still white. That is mixture of cloud and other objects, so that is difficult to define. This problem will be solved by extension function in the Refining Cloud section.

Integrating TRRI index and CSI index can separate cloud and non-cloud quite well. This model can apply for every type of multi-spectral optical image.

3.3.2. Refining cloud

The Clouds after defining still has some mistakes. Single pixels exist in some places. These pixels were estimated by visually that are some dry objects like buildings and something like that. To correct these mistakes, a function was developed to remove single pixels called Remove Single Pixels function (Figure 3.8).

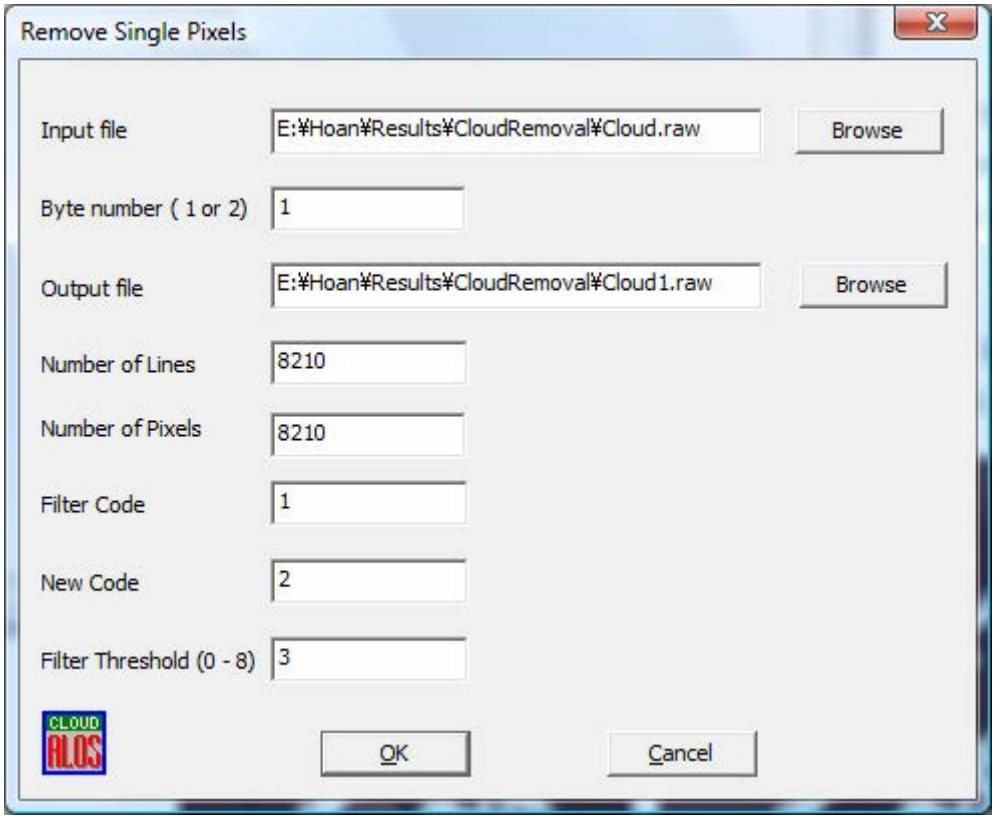

Figure 3.8: Window and parameters of the Remove Single Pixels function

After defining cloud, if result has some single pixels, the Remove Single Pixels function can be used to make a better result. An example is shown in Figure 3.9.

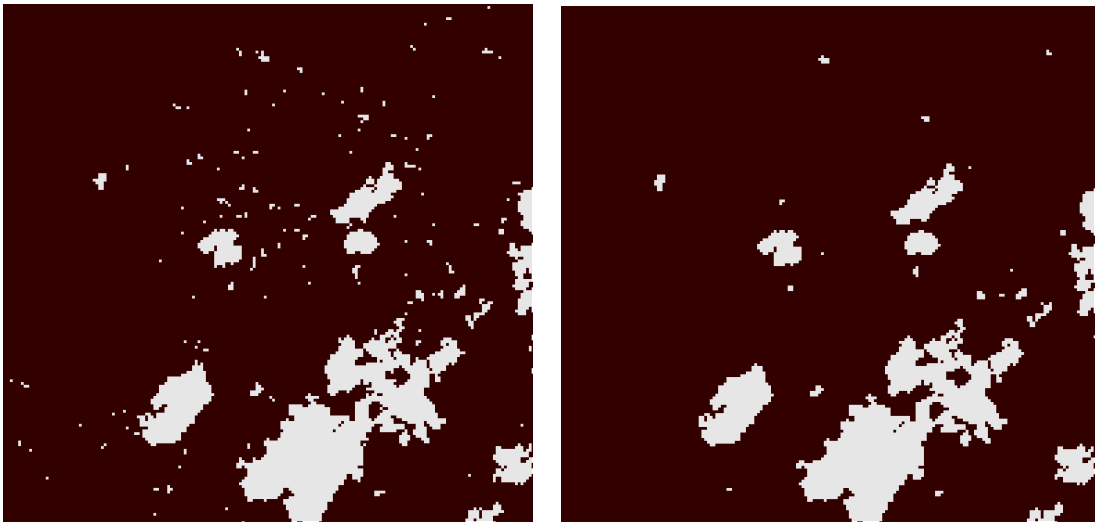

(*a*) (*b*)

Figure 3.9: Removing single pixel (the small white dots); (*a*) before removing and (*b*) after removing

The around-cloud pixels are mixture of cloud and other objects. So, that is very difficult to define. In this study, the around-cloud pixels are extended from cloud. Another individual function was developed for this purpose. By this extension function, the cloud after defining can be extended to cover all real cloud. A result example of this function is shown in Figure 3.13.

3.3.3. Extraction of shadow

Shadow is always difficult problem. Shadows of clouds on the different objects will have different values. Therefore they are very difficult to define. In this study, shadows are interpolated from clouds. For each image, average distance from clouds to their shadows is determined. Direction of shadow is also estimated. Based on these parameters, a function was developed to interpolate shadows from clouds called Get

Shadow function as shown in Figure 3.10.

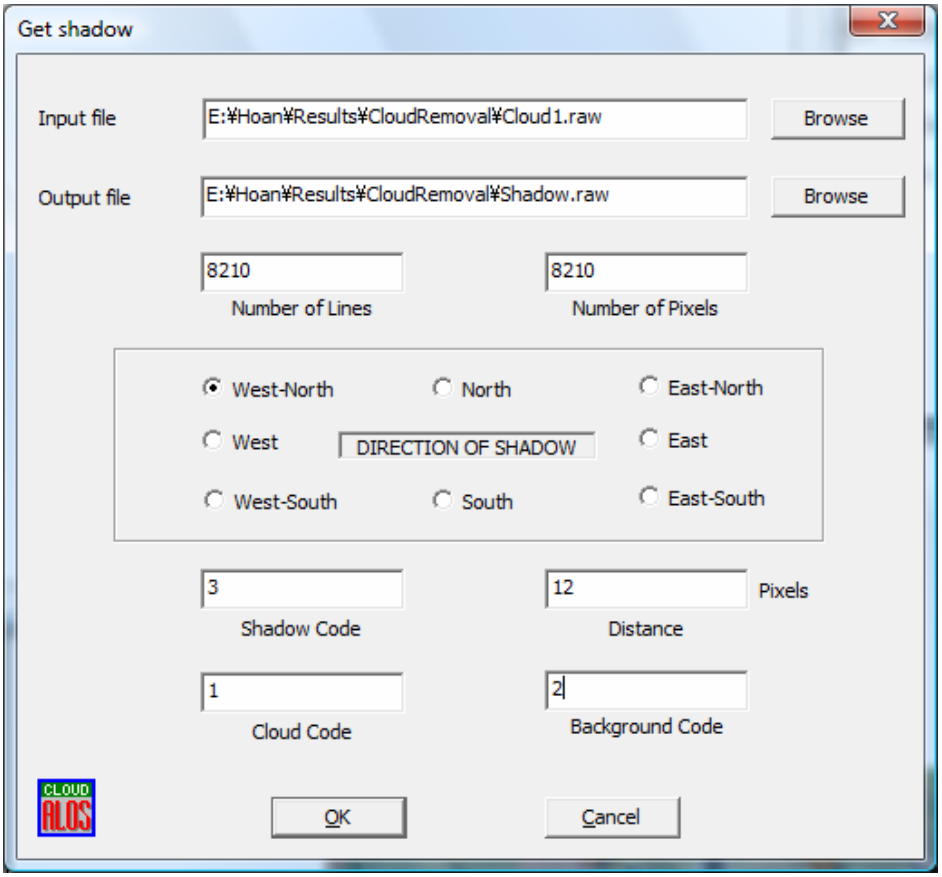

Figure 3.10: Window and parameters of the Get Shadow function

The interpolated result of shadow is illustrated in Figure 3.11.

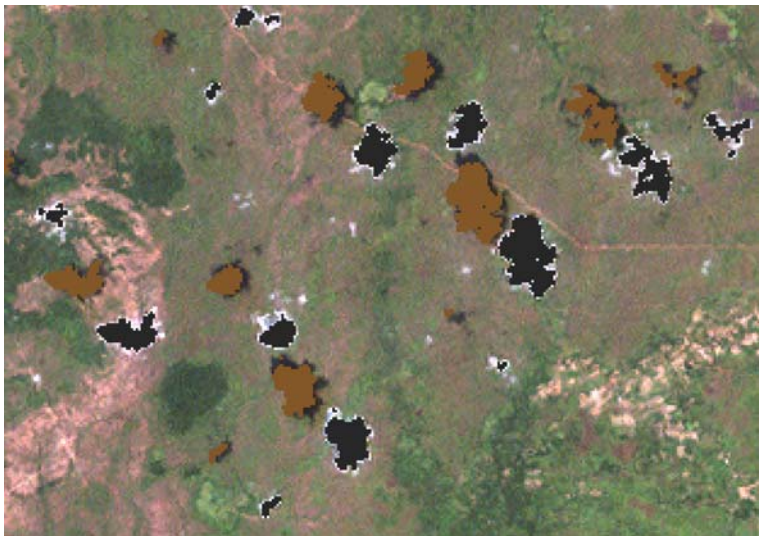

Figure 3.11: Shadows (dark-yellow) of clouds are interpolated from clouds (black)

Normally, clouds are in different heights. Elevations of terrain under shadows are also different. So, distance from clouds to shadows will be not constant. In this function, average distance is used and of course it will be not a perfect distance. Therefore, interpolated shadow does not cover whole real shadow. After interpolating, shadow result will be extended to cover all real shadow of cloud. A program was developed to do this called Extend Cloud function as shown in Figure 3.12.

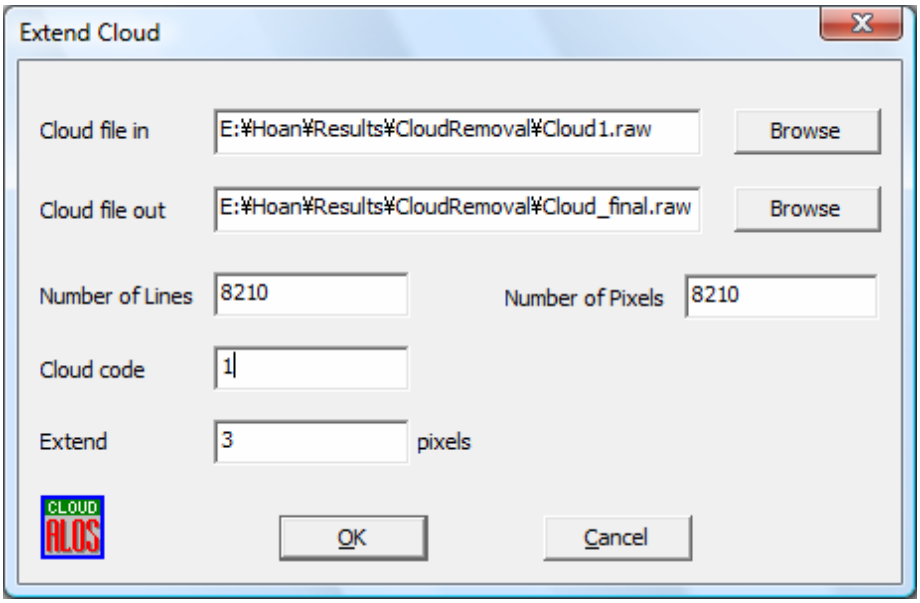

Figure 3.12: Window and parameters of Extend Cloud function

Clouds and Shadows after extension are shown in Figure 3.13.

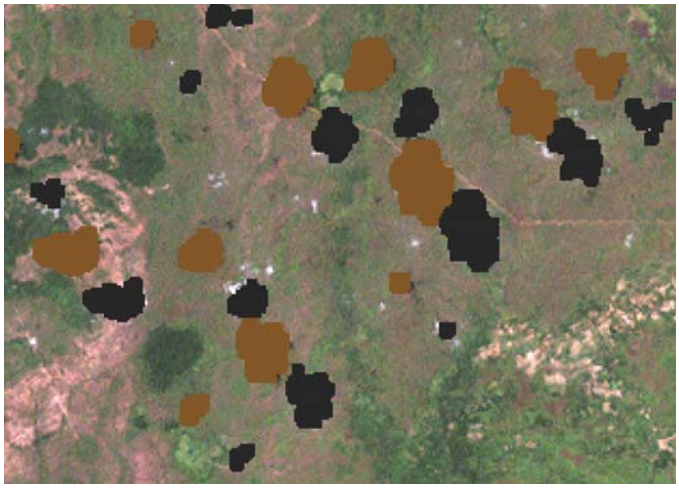

Figure 3.13: Clouds and Shadows after extension

3.3.4. Interpolating to remove cloud

To remove clouds and shadows, pixel values of clouds and shadows will be replaced by new values. These new values are interpolated from radar image. An interpolation function was developed to describe this algorithm.

With each cloud or shadow pixel in optical image, the interpolation function will find the corresponsive pixel (same location pixel) in radar image and get DN value of this pixel in the radar image. Then, the function will search from the nearest pixels to farther pixels in the radar image to find a similar pixel with the centre pixel. When meet the pixel that satisfy the condition as the Eq. (3.3) and it is not cloud or shadow in optical image, the searching will be stopped.

$$abs(DN_i - DN_j) \leq a \qquad (3.3)$$

Where,

a is threshold value

DN_i is digital number of centre pixel

DN_j is digital number of searching pixel

From DN_j position, program will find in the reverse direction to corresponsive pixel in the optical image. Then, DN value in this position will be gotten to replace for cloud or shadow pixel in the central position of searching window. Processing will be done one pixel by one pixel. The schematic image of this algorithm is described in Figure 3.10.

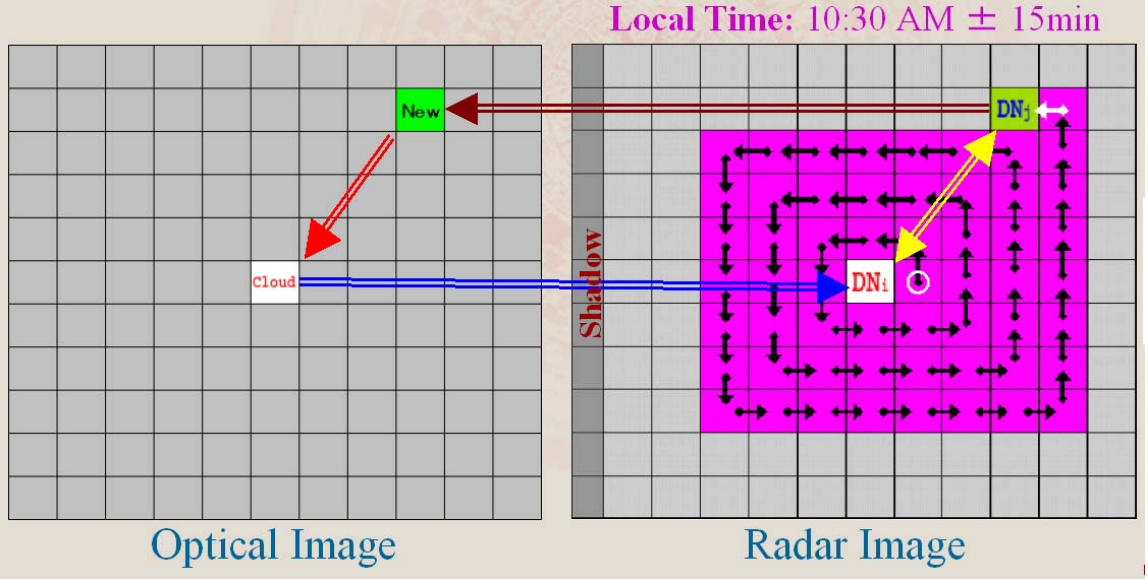

Figure 3.14: Interpolation model to remove cloud

Local time of ALOS satellite is 10:30 am ± 15 minutes. It means that the sun will be in the right side of image and shadow will be in the left side of image. To reduce effects of shadow, interpolation will be started from right-down pixel of each distance. This interpolation is illustrated by arrows in Figure 3.14. The white circle is started pixel of interpolation. A program was developed to interpolate for under cloud and shadow pixels based on the interpolation model. It is called Remove Cloud function in the menu File of the Cloud Removal Program. Window and parameters of this function are shown in Figure 3.15.

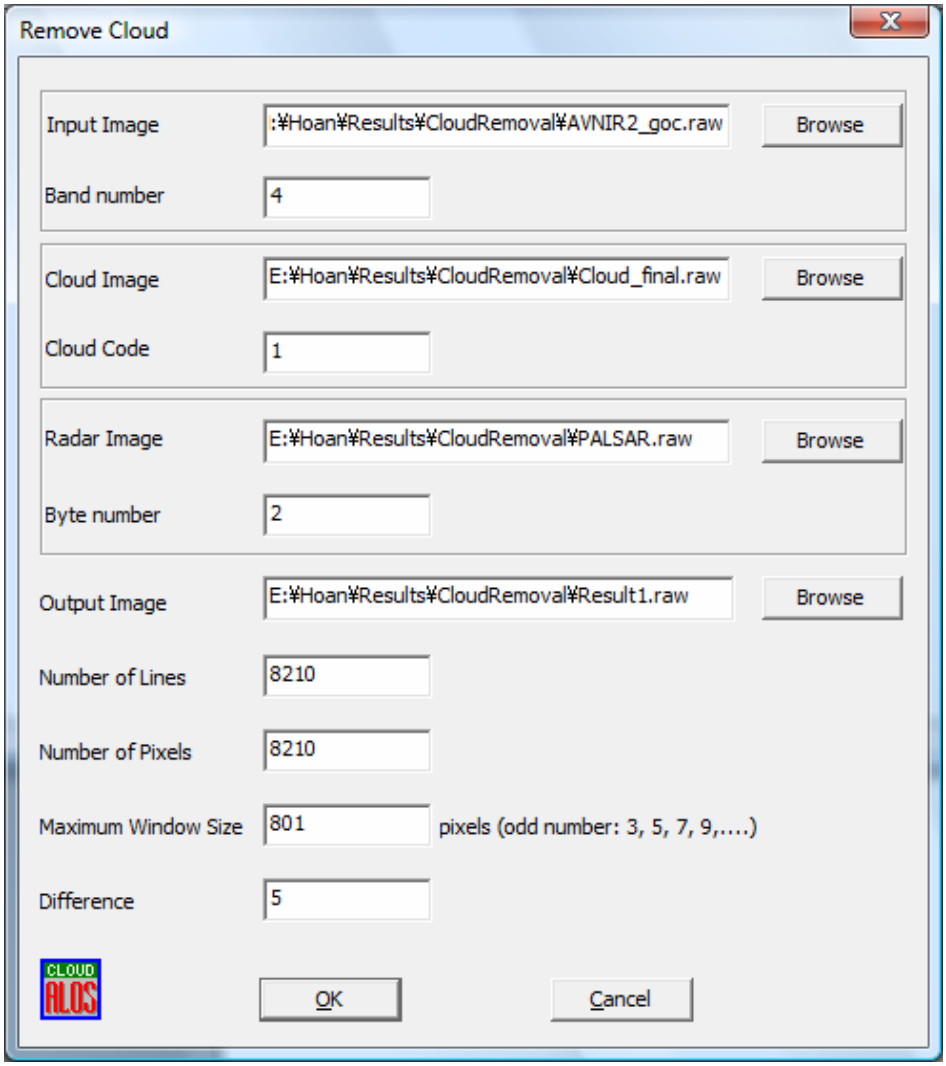

Figure 3.15: Window and parameters of Remove Cloud function

As we know, optical data and microwave data are very different together. The same values in microwave data do not guarantee that values in optical data will be the same. However, if the pixels are near together, likelihood of the same objects in optical data will be higher because the same objects are usually distributed in the same geographic regions. So, result image will have more information than cloud image and microwave image if using them independently.

In addition, some other functions were developed to support for image processing like Mask Cloud function and Change Code function.

3.4. Results and discussions

Result of this section is a package program with many functions for cloud removal of optical remote sensing image. After finish one processing, program will summarize and display every parameters of progress. An example is shown in Figure 3.16.

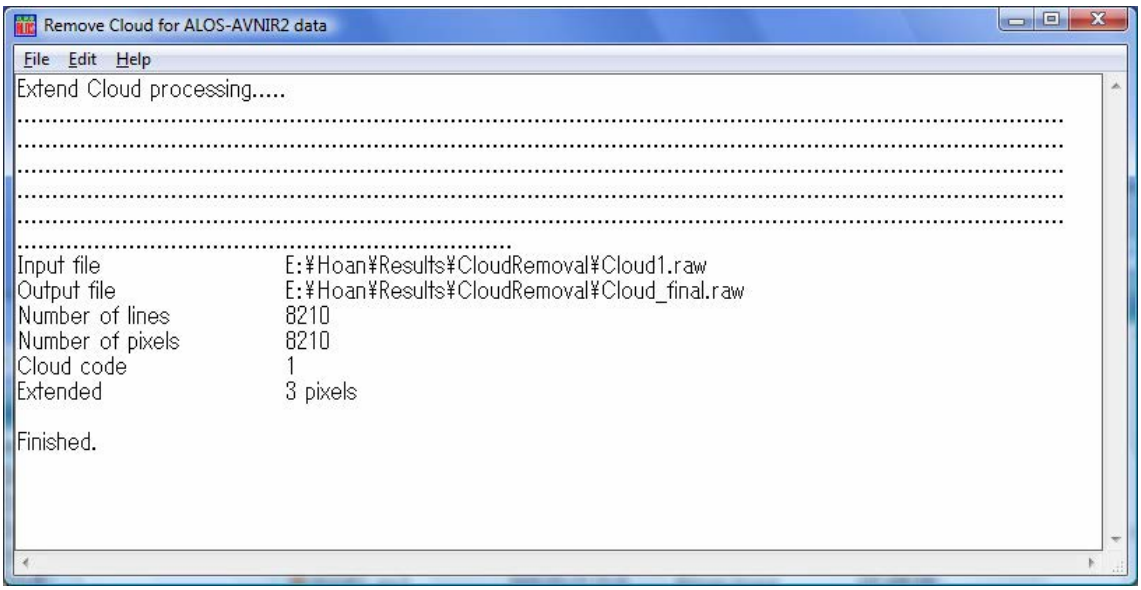

Figure 3.16: Main window and output screen of the Cloud Removal Program

Input images are in RAW format without header. This information is written in the About window of the program as shown in Figure 3.17.

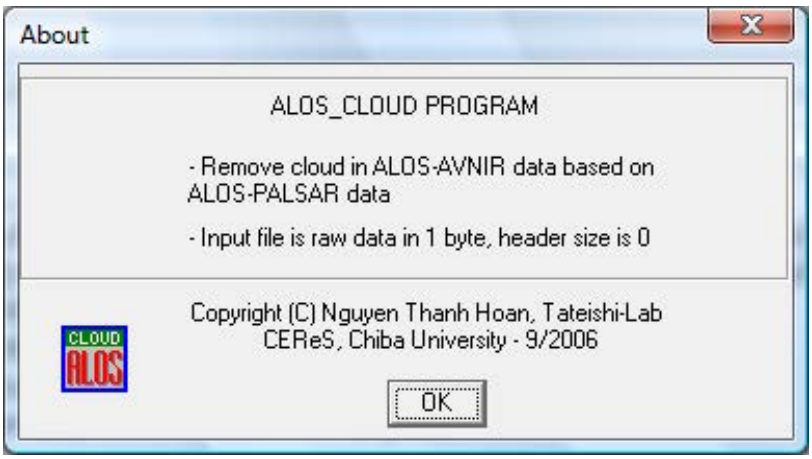

Figure 3.17: About window of the Cloud Removal Program

The Cloud Removal Program will be experimented on the simulated ALOS data, ASTER data, Landsat/ETM data, and finally applied for real ALOS data. These experiment result will be presented in the next sections.

3.4.1. On simulated ALOS data

The result is a cloud free and shadow free image. Interpolated image is compared with the original image (before overlaid by cloud) by visually. The result looks very good as Figure 3.18.

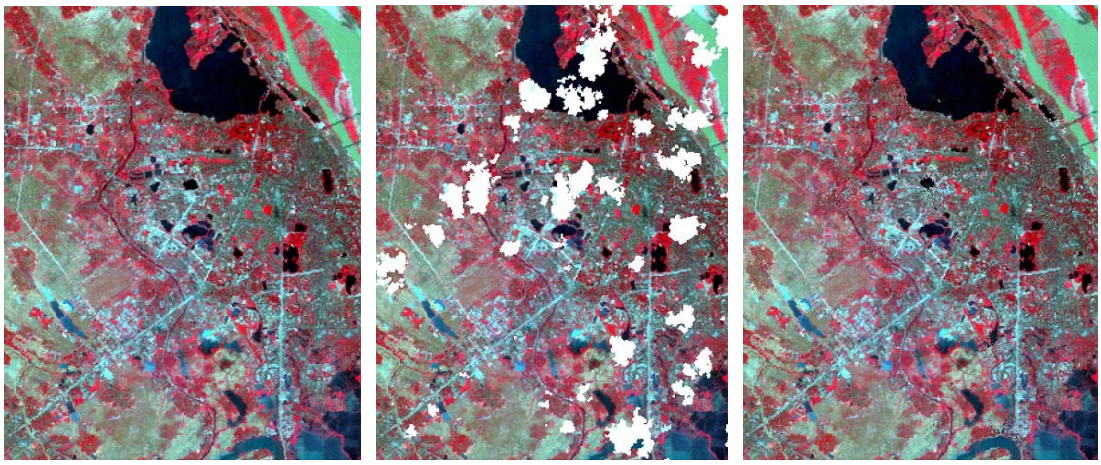

(*a*) (*b*) (*c*)

Figure 3.18: Comparison of original and interpolated image; (*a*) Original image, (*b*) Cloud image, and (*c*) Interpolated image

However, some objects in some parts have some mistakes. Comparison of red object (inside the yellow circle in Figure 3.19) in the interpolated image and original image is not the same together. Shape of these objects in original image is very clear, but shape of them in interpolated image is not clear. This problem is shown in Figure 3.19.

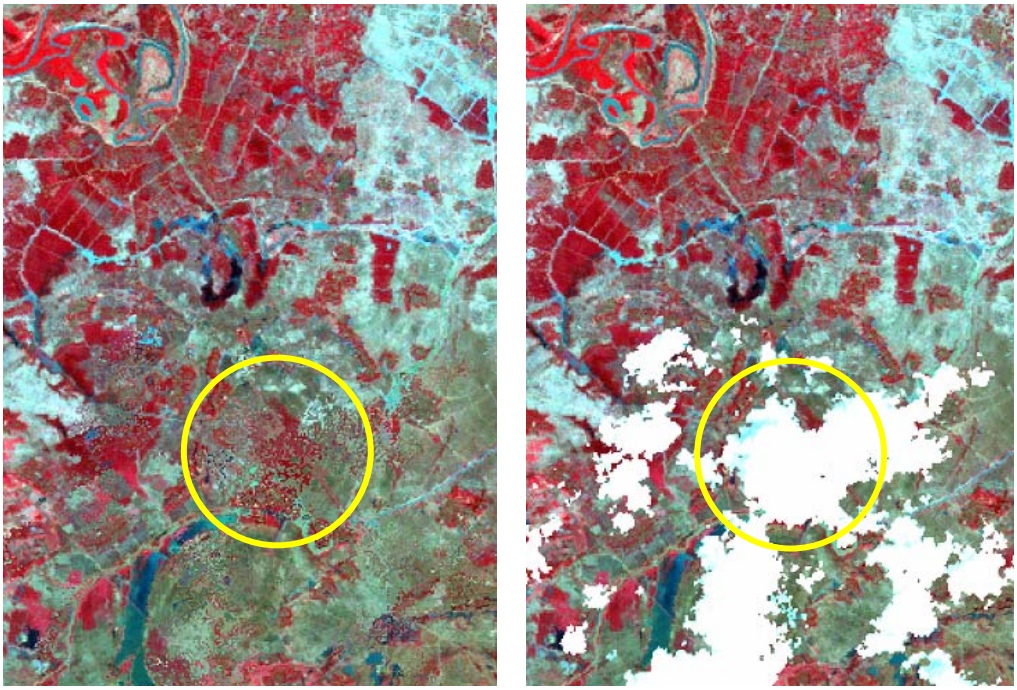

(*a*) (*b*)

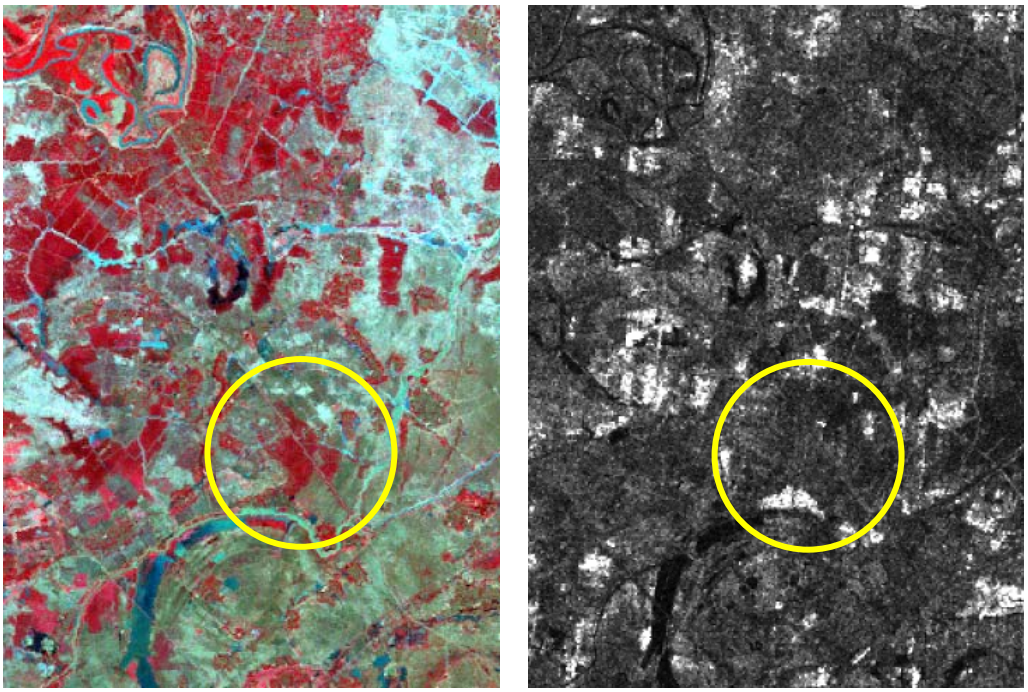

(*c*) (*d*)

Figure 3.19: Problems of interpolated image; (*a*) Interpolated image, (*b*) Cloud image, (*c*) Original optical image, and (*d*) radar image

This object was checked in radar image but that cannot be determined by radar image from around objects. This problem may be because of radar image (backscatter is the same with around objects) or change of the object (radar image and optical image are different 6 days). This checking is illustrated in Figure 3.19.

These objects were already confirmed by local native farmers. That is one type of vegetable. Height of this vegetable is about 20-30cm. It covers nearly 100% of land. Maybe, it looks like a flat surface by radar L-band. In Figure 3.19, the big vegetable fields can be seen very clearly in the left-top corner of optical image (red color), but they cannot be determined by JERS-1/SAR images. Therefore, cause of radar image (can not separate this object by radar image) is higher probability than cause of change of object. So, interpolation of under cloud data based on radar image will be not so good at some special objects like that. However, by using combination of threshold level (a value) for radar image and searching the nearest pixel to interpolate cloud pixel, the result will have more information than using threshold of whole radar image and cloud optical image independently.

3.4.2. Cloud removal of ASTER image based on Landsat/ETM image

This Cloud Removal program also can be applied for combination of two optical images to remove cloud if the change of objects is not so much. By the same way, cloud was gotten from another image to overlay on ASTER image date 2001/11/16. The NDVI of Landsat/ETM image date 2000/11/04 was used instead of radar image. Interpolated image is compared with original image by visually. Result is very good. Almost there are no change between interpolated result and original ASTER image. An illustration is shown in Figure 3.20.

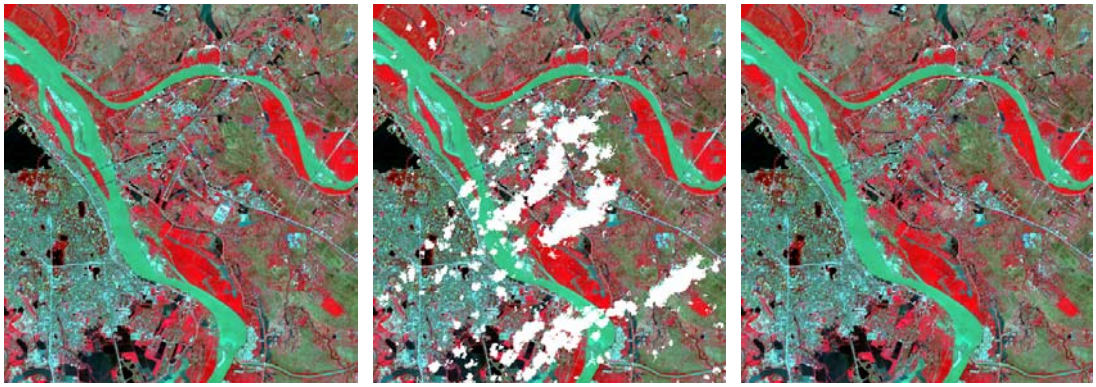

(*a*) (*b*) (*c*)

Figure 3.20: Removing Cloud of ASTER image date 2001/11/16; (*a*) Original image, (*b*) Cloud image, and (*c*) Interpolated image

By this way, many types of different optical images can be combined together to remove cloud. It can be used to make a series of cloud free multi-temporal data from many types of satellite data for studies about monitoring the change in environment and natural resource.

3.4.3. Combination of two Landsat/ETM images

Here is another application of the Cloud Removal Program. Two Landsat/ETM images date 2002/01/05 and 2001/02/03 were used. Both of them have clouds. These two images can be combined together to make two cloud free images. In this case, wavelengths of two images are the same together. So, interpolation is done based on band by band. That means using band 1 to interpolate for band 1, band 2 to interpolate for band 2, band 3 to interpolate for band 3 and so on. The first, cloud parts in the image date 2001/02/03 were removed based on the image date 2002/01/05. The result is shown in Figure 3.21.

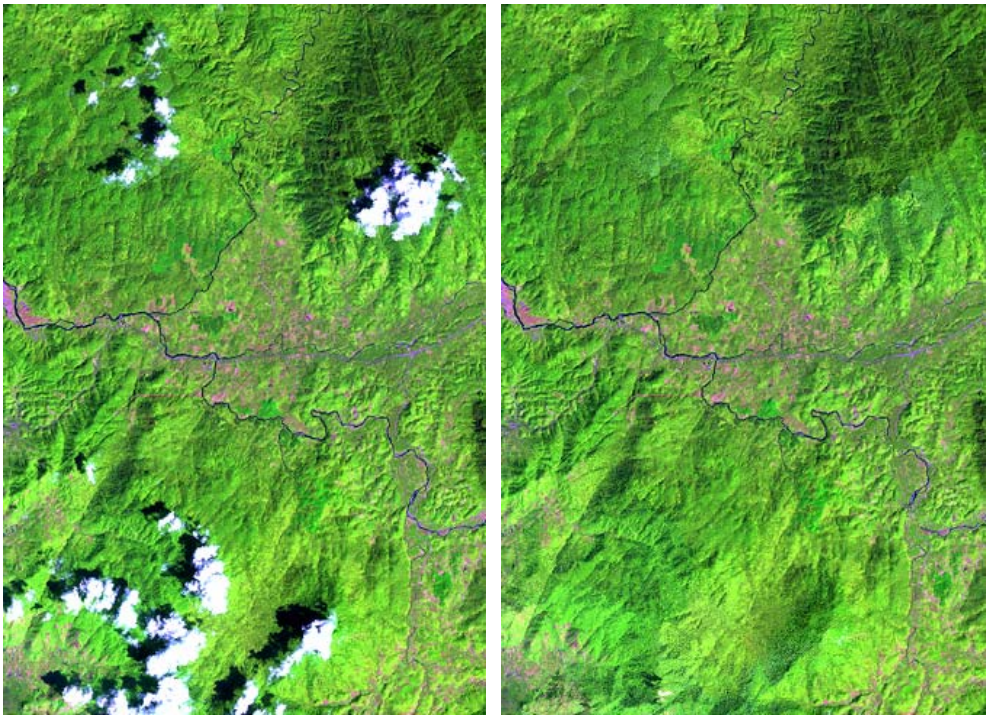

(*a*) (*b*)

Figure 3.21: Removing cloud from Landsat/ETM image on 2001/02/03; (a) Cloud image and (b) interpolated image

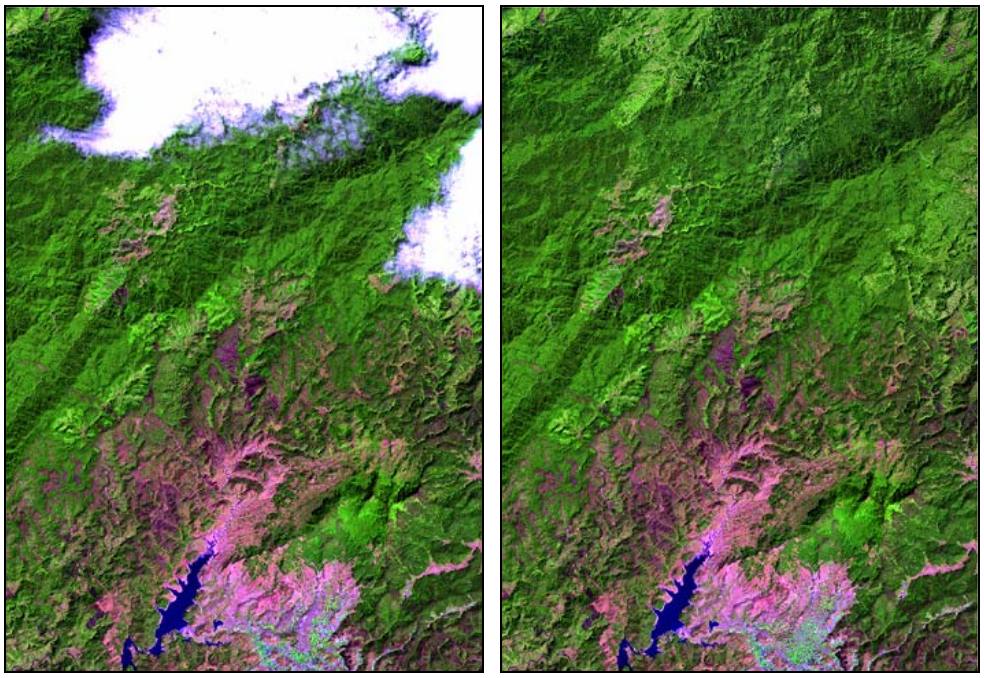

(*a*) (*b*)

Figure 3.22: Removing cloud from Landsat/ETM image on 2002/01/05; (*a*) Cloud image and (*b*) interpolated image

By the same way, cloud parts in the image date 2002/01/05 were removed based on the image date 2001/02/03. The result is shown in Figure 3.22.

Result shows as two cloud free images. These images are really perfect results. Every object in the interpolated images looks very natural and logical. If spatial change of objects covered by cloud is not so much, this method is perfect way for removing cloud to make a multi-temporal dataset for one type of data or for the types of data that have similar wavelengths.

3.4.4. Applying the Cloud Removal Program for real ALOS data

- *The first step - Defining cloud:* The Define Cloud function of the Cloud Removal Program was used to extract cloud in the ALOS/AVNIR-2 image as presented in the section 3.3.1 but it is not very successful. The input parameters for this program were estimated as shown in Figure 3.6. Because of calibration of ALOS/AVNIR-2 data, DN values of some objects become 255 (top value of 8bits data as ALOS/AVNIR-2 image) in some bands, including thick clouds and some parts of dry bare land, dry sand. Therefore, they cannot be separated together by the defining cloud method. In this case, the some parts of dry bare land and dry sand that confused with clouds were separated from clouds by manually.
- *The second step - Refining cloud:* The cloud extracted from the first step includes some single pixels. That almost is error as explained in the section 3.3.2. The Remove Single Pixels function was used to solve this problem. Result is good, every single pixels were already removed. Input parameters for this processing is shown in Figure 3.8
- *The third step - Getting shadow:* The result of the second step is input data for this step. The Getting Shadow function of the Cloud Removal program was used.

Direction of shadow was determined as West-North and average distance from cloud to shadow was estimated as 12 pixels (Figure 3.10). This function worked well, and shadows of clouds were already gotten.

- *The fourth step - Extend cloud and shadow:* Boundary of cloud cannot be extracted by the Define Cloud function as presented in the section 3.3.2 (Refining cloud). And shadows interpolated from clouds cover not fully real shadows as presented in the section 3.3.3 (Getting shadow). Both problems were solved by the Extend Cloud function of the Cloud Removal Program. Input parameters for this function are shown in Figure 3.12. The program worked well. Clouds and shadows were already extended to cover all boundary of clouds and real shadows.
- *The fifth step - Interpolating to remove cloud and shadow:* This is the most important step. Currently, this processing cannot be found in any other software. The Remove Cloud function of the Cloud Removal Program was used to interpolate values for under cloud and shadow pixels. This processing was presented clearly in the section 3.3.4 (Interpolating to remove cloud). Input parameters for this processing are shown in Figure 3.15. Where, radar data is the ALOS/PALSAR single-polarized image after applying FROST filter method by window size 5x5 pixels as presented in the section 2.1 (Data acquisition).

Final result of above processing is a cloud free and shadow free image of ALOS/AVNIR-2 as shown in Figure 3.23.

As a whole, the result is good. The under cloud pixels after interpolation look smooth and natural by visually. More detail, some parts were zoomed in and checked by classification result. In Figure 3.24, the main objects covered by clouds and shadows are forests and some water. These objects look good in the interpolated image (after cloud removal) and in classification result.

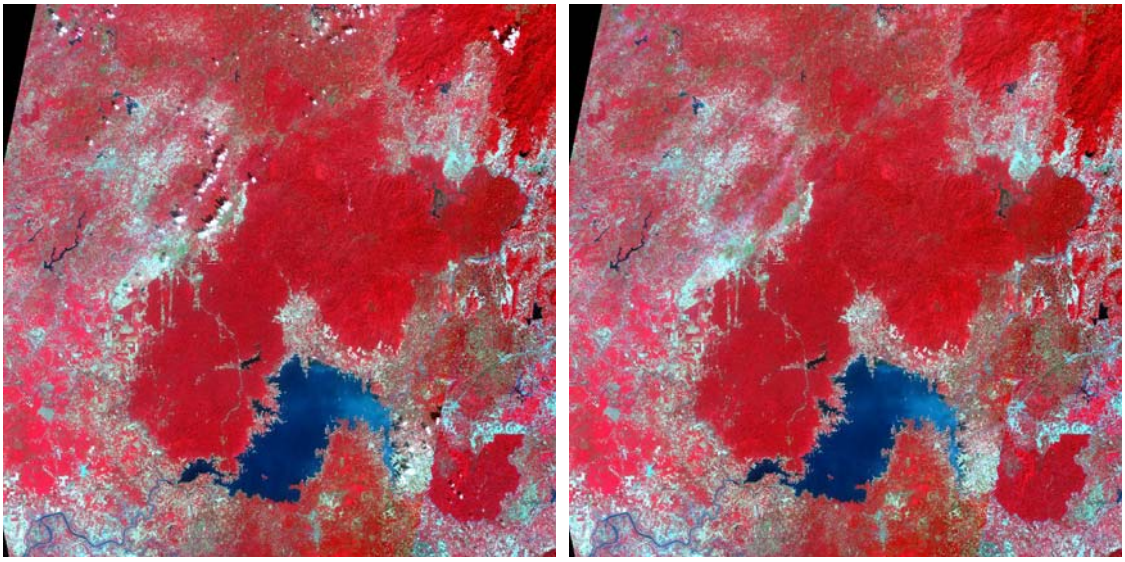

(*a*) (*b*)

Figure 3.23: ALOS/AVNIR-2 image, (a) before cloud removal and (b) after cloud removal (Color composite: R-NIR; G-Red; B-Green)

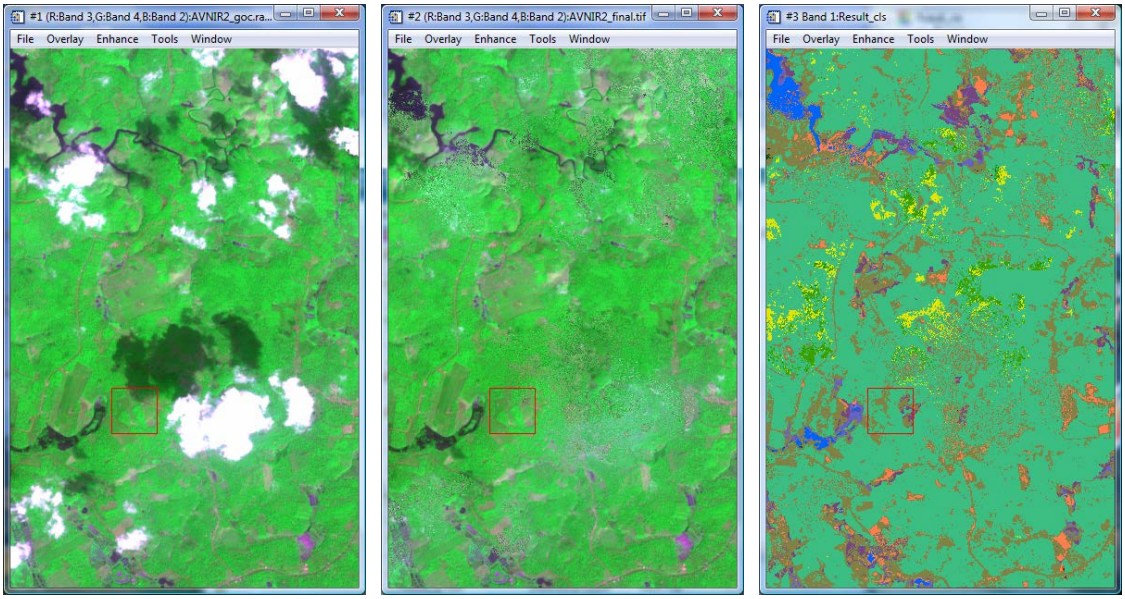

(*a*) (*b*) (*c*)

Figure 3.24: Water and forest in cloud removal result of ALOS/AVNIR-2 image, (*a*) before cloud removal, (*b*) after cloud removal, and (*c*) classification result (Color composite: R-Red; G-NIR; B-Green)

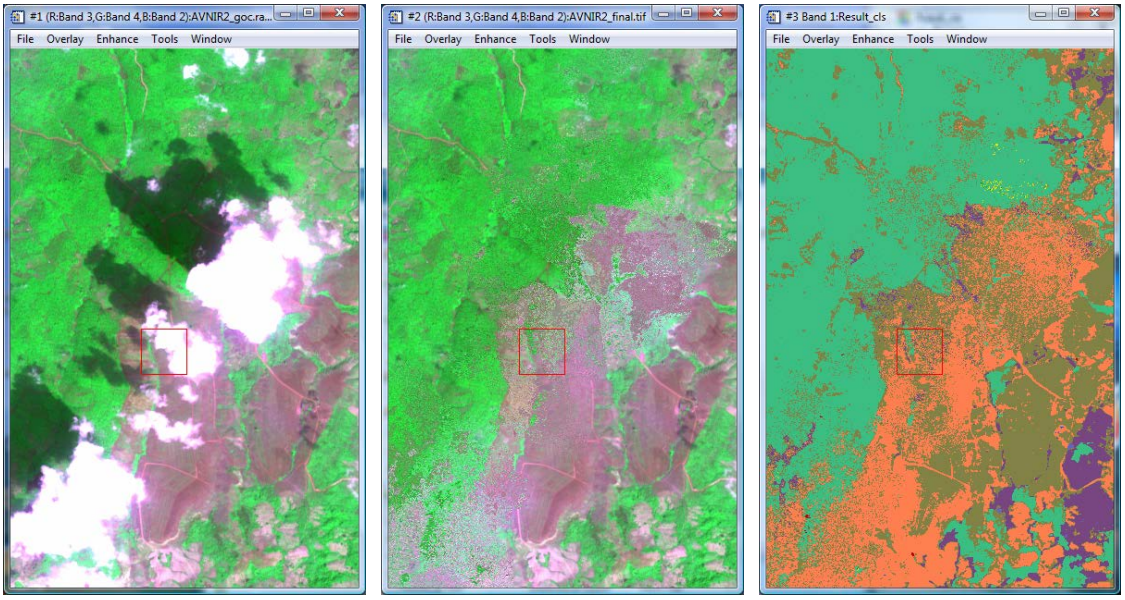

(*a*) (*b*) (*c*)

Figure 3.25: Cropland and forest in cloud removal result of ALOS/AVNIR-2 image, (*a*) before cloud removal, (*b*) after cloud removal, and (*c*) classification result

(Color composite: R-Red; G-NIR; B-Green)

In Figure 3.25, the main objects covered by clouds and shadows are forest, some croplands and grass land. The result looks good at the center part of the image (that is boundary of forest and grass land). But it looks not very good at the place that is boundary of cropland and grass land (the clouds in the left-bottom corner of Figure 3.25). This situation is the same as the problem presented in the section 3.4.2 (On simulated ALOS data - Figure 3.19) because the radar image L band cannot separate some types of land cover like cropland, grass land and bare land together. Therefore, cloud removal result should be not good at the parts that are boundaries of those objects.

3.5. Conclusions

Combination of TRRI index and CSI index to define cloud showed a good result. This

method can be applied for every multi-spectral optical image to extract cloud.

Shadow interpolated from cloud will be larger than real shadow. It is one of limitations of the Cloud Removal Program

Result image after removing cloud based on radar image is good, no cloud and shadow. Distribution of objects under cloud and shadow after interpolation processing almost is good, smooth and natural by visually. However, some parts are not so good after interpolation if they are boundaries of some types of vegetable, cropland, grass land and bare land.

Combination of two optical images to remove cloud is good way to make cloud free multi-temporal dataset. Condition to apply this method is satisfied when the change of objects that covered by clouds and shadows are not so much.

Final result of this section is a program with many functions like: define cloud, extend cloud, get shadow, remove cloud and so on. This is free software for every one.

CHAPTER 4

COMBINATION OF OPTICAL AND MICROWAVE DATA OF ALOS FOR TROPICAL FOREST MAPPING

In whole the year 2007, only one-time good quality images of ALOS/AVNIR-2 were observed in the study area. These images are not enough to describe phenology of land cover objects for forest mapping. Therefore, they cannot separate between forests and growing paddy/croplands and so on. Radar data can get information of forest structure which cannot be collected by optical images. Radar sensor can collect image many times in one year because it is not affected by weather condition. This section will present a method for combination of **single-temporal** ALOS/AVNIR-2 image and **multi-temporal** ALOS/PALSAR images for tropical forest mapping.

4.1. Forest classes definition

The forest classes were mainly determined after visual interpretation of the ALOS/PRISM sharpen image, 2.5 meter spatial resolution. In addition, other concerned documents were used as references including: National Forest Inventory - Field Manual (FAO 2004), the Forest Vegetation of Vietnam (Vietnamese, Thai Van Trung 1997), Vegetation and Special Vegetation of Forest (Vietnamese, Chan and Dung 1992), and the Vietnam Forest Map 2005. The initial number of categories visually discriminated was 16, but some classes were found very similarly in digital processing products (by unsupervised classification - Kmean method). Finally, eleven classes were used for tropical forest classification in the study area, in which, there are five classes of forest as shown in Table 4.1.

Table 4.1: Physiognomic and structural forest types within the Cat Tien national park and surrounding areas in southern part of Vietnam

Class name (color: R, G, B)	Description
1. Primary forest (0,60,0)	Undisturbed Broad-leaf evergreen and semi-deciduous forest stands. Canopy closure is more than 60% by high trees
2. Degraded forest (60,160,0)	Forest areas with a considerable human disturbance. These areas might include forest growing back from clear-felling, resulting from either shifting cultivation of logging (secondary forest) or areas affected by pronounced selective logging. Canopy of high trees is usually small and canopy closure of high trees is less than 30%
3. Bamboo (230,230,0)	Areas dominated by bamboo. The term bamboo refers to old, naturally occurring bamboo areas as well as to second growth bamboo following clear-felling.
4. Mixed forest (0,120,0)	Mixture of high trees, bamboo and shrubs. These areas are almost affected by selective logging. Canopy of trees is still big but sparse. Canopy coverage of high trees is about from 30-60%
5. Planted forest (60,190,130)	The forest is planted by reforestation projects, rubber forest and so on
6. Shrub & Grass (255,127,80)	Areas dominated by shrub, bushes or grass reaching a

	height less than 5m.
7. Mosaic (130,130,70)	Mixture of natural vegetation and cropland, or family gardens
8. Paddy/Cropland (120,70,130)	Paddy fields or croplands
9. Built-up (200,0,0)	Urban, high density residential areas or built-up areas
10. Wetland (100,100,200)	Swamps covered by some types of herbaceous
11. Water (0,100,250)	Water bodies

* Hence, the color table as shown in Table 4.1 will be used for all classification results.

4.2. ALOS/AVNIR-2 classification

Forest mapping and land cover mapping from remote sensing images are usually performed using either supervised or unsupervised techniques. In classification, there are two types of classes that need to be distinguished: user classes and spectral classes. User classes are those categories of interest that the analysis is actually trying to identify in the imagery. In contrast, spectral classes are groups of pixels that are uniform with respect to their brightness values in the different spectral channels of the data. Actually, rarely there is a simple one-to-one match between these two types of classes. In addition, spectral classes are always more detailed then user classes. In this study, to determine ability of ALOS/AVNIR-2 images in tropical forest mapping, all main spectral classes were used as training data to estimate user classes. The first step, unsupervised classification (K_mean) method was used to divide image to 60 spectral classes. Each

class of the spectral classes was compared with PRISM-sharpen image and other reference data like local forest map 2005 and Tree-Height map to determine that belong in which user class name. The user classes are defined in Table 4.1. Only main spectral classes that are easy to determine user class name and cover large areas were used. Subsequently, 30 spectral classes were already chosen. Other spectral classes are very small or difficult to determine user class name. The 30 chosen classes as shown in Figure 4.1(*a*) will be used as training data for supervised classification technique to make tropical forest map.

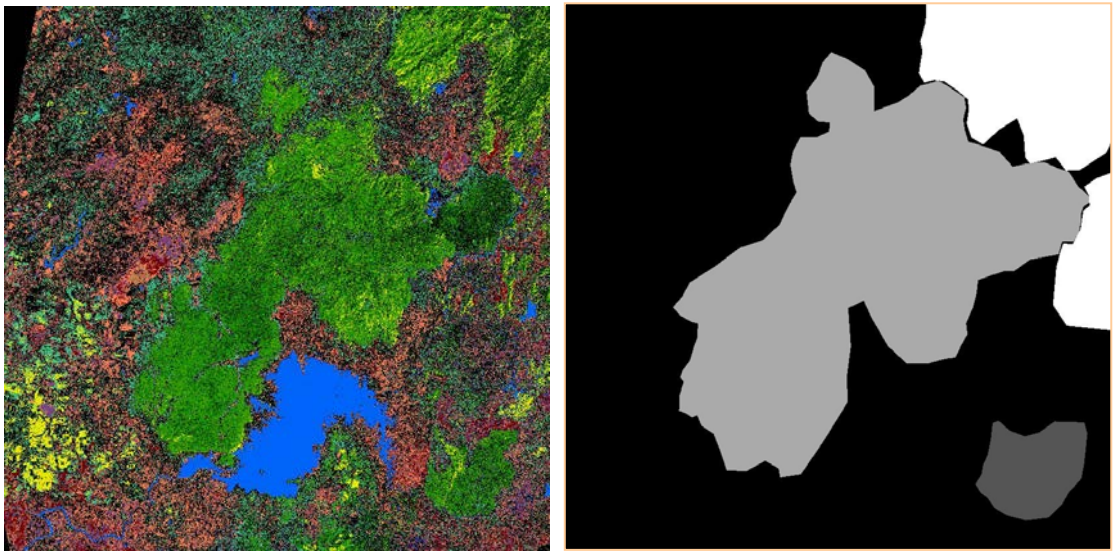

(*a*) (*b*)

Figure 4.1: (*a*) the 30 main classes of unsupervised classification result; and (*b*) the simple manual mask of natural forest

One of the most important purposes of this study is to discriminate planted forest and natural forest. However, clustering spectral classes of ALOS/AVNIR-2 image using K_mean method was not successful for this purpose. Thus, discrimination will be tried one more time by supervised techniques. To separate planted forest and natural forest for training data, one simple mask was drawn manually for the main locations of natural forest (Figure 4.1(*b*)). All planted forests inside of this mask were deleted, while natural forests outside of this mask were converted to a new planted forest class.

Therefore, total of 31 classes were used as training data for supervised classification to represent for 9 user classes as shown in Table 4.1 without paddy/cropland and built-up area. Because paddy/cropland and built-up area are confused totally with forests and other land cover types, so they have no training data for supervised classification. They will be estimated later by ALOS/PALSAR data.

Single pixel is usually the error of the classification result. The boundary of two objects always includes pixels that are mixture of the two objects. They have not specific reflectance value of any object and they were usually considered as errors in the classification result. In this study, to get good training areas, all single pixels were removed. The Remove Single Pixels function of the Cloud Removal Program (as presented in the section 3.3.2) was used to solve this problem. As a result 31 classes without single pixels were used as training areas for classifying ALOS/AVNIR-2 image by Maximum Likelihood method (Figure 4.2(*a*)).

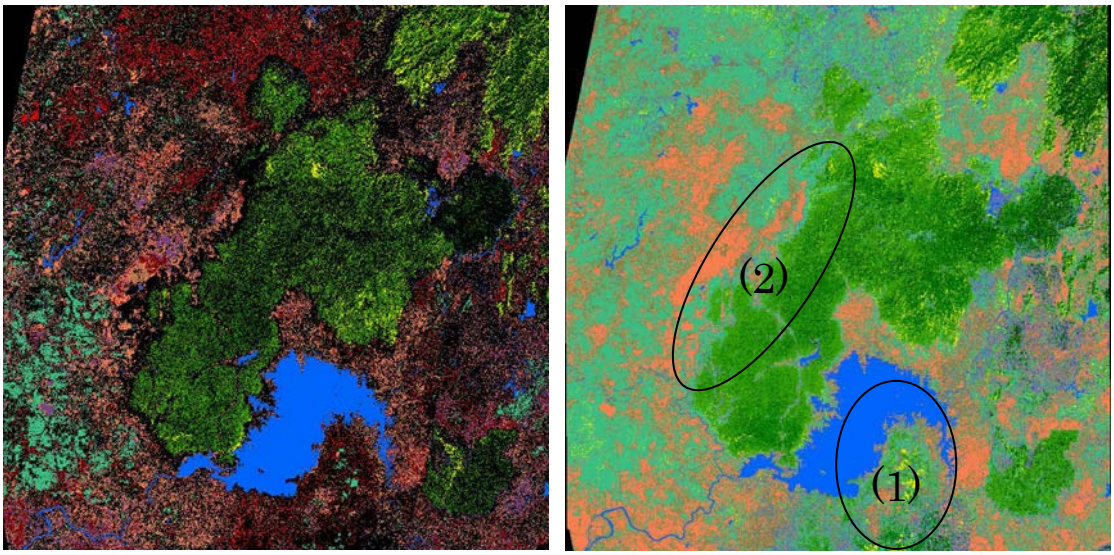

(*a*) (*b*)

Figure 4.2: (*a*) The 31 classes of unsupervised classification method used as training data for supervised classification, and (*b*) Classification result of ALOS/AVNIR-2 image by Maximum Likelihood method

Figure 4.2(*a*), illustrated the new planted forest class in a red color while black color is

the unused pixels and other colors are shown in Table 4.1. The classification result is shown in Figure 4.2(*b*).

Figure 4.2(*b*) shows some examples that Maximum Likelihood method also cannot discriminate between planted forest and natural forest from ALOS/AVNIR-2 image: one example presented in the region (1), which is a location of planted forests but there are many natural forests in the classification result; on the other hand in the region (2), many natural forests become planted forest in the classification result. There are many similar mistakes in other places.

The observed time of the ALOS/AVNIR-2 image is in the growing season of paddy/croplands in the study area. Single-temporal ALOS/AVNIR-2 images also cannot separate between forests and growing paddy/croplands. Figure 4.3 is an example.

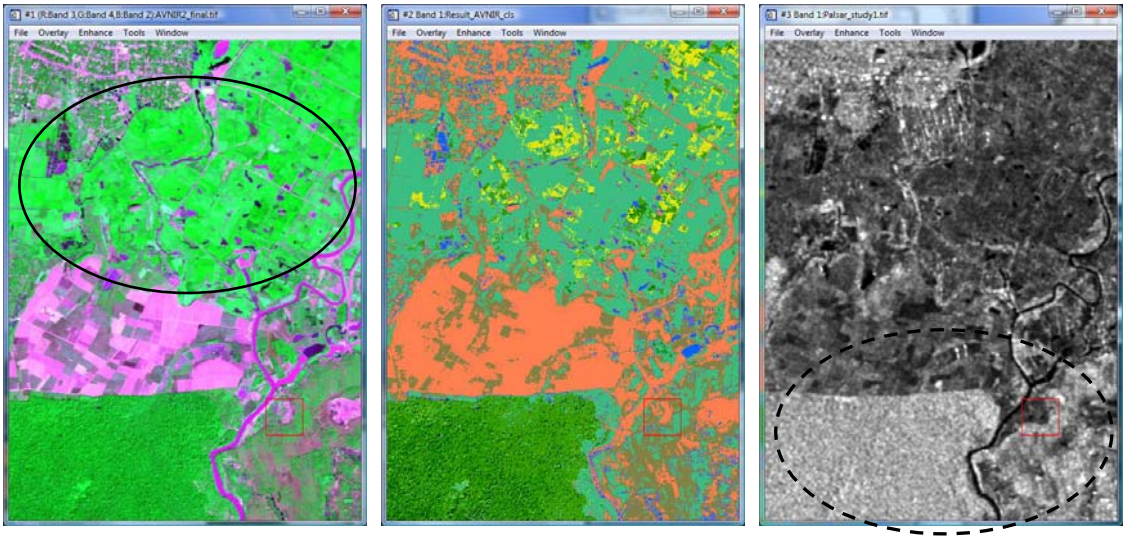

(*a*) (*b*) (*c*)

Figure 4.3: Confusion of paddy/croplands and forests in ALOS/AVNIR-2 classification result, but that can be separated clearly in PALSAR image by visually, (*a*) AVNIR-2 image (R-red, G-NIR, B-green), (*b*) classification result, and (*c*) PALSAR image

In Figure 4.3(*a*), the black ellipse is a place of paddy/cropland, but in classification result from ALOS/AVNIR-2 image (Figure 4.3(*b*)), paddy/cropland almost becomes planted forest, bamboo or other forest types. At the same time in Figure 4.3(*c*), the black

ellipse (dashed line) is a location of forests in PALSAR image, they are easy to be separated with the paddy/cropland area in the radar image by visually. In addition, some other land cover types like built-up also cannot be discriminated from others by ALOS/VNIR-2 image, but it can be separated easily by ALOS/PALSAR image as shown in Figure 4.4.

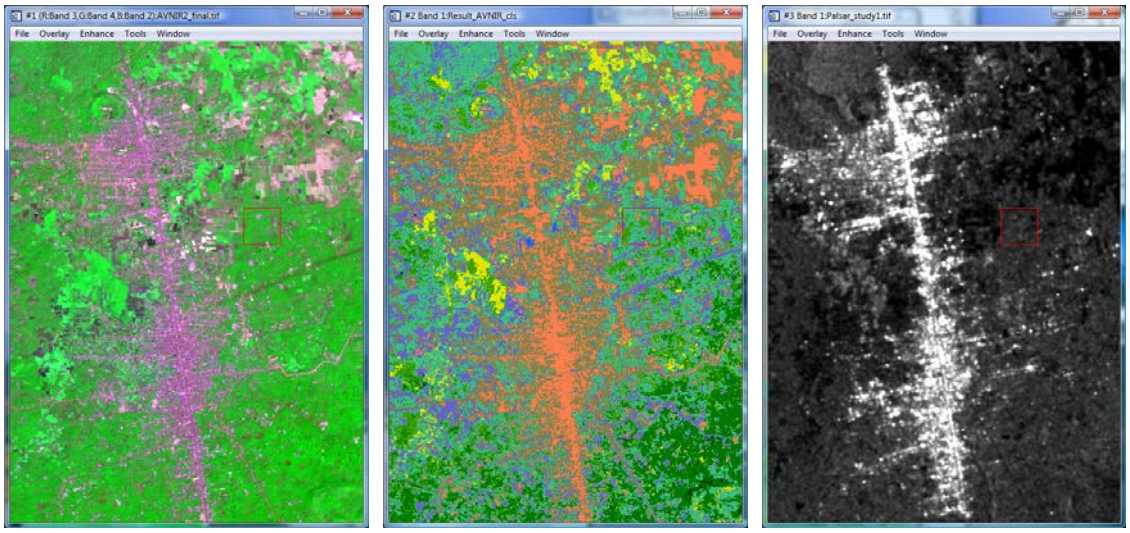

(*a*) (*b*) (*c*)

Figure 4.4: Confusion of built-up and others in ALOS/AVNIR-2 classification result, but that can be separated clearly in ALOS/PALSAR image by visually, (*a*) AVNIR-2 image (R-red, G-NIR, B-green), (*b*) classification result, and (*c*) PALSAR image

From the analyses above, it can be concluded that using ALOS/AVNIR-2 image (single-temporal) cannot separate between planted forest and natural forest, between forest and growing paddy/cropland, between built-up area and some other land cover types. ALOS/PALSAR data will be used to solve these problems.

4.3. ALOS/PALSAR analysis

The interest in using radar remote sensing for monitoring forest cover raises from the

two assets of radar data. The first, radar can provide information related to the canopy volume, which cannot be collected by other means. The other advantage of radars is the possibility to acquire data over areas with frequent cloud or haze coverage as tropical regions (Thuy Le Toan et al. 2001). In this study, radar data were used for two purposes: the first, to separate forests and growing paddy/croplands that cannot be separated by single-temporal optical image; and the second, to discriminate planted forest and natural forest by analyzing structure of forest.

According to Alvin Wong (Alvin Wong et al. 1997), there are four main scattering mechanisms of radar as shown in Figure 4.5.

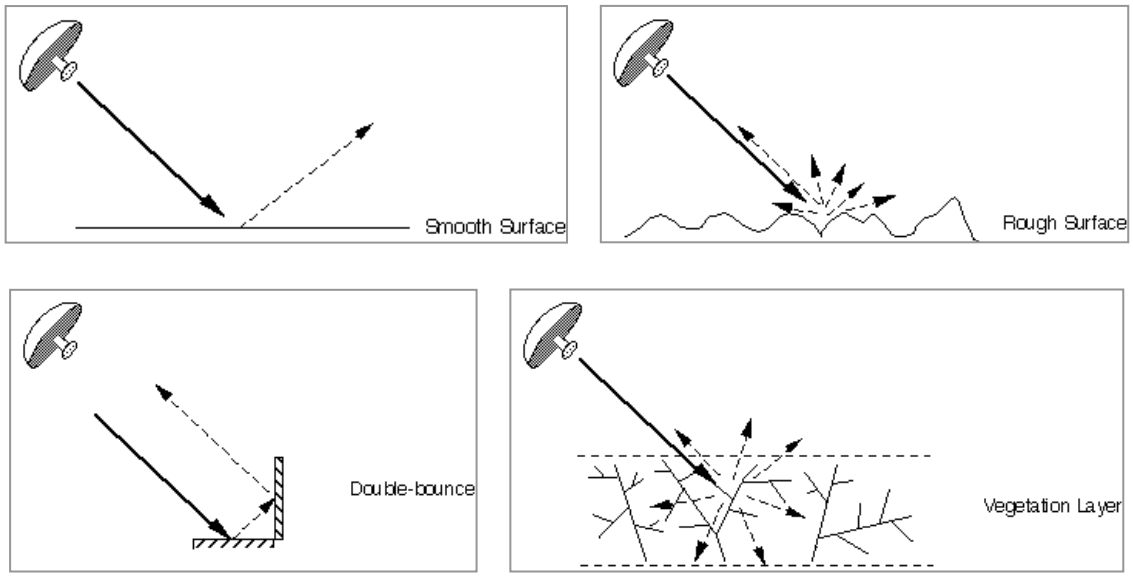

Figure 4.5: The four main scattering mechanisms of radar

Where, backscatter in the scattering mechanism of "Smooth Surface" is the weakest. Backscatter in the scattering mechanism of "Double-bounce" is the strongest. These scattering mechanisms will be used to analyze the differences of the interested objects in the next sections.

4.3.1. Discrimination of planted forest and natural forest

[AVNIR-2] 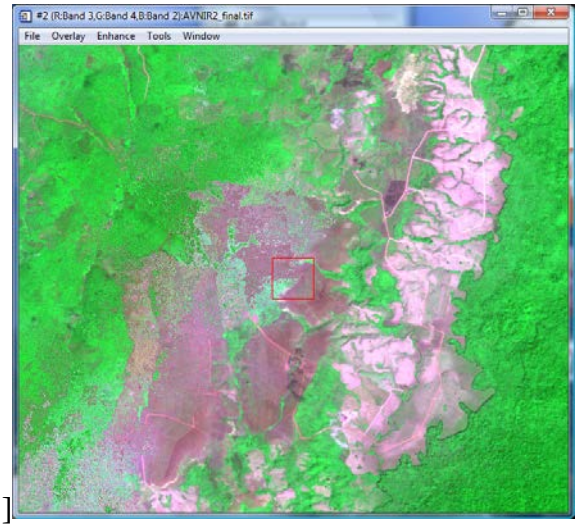

[HH] 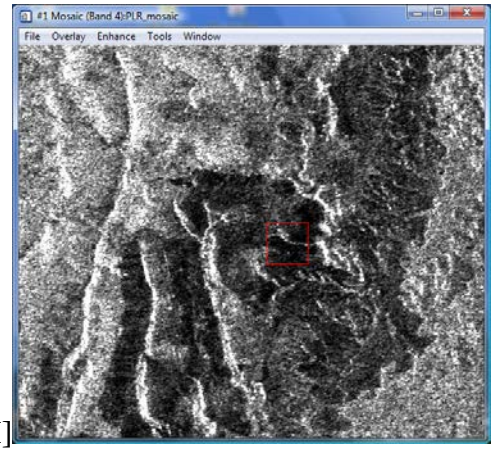

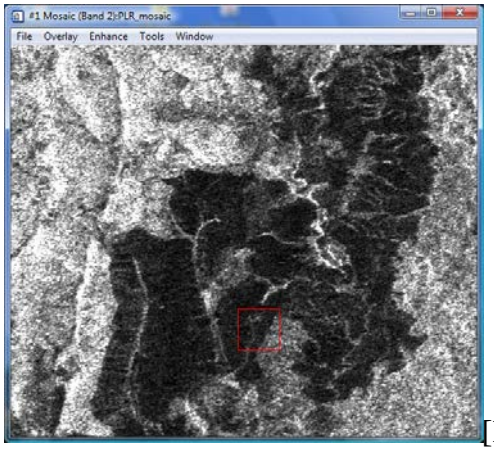

[HV]

[VV] 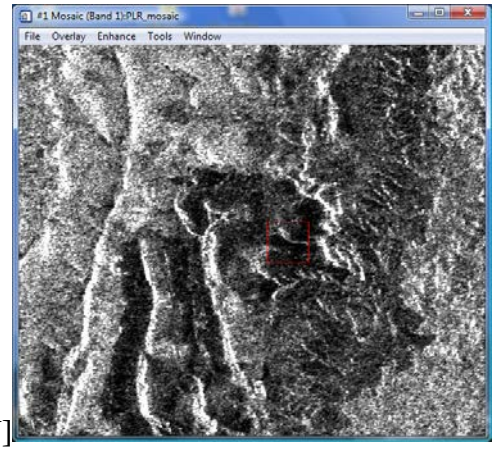

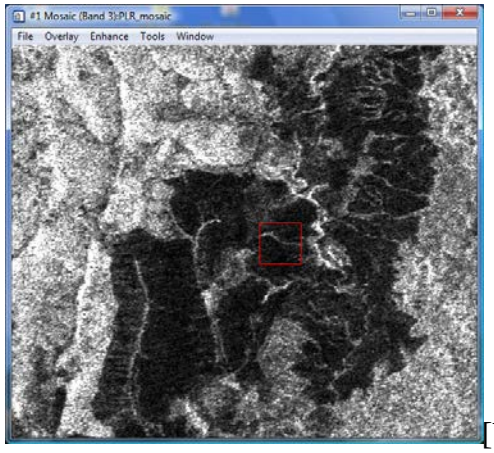

[VH]

Figure 4.6: Difference of polarizations between natural forest and planted forest, between forest and non-forest

Figure 4.6 shows the differences of the four polarizations of ALOS/PALSAR

multi-temporal image. Where, the left side of each image is planted forest, the right side is natural forest, and the middle part is non-forest.

By visual comparison, for separating between planted forest and natural forest, between forest and non-forest, ability of HH polarization is similar to that of VV polarization. And ability of HV polarization is similar to that of VH polarization. In addition, there are very few ALOS/PALSAR multi-temporal data in the study area as mentioned in the section 2.1. Therefore, ALOS/PALSAR dual-polarization image including HH and HV polarizations was selected to separate between tropical planted forest and tropical natural forest. ALOS/PALSAR multi-polarized images were not used in this study.

The main difference of tropical planted forest and tropical natural forest is their structure. Tropical planted forest normally has only one layer of wood tree and density of the tree is not very high (Figure 4.6). Conversely, tropical natural forest always has more than one layer of wood tree, density of the tree is usually very high and there are many branches and lianas (Figure 4.7). According to Thuy Le Toan (Thuy Le Toan et al. 2001), main scatterers of tropical natural forest are shown in Table 4.2.

Table 4.2: Main scatterers of tropical natural forest

Frequency band	X	C	L	P	VHF
Main scatterers	Leaves, Twigs	Leaves, Small branches	Branches	Branches & Trunk	Trunk

Using ALOS/PALSAR (L-band), the scattering is affected mainly by branches of trees. Meanwhile, number of branches is one of the main differences between tropical planted forest and tropical natural forest. It means that tropical planted forest and tropical natural forest can be discriminated together by ALOS/PALSAR image in theory.

Based on the scattering mechanisms, backscatter of tropical natural forest with many branches and lianas is affected mainly by the scattering mechanism of "Vegetation layer" (Figure 4.5). Figure 4.7 is two examples of typical planted forest types in the study area. The left photo is planted rubber forest and the right photo is planted pine forest. Both of them have only one layer of wood tree and almost have no shrub. Density of trees is not high and branches of trees are also not many. Therefore, backscatter of tropical planted forest should be stronger with a significant amount of the "Double-bounce" scattering mechanism (Figure 4.5), because some radar signals can go through the planted forest canopy to ground and be affected by backscatter of ground and trunks.

Figure 4.7: Two examples of planted forest, Rubber (left) and Pine (right)

Figure 4.8 is a photo of tropical natural forest and its model (This model was gotten from the website of Learning about Rainforests (MT&PK 2009)). It has many layers with many branches and lianas. Therefore, backscatter of this forest type mostly should be from branches of trees and affected mainly by the scattering mechanism of "Vegetation Layer".

(*a*) (*b*)

Figure 4.8: Tropical natural forest with many layers: (*a*) real photo, (*b*) model of tropical forest layers (four layers)

In ALOS images, differences of tropical planted forest and tropical natural forest are shown in Figure 4.9.

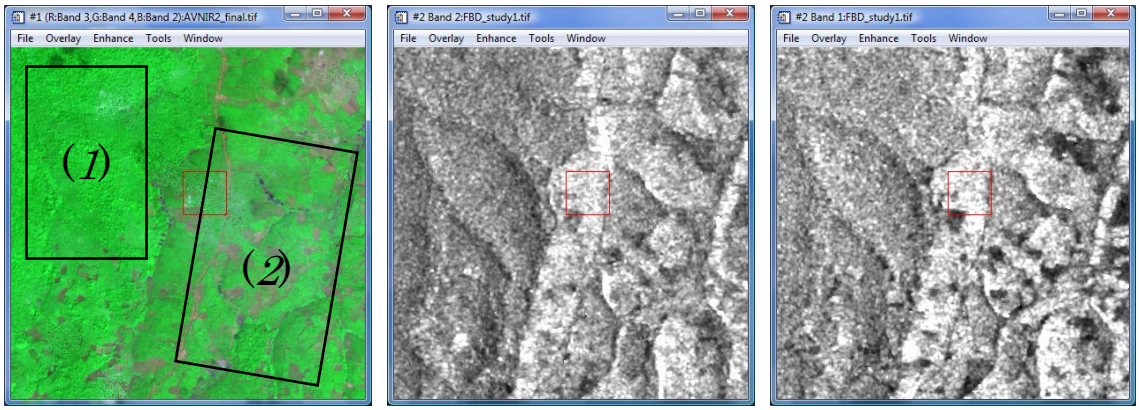

AVNIR-2 PALSAR-HH PALSAR-HV

Figure 4.9: Differences of natural forest and planted forest in ALOS images: region (1) is natural forests, and region (2) is planted forests

Where, planted forest and natural forest cannot be separated in the ALOS/AVNIR-2 image, while boundary of them can be determined in ALOS/PALSAR images by

visually. Natural forest looks darker and planted forest looks lighter. The boundary of them in HH polarization image is clearer than in HV polarization image (Figure 4.9). In this study, both polarization HH and HV were used to separate between planted forest and natural forest.

When planed forest or natural forest areas in ALOS/PALSAR images are zoomed in, they are become visible not homogeneous regions. They are mixtures of many different dots (pixels), in that case, darker dots (for natural forest) or lighter dots (for planted forest) is dominated. Consequently, these images cannot be used to classify forest types directly. To solve this problem, one filtering method is necessary to get mean values of objects and at the same time, still keep their boundaries well as possible. FROST filtering method, the best suitable, window size 15x15 was chosen (Lopes et al. 1993, Zhenghao and Fung 1994). Then, the dual-polarized image (including HH and HV) of ALOS/PALSAR was classified by unsupervised classification - Kmean method - to 20 classes. These classes were labeled to two user classes: natural forest and others. After that, every natural forest region that is smaller than 500 pixels (~5 hectares) was deleted. Finally, natural forest mask was completed as shown in Figure 4.10.

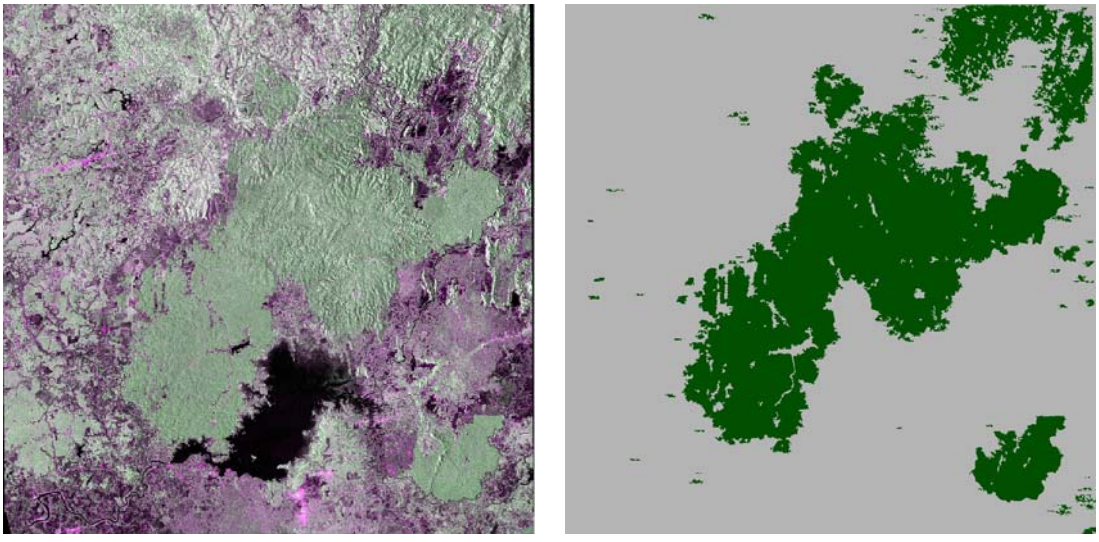

Figure 4.10: Natural forest mask (right) derived from ALOS/PALSAR dual-polarized images (left) - color composite: R-HH, G-HV, B-HH

The mistakes of planted forest and natural forest as mentioned in Figure 4.2(*b*) do not appeared in the natural forest mask. This mask will be used in combination model to make final tropical forest map as presented in the section 4.4.

4.3.2. Discrimination of forests and growing paddy/croplands

ALOS/PALSAR is SAR of L band, long wavelength. Paddy/cropland is considered like quite smooth surface by L band SAR in any season (Naoki Ishitsuka 2007), in this case, backscatter of paddy/cropland is almost affected by the "Smooth surface" scattering mechanism (Figure 4.5). This reason is due to the weakness of backscattering of paddy/croplands in ALOS/PALSAR images. Figure 4.11 is two typical types of paddy (left photo) and cropland (right photo) in the study area.

Figure 4.11: An example of Paddy (left) and Cropland (right)

Backscatters of forests are in "vegetation layer" and "double-bounce" scattering mechanisms as presented in the section 4.3.1. Therefore, backscatters of forests should be higher than that of paddy/croplands. In this study, ALOS/PALSAR single-polarized (HH) images were used to extract the paddy/cropland mask because the observed time of the single-polarized images are close to the received optical images and also it is enough to separate between forests and paddy/croplands. In addition, another reason of selecting ALOS/PALSAR single-polarization HH image is to separate Built-up and

others. As shown in Figure 4.12, ALOS/PALSAR HH polarization can separate between Built-up and others clearly, but ALOS/PALSAR HV polarization cannot.

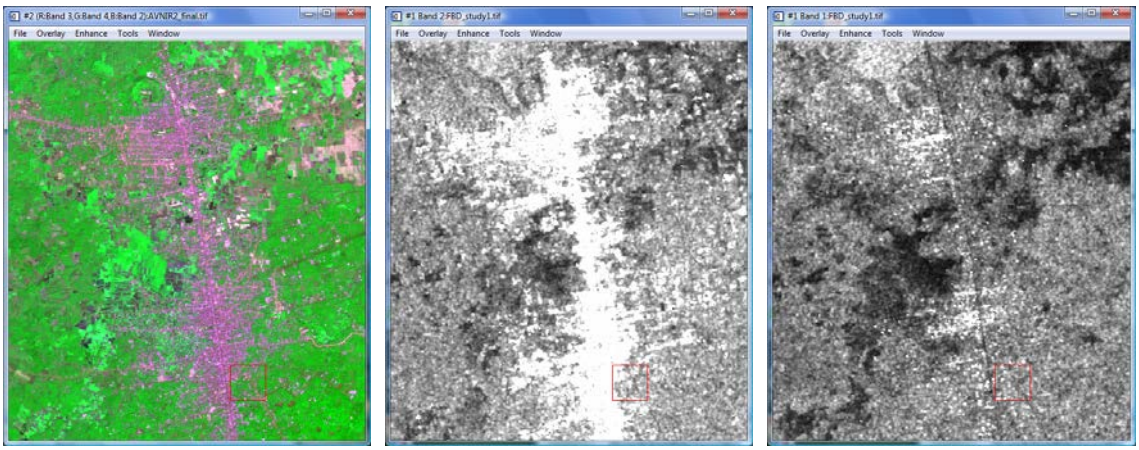

AVNIR-2 PALSAR-HH PALSAR-HV

Figure 4.12: Ability of HH and HV polarization images for separating between Built-up and Others

Level slicing method was applied to divide the ALOS/PALSAR HH-polarized image to four layers. The Built-up class is also one of them. Final result is shown in Figure 4.13, where, blue color is water and no-data, green-yellow color is paddy/croplands, red color is built-up area and grey color is other.

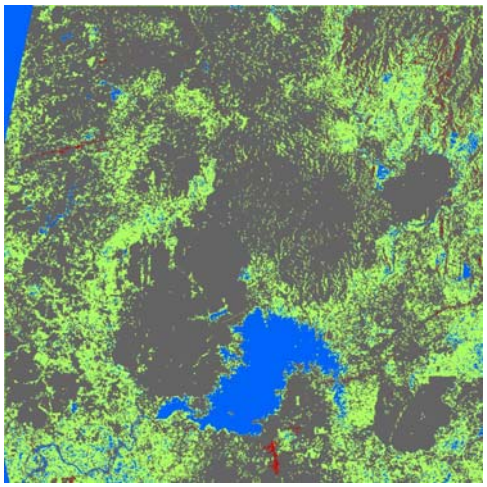

Figure 4.13: Paddy/Cropland and Built-up mask derived from ALOS/PALSAR single-polarized image

The paddy/cropland and built-up layers will be used as masks in the combination model to make final forest map.

4.4. Combination model

According to Feilong Ling (Feilong Ling et al. 2008), multi-temporal ALOS/PALSAR dual-polarization data can create accurate maps for forest in flat areas. The capability to map forest in hilly regions is still limited. Furthermore, the analyses in this study showed a similar result. Figure 4.14 is one example of terrain effects to backscatter values in ALOS/PALSAR images. One side of mountains is too light and another side is too dark. Therefore, the objects that are derived from ALOS/PALSAR images in high slope areas should have errors.

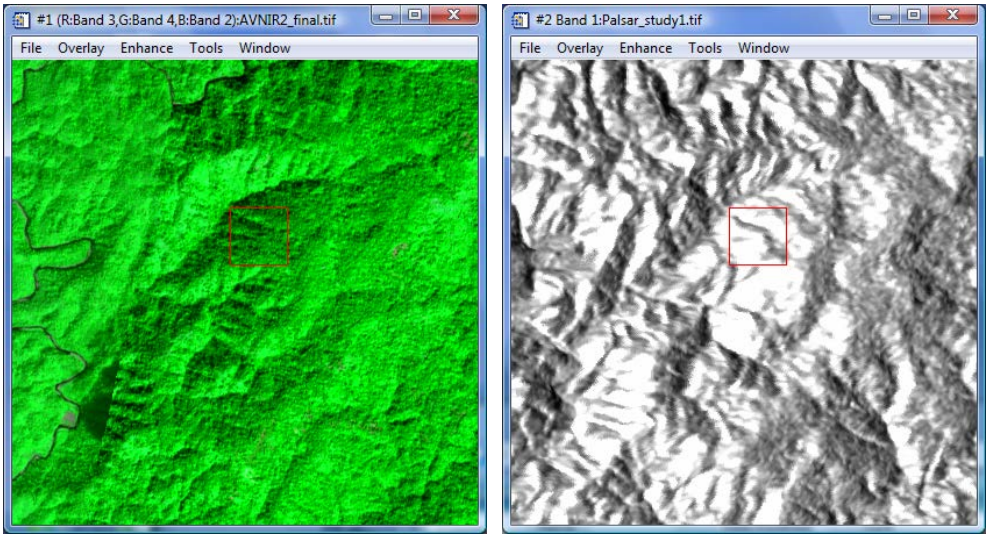

AVNIR-2 PALSAR

Figure 4.14: Effects of terrain to backscatter values of ALOS/PALSAR images

In this study, slope map developed from DEM 10 meter resolution was used to remove the high slope areas as shown in Figure 4.15. In the combination model, the areas that have slope higher than 10^{o} will be kept as ALOS/AVNIR-2 classification result.

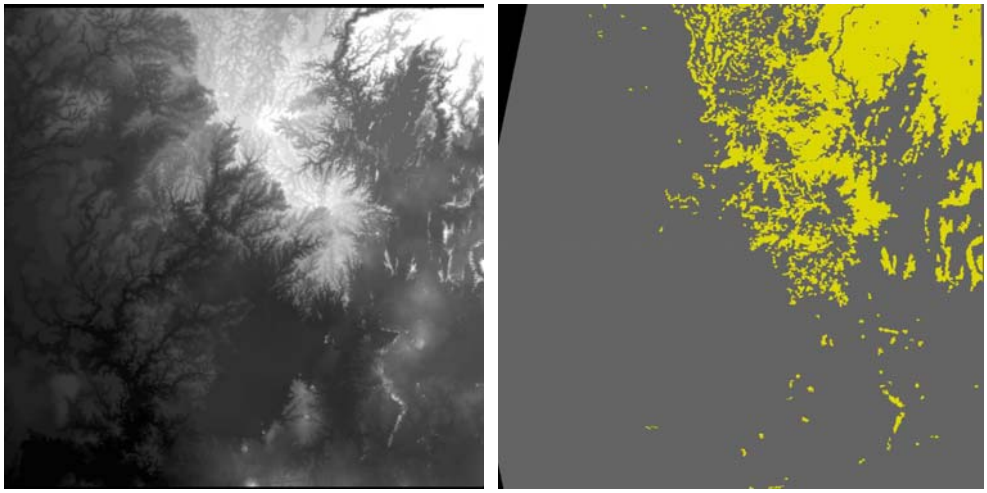

Map-DEM High Slope (>10^{o})

Figure 4.15: High slope areas (right) derived from Map-DEM (left)

Combination model was developed to combine the classification result of ALOS/AVNIR-2 (31 classes to represent for 9 classes as presented in Table 4.1 without Paddy/cropland and Built-up) with results derived from ALOS/PALSAR images and the high slope map to make final tropical forest map. This combination model was summarized in a flow chat as shown in Figure 4.16. The result classified from ALOS/AVNIR-2 image was used as a background image to combine with the natural forest mask, paddy/cropland mask and built-up mask derived from ALOS/PALSAR images for producing final tropical forest map.

In Figure 4.16, the continuous vectors present for AND condition. That means, the parameters at begin of the vectors will be used AND function to combine with other parameters. The dashed vectors present for OR condition. The parameters at begin of the vectors will be used OR function to combine with other parameters. The dashed vectors will be used in direct conversions only. That means, the parameters at begin of the dashed vectors will be used to combine with other parameters only when destination has the same class name with original class, e.g. converting from Primary F of AVNIR-2 box to Primary F of RESULT box, from Bamboo of AVNIR-2 box to Bamboo of

RESULT box, and so on.

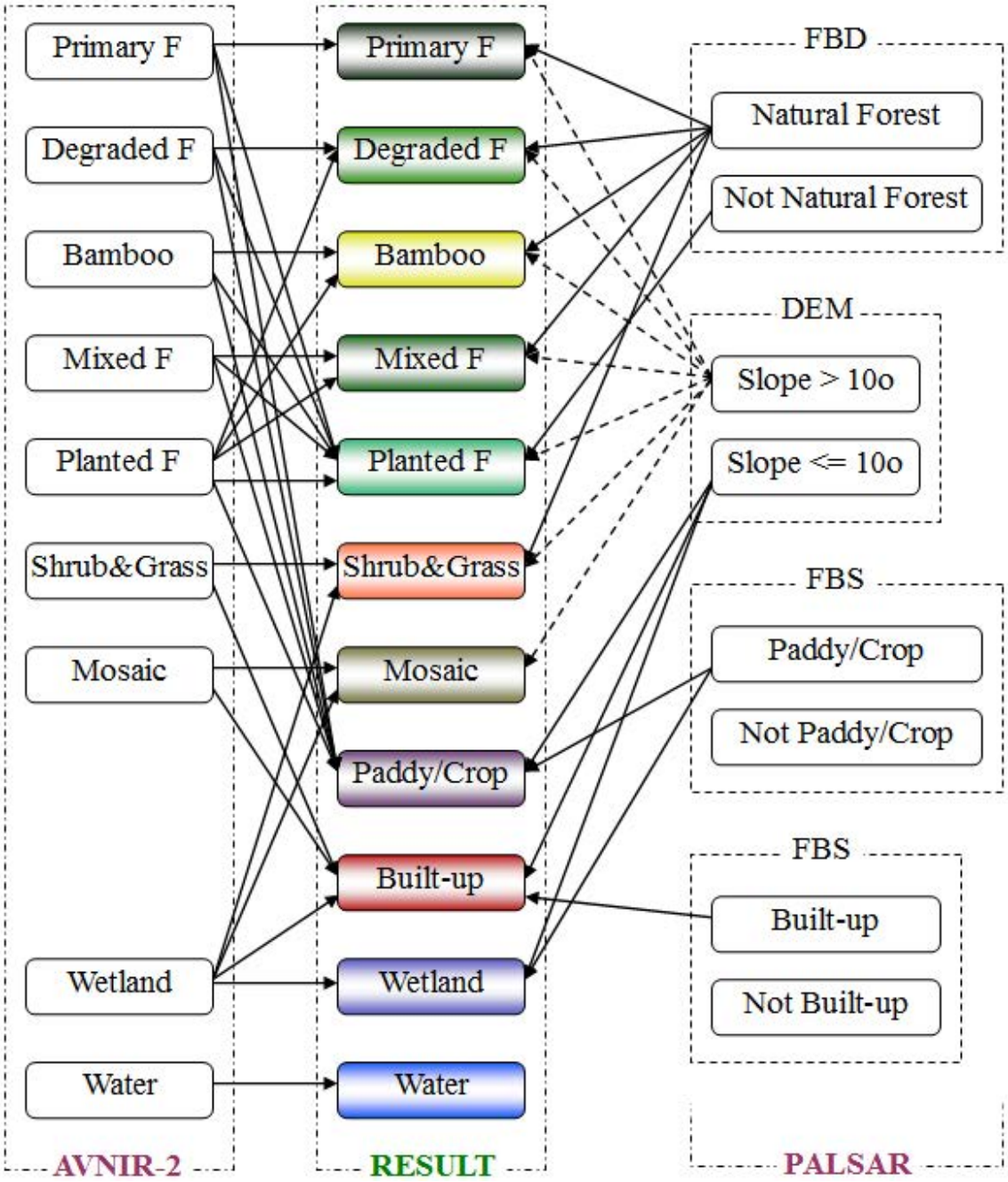

Figure 4.16: The combination model of ALOS/AVNIR-2 and ALOS/PALSAR images for tropical forest mapping

→ AND condition

- - - - - → OR condition (for only direct conversions)

One example to explain the combination model, from original Primary Forest as shown in the box of AVNIR-2 will have three destinations presented in the RESULT box: to Primary F when the pixel is in natural forest mask OR slope is higher than 10^{o}; to Planted F when the pixel is not in natural forest mask; and to Paddy/Crop when the pixel is in paddy/crop mask AND slope is lower or equal 10^{o}. Order of priority functions is from up to down. Other classes were done by similar ways.

This combination model was written by EASI Modeling language of PCI software as following:

```
DOC - COMBINATION MODEL OF ALOS/AVNIR-2 AND ALOS/PALSAR
DOC - Written by Nguyen Thanh Hoan, CEReS, Chiba University, 05/2009
DOC - ********************************************** -
                        DOC - *** - Variants - *** -
local int fin1, fin2, fin3, fin4, fin5, fin6, fin7, fin8, fin9
                        DOC - *** - Output file - *** -
MODEL ON "D:¥Hoan¥PhD_data¥Results¥Result.tif"
                        DOC - *** - Input data - *** -
!! Classification result from ALOS/AVNIR-2, 31 classes
      fin1=DBOpen("D:¥Hoan¥PhD_data¥Results¥AVNIR2_Result1.tif","r")
!! Natural Forest mask derived from ALOS/PALSAR dual-polarization
      fin2=DBOpen("D:¥Hoan¥PhD_data¥Results¥NaturalF_mask.tif","r")
!! Paddy/Crop mask and Built-up mask derived from ALOS/PALSAR single-polarization
      fin3=DBOpen("D:¥Hoan¥PhD_data¥Results¥Paddy_mask.tif","r")
!! High slope mask derived from Map-DEM
      fin5=DBOpen("D:¥Hoan¥PhD_data¥Results¥HighSlope10o.tif","r")
!! Source data (to remove no data areas)
      fin6=DBOpen("E:¥Hoan¥PhD_Thesis¥Data_final¥AVNIR2_final.tif","r")
      fin7=DBOpen("E:¥Hoan¥PhD_Thesis¥Data_final¥FBD_study1.tif","r")
      fin8=DBOpen("E:¥Hoan¥PhD_Thesis¥Data_final¥Palsar_study1.tif","r")
      fin9=DBOpen("E:¥Hoan¥PhD_Thesis¥Data_final¥DEM_Map.tif","r")
DOC - ********************************- CODING - ************************************** -
%1 = 0
!! From Primary Forest
IF ((%{fin1,1}=12) OR (%{fin1,1}=23 OR %{fin1,1}=27)) THEN
         IF (%{fin2,1}<>3) %1 = 5
```

```
        IF (%{fin5,1}=3) %1 = 1
        IF ((%{fin3,1}=1 OR %{fin3,1}=2) AND (%{fin5,1}<>3)) %1 = 8
        IF (%{fin2,1}=3) %1 = 1
ENDIF
!! From Degraded Forest
IF ((%{fin1,1}=3 OR %{fin1,1}=4)OR (%{fin1,1}=6 OR %{fin1,1}=29)) THEN
        IF (%{fin2,1}<>3) %1 = 5
        IF (%{fin5,1}=3) %1 = 2
        IF ((%{fin3,1}=1 OR %{fin3,1}=2) AND (%{fin5,1}<>3)) %1 = 8
        IF (%{fin2,1}=3) %1 = 2
ENDIF
!! From Bamboo
IF (%{fin1,1}=7) THEN
        IF (%{fin2,1}<>3) %1 = 5
        IF (%{fin5,1}=3) %1 = 3
        IF ((%{fin3,1}=1 OR %{fin3,1}=2) AND (%{fin5,1}<>3)) %1 = 8
        IF (%{fin2,1}=3) %1 = 3
ENDIF
!!From Mixed Forest
IF ((%{fin1,1}=2 OR %{fin1,1}=5) OR (%{fin1,1}=30 OR %{fin1,1}=31)) THEN
        IF (%{fin2,1}<>3) %1 = 5
        IF (%{fin5,1}=3) %1 = 4
        IF ((%{fin3,1}=1 OR %{fin3,1}=2) AND (%{fin5,1}<>3)) %1 = 8
        IF (%{fin2,1}=3) %1 = 4
ENDIF
!! From Planted Forest 1 (converted to Degraded Forest)
IF ((%{fin1,1}=8 OR %{fin1,1}=9)OR (%{fin1,1}=16)) THEN
        IF (%{fin2,1}<>3) %1 = 5
        IF (%{fin5,1}=3) %1 = 5
        IF ((%{fin3,1}=1 OR %{fin3,1}=2) AND (%{fin5,1}<>3)) %1 = 8
        IF (%{fin2,1}=3) %1 = 2
ENDIF
!! From Planted Forest 2 (converted to Bamboo)
IF ((%{fin1,1}=10) OR (%{fin1,1}=11 OR %{fin1,1}=25)) THEN
        IF (%{fin2,1}<>3) %1 = 5
        IF (%{fin5,1}=3) %1 = 5
        IF ((%{fin3,1}=1 OR %{fin3,1}=2) AND (%{fin5,1}<>3)) %1 = 8
        IF (%{fin2,1}=3) %1 = 3
```

```
ENDIF
!! From Planted Forest 3 (converted to Mixed Forest)
IF ((%{fin1,1}=13) OR %{fin1,1}=28))THEN
        IF (%{fin2,1}<>3) %1 = 5
        IF (%{fin5,1}=3) %1 = 5
        IF ((%{fin3,1}=1 OR %{fin3,1}=2) AND (%{fin5,1}<>3)) %1 = 8
        IF (%{fin2,1}=3) %1 = 4
ENDIF
!! From Shrub&Grass
        IF (%{fin1,1}=19) %1 = 6
        IF (%{fin1,1}=20) %1 = 6
        IF (%{fin1,1}=21) %1 = 6
        IF (%{fin1,1}=22) %1 = 6
        IF (%{fin1,1}=24) %1 = 6
!! From Mosaic
        IF (%{fin1,1}=14) %1 = 7
        IF (%{fin1,1}=15) %1 = 7
        IF (%{fin1,1}=17) %1 = 7
        IF (%{fin1,1}=18) %1 = 7
!! From Wetland
IF (%{fin1,1}=26)THEN
        IF (%{fin2,1}<>3) %1 = 7
        IF (%{fin5,1}=3) %1 = 7
        IF (%{fin2,1}=3) %1 = 6
        IF ((%{fin3,1}=1 OR %{fin3,1}=2) AND (%{fin5,1}<>3)) %1 = 10
ENDIF
!! From Water
        IF (%{fin1,1}=1) %1 = 11
!! Built-up class
        IF ((%1>=6 AND %1<=8) AND (%{fin3,1}=4 AND %{fin2,1}<>3)) %1 = 9
!! No data
        IF ((%{fin6,1}=0 OR %{fin7,1}=0) OR (%{fin8,1}=0 OR %{fin9,1}=0)) %1 = 0
ENDMODEL
```

The class codes in the above source code are class numbers of the categories as shown in Table 4.1.

Finally, tropical forest map was completed as shown in Figure 4.17.

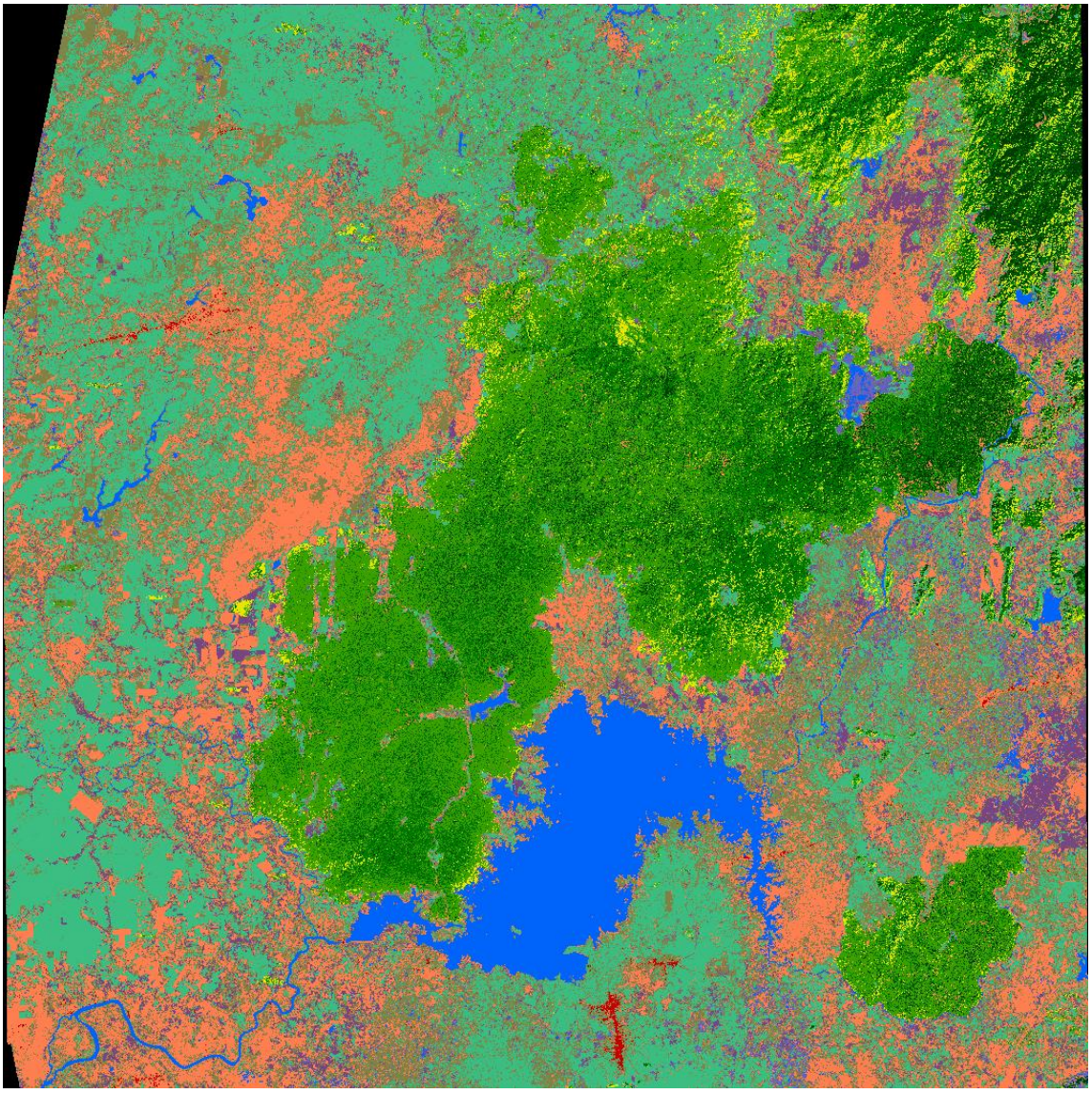

Figure 4.17: The final tropical forest map 2007

This map will be validated to estimate accuracy in the next chapter.

CHAPTER 5

VALIDATION AND DISCUSSIONS

Accuracy assessment always is an important step of forest mapping to verify the quality of information that resultant from remotely sensed data. In this study, validation database was developed based on visual interpretation of very high resolution - PRISM sharpen - images (2.5m) and other reference data like local forest map 2005 and Height-Tree map. 330 random points were selected by PCI software to validate for 11 classes of the categories, averagely, 30 random points for one class. Distribution of these points was shown in Figure 5.1.

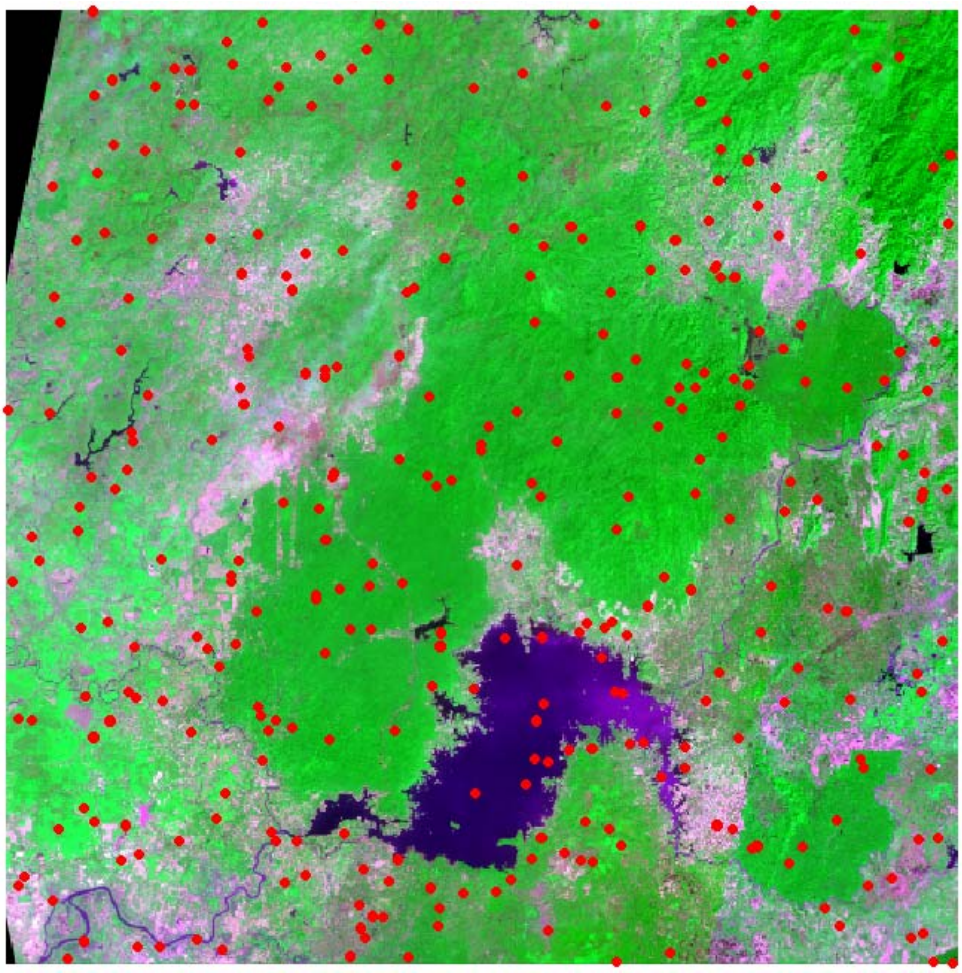

Figure 5.1: Distribution of 330 random points for validation

Currently, the random points are in vector format, but the required database is polygons that cover pixel by pixel of the final tropical forest map. To build this database, the first, the random points were converted to raster pixels based on pixel size and image size of the final tropical forest map. Then, these raster pixels were converted again to polygons in vector format.

To set attributes for the polygons of database, each random point (pixel) was compared very carefully with PRISM sharpen images and other reference data like forest map 2005 and Tree-Height map to determine class name which was already mentioned in the categories (table 4.1). This work was done independently with classification steps. Database was built by ArcGIS/ArcInfo software version 9.1 as shown in Figure 5.2.

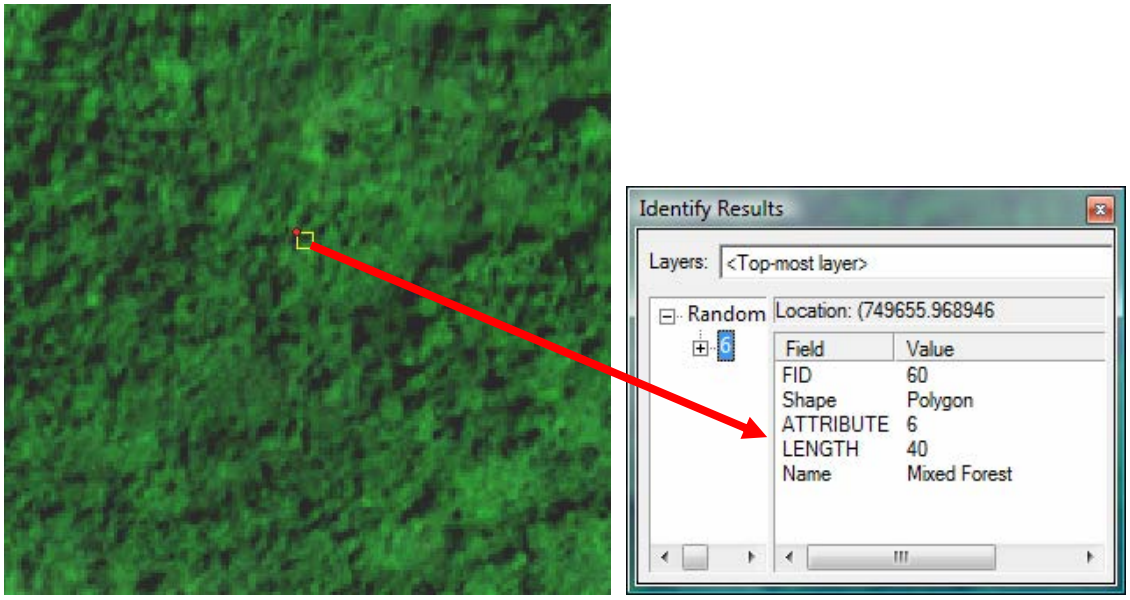

Figure 5.2: An example of validation database

Figure 5.2 is an example of one polygon in the validation database. Where, the left photo is one polygon displayed on PRISM sharpen image, and the right photo is the attribute table of it.

This validation database was used to estimate accuracies for both classification result derived from ALOS/AVNIR-2 image only and the final combination result of AVNIR-2 and PALSAR. Error matrices were shown in Table 5.1 and Table 5.2.

Table 5.1: Error matrix of classification result from ALOS/AVNIR-2 image only

Classified	Reference data											Total	User's
	[1]	[2]	[3]	[4]	[5]	[6]	[7]	[8]	[9]	[10]	[11]	(pixels)	accuracy
[1] Primary forest	11	0	0	1	0	0	0	0	0	0	0	12	91.7%
[2] Degraded Forest	1	37	2	4	3	0	0	0	0	0	0	47	78.7%
[3] Bamboo	0	1	5	2	2	0	0	0	0	0	0	10	50.0%
[4] Mixed forest	1	1	0	25	2	0	0	0	0	0	0	29	86.2%
[5] Planted forest	1	2	3	4	72	0	5	13	0	0	0	100	72.0%
[6] Shrub & Grass	0	0	0	0	0	43	4	0	2	0	0	49	87.8%
[7] Mosaic	0	0	0	0	0	7	40	0	2	0	0	49	81.6%
[8] Paddy/Cropland	0	0	0	0	0	0	0	0	0	0	0	0	0.0%
[9] Built-up	0	0	0	0	0	0	0	0	0	0	0	0	0.0%
[10] Wetland	0	0	0	0	2	0	9	2	0	5	0	18	27.8%
[11] Water	0	0	0	0	0	0	0	0	0	0	16	16	100.0%
Total (pixels)	14	41	10	36	81	50	58	15	4	5	16	330	
Producer's accuracy	78.6%	90.2%	50.0%	69.4%	88.9%	86.0%	69.0%	0.0%	0.0%	100.0%	100.0%		

Table 5.2: Error matrix of combination result between ALOS/AVNIR-2 and ALOS/PALSAR images

Classified	Reference data											Total	User's
	[1]	[2]	[3]	[4]	[5]	[6]	[7]	[8]	[9]	[10]	[11]	(pixels)	accuracy
[1] Primary forest	11	0	0	1	0	0	0	0	0	0	0	12	91.7%
[2] Degraded Forest	1	38	0	4	0	0	0	0	0	0	0	43	88.4%
[3] Bamboo	0	1	8	2	0	0	0	0	0	0	0	11	72.7%
[4] Mixed forest	2	2	0	28	0	0	0	0	0	0	0	32	87.5%
[5] Planted forest	0	0	2	1	77	0	4	0	0	0	0	84	91.7%
[6] Shrub & Grass	0	0	0	0	0	43	4	0	0	0	0	47	91.5%
[7] Mosaic	0	0	0	0	2	7	48	0	0	0	0	57	84.2%
[8] Paddy/Cropland	0	0	0	0	2	0	1	13	0	0	0	16	81.3%
[9] Built-up	0	0	0	0	0	0	0	0	4	0	0	4	100.0%
[10] Wetland	0	0	0	0	0	0	1	2	0	5	0	8	62.5%
[11] Water	0	0	0	0	0	0	0	0	0	0	16	16	100.0%
Total (pixels)	14	41	10	36	81	50	58	15	4	5	16	330	
Producer's accuracy	78.6%	92.7%	80.0%	77.8%	95.1%	86.0%	82.8%	86.7%	100.0%	100.0%	100.0%		

To imagine the difference easily, user's accuracy and producer's accuracy of the two error matrices were compared together in Table 5.3 and Table 5.4.

Table 5.3: Comparison table of User's accuracy before and after combination

Class name	AVNIR-2 only	AVNIR-2 + PALSAR
[1] Primary forest	91.7%	91.7%
[2] Degraded Forest	78.7%	88.4%
[3] Bamboo	50.0%	72.7%
[4] Mixed forest	86.2%	87.5%
[5] Planted forest	72.0%	91.7%
[6] Shrub & Grass	87.8%	91.5%
[7] Mosaic	81.6%	84.2%
[8] Paddy/Cropland	0.0%	81.3%
[9] Built-up	0.0%	100.0%
[10] Wetland	27.8%	62.5%
[11] Water	100.0%	100.0%

Table 5.4: Comparison table of Producer's accuracy before and after combination

	[1]	[2]	[3]	[4]	[5]	[6]	[7]	[8]	[9]	[10]	[11]
AVNIR-2 only	78.6%	90.2%	50.0%	69.4%	88.9%	86.0%	69.0%	0.0%	0.0%	100.0%	100.0%
AVNIR-2 + PALSAR	78.6%	92.7%	80.0%	77.8%	95.1%	86.0%	82.8%	86.7%	100.0%	100.0%	100.0%

The results showed that the overall accuracy before combination is 77.0%, after combination the overall accuracy is increased up to 88.2%.

Planted forest almost has only one layer of wood tree and it looks smooth in ALOS/AVNIR-2 images, also Bamboo has only one layer, and it looks smooth and light in ALOS/AVNIR-2 images. Actually, planted forest and bamboo are confused together totally in optical data. That is why accuracy of bamboo is increased more than that of the other forest classes, from 50% to 72.7% for user's accuracy and from 50% to 80% for producer's accuracy. Outside of confused with bamboo, planted forest is also confused very much with other types of forest like degraded forest and mixed forest. In addition, many paddy/cropland fields become planted forest in ALOS/AVNIR-2 classification result. Therefore, accuracy of planted forest also increased much after combination, from 72% to 91.7% for user's accuracy and from 88.9% to 95.1% for producer's accuracy. Accuracies of paddy/cropland and built-up increased very much because they have no training data for ALOS/AVNIR-2 classification. Final accuracies of built-up area and wetland maybe not correct because number of validation points distributed in these classes is very few, only 4 points for built-up and 5 points for wetland. Any way, this problem doesn't affect so much to purpose of this study.

Primary forest, degraded forest and mixed forest are natural forest, which are usually confused together. Some time, it is very difficult to separate between them even by visual interpretation using very high resolution images like PRISM sharpen images. For forest management purposes, they could be merged together to become one natural forest class only. In this case, error matrices of main forest classes are shown in Table 5.5 and Table 5.6.

Table 5.5: Error matrix of main forest classes before combination

	Reference data				
Classified	Natural forest	Planted forest	Bamboo	Total	User's accuracy
Natural forest	81	5	2	88	92.0%
Planted forest	7	72	3	100	72.0%
Bamboo	3	2	5	10	50.0%
Total	91	81	10	182	
Producer's Accuracy	89.0%	88.9%	50.0%		

Overall accuracy of the main forest classes before combination is 86.8%.

Table 5.6: Error matrix of main forest classes after combination

	Reference data				
Classified	Natural forest	Planted forest	Bamboo	Total	User's accuracy
Natural forest	87	0	0	87	100.0%
Planted forest	0	77	2	84	91.7%
Bamboo	2	0	8	11	72.7%
Total	91	81	10	182	
Producer's Accuracy	95.6%	95.1%	80.0%		

Overall accuracy of the main forest classes after combination is 94.5%.

Accuracies of natural forest and planted forest become very high after combination. That means, combination of ALOS/AVNIR-2 and ALOS/PALSAR images in order to separate between natural forest and planted forest shows a good result, in the other hand ALOS/AVNIR-2 image has some limitations in discrimination of primary forest, degraded forest and mixed forest together. Accuracy of bamboo is still not high after combination. Actually, bamboo includes natural bamboo and planted bamboo, but they are almost similar together. Validation result shows that some time bamboo is confused with natural forest, but in some other places it is confused with planted forest. So, separating bamboo from other forest types is a very difficult work. In any case, accuracy of bamboo was already increased after combination so much more than before combination. That is also a success, however, not very perfect.

CONCLUSIONS

Some geometric problems are existing in the highest processing levels of ALOS standard products (L1B2 for AVNIR-2 and PRISM, L1.5 for PALSAR). The methodology of geometric correction as proposed in this study can correct all ALOS data. After geometric correction, all ALOS data and existing local maps can overlay well together.

The difference of grey level (DN value) is usually met not only in ALOS/AVNIR-2 data, but also in other types of optical remote sensing data, especially in high resolution images. The reflectance conversion is a good way, but sometime it cannot be applied due to the lack of information. In that case, normalization is a suitable choice. This study is successful in using mean and standard deviation values of a common area to normalize DN value for ALOS/AVNIR-2 image. After normalization, boundary of two images cannot be determined visually in mosaic image and in classification result, although it is very clear in the mosaic image before normalization.

Cloud removal is one of the new points of this study. Result is a program with many functions for cloud removal progress called Cloud Removal Program. This program was already experimented successfully on simulated ALOS data, on Landsat/ETM and ASTER images. Combination of two optical images to remove cloud is a good way to make cloud free multi-temporal dataset. Condition to apply this method is suitable if the change of objects that are covered by cloud is not so much. When applying on real ALOS data, it is not very successful in the Define Cloud function because of calibration problem of ALOS/AVNIR-2 (DN values of some objects become 255). Other processing shows good results. Interpolation result is a cloud free and shadow free image of ALOS/AVNIR-2. Almost the objects under clouds and shadows after interpolation look smooth, natural and logical. However, some of them look not very good if they are boundaries between cropland, grassland, bare land or the similar objects

that cannot be separated together by PALSAR data. By using a threshold value for radar image and searching the nearest pixel to interpolate cloud pixels for optical image, the cloud removal result should have more information than using the radar image and the cloud optical image independently.

In whole the year 2007, only one-time good quality images of ALOS/AVNIR-2 were observed for the study area. Collecting multi-temporal optical images of high-resolution satellites for tropical regions in one-year cycle to describe phenology of objects for forest mapping is usually very difficult, maybe impossible because of the presence of the cloud and the long repeat cycle of satellite. ALOS/PALSAR is not affected by cloud, in one year, it has many images. Therefore, combination of single-temporal image of ALOS/AVNIR-2 and multi-temporal images of ALOS/PALSAR for tropical forest mapping is a feasible way for every year. Tropical forest mapping annually by high resolution images becomes possible with ALOS data.

Using only single-temporal optical data like ALOS/AVNIR-2 is not adequate to separate between forests and growing paddy/croplands, between planted forests and natural forests, between built-up area and others, and so on. However, using ALOS/PALSAR single-polarized image (HH) is sufficient to discriminate forests and growing paddy/croplands; built-up and others easily. On the other hand, using ALOS/PALSAR dual-polarized images (HH and HV) can separate between planted forests and natural forests.

In the combination model, high slope map was already used to reduce effects of terrain in ALOS/PALSAR data. That means, accuracy in the high slope areas is not increased. That is one of the limitations of this study. Actually, Radiometric Terrain Correction (RTC) is necessary for PALSAR data, but it has not applied yet. Using combination of the PALSAR images observed in the decreasing path and the increasing path of ALOS satellite to reduce terrain effects is also another idea, however it has not yet studied in this thesis. To solve this problem, it needs to be studied more.

In the final goal, combination of optical and microwave data of ALOS can improve accuracy of tropical forest mapping. The accuracy is increased after combination so much more than before combination. The final tropical forest map has a high accuracy, especially for main forest classes.

REFERENCES

ALMEIDA-FILHO, R., SHIMABUKURO, Y.E., ROSENQVIST, A., SANCHEZ, G.A., 2009, Using dual-polarized ALOS PALSAR data for detecting new fronts of deforestation in the Brazillian Amazonia. *International Journal of Remote Sensing*, **30**, pp. 3735-3743.

ALOS, 2009, Advanced Land Observing Satellite "DAICHI". RESTEC 2009. Available online at: http:/www.alos-restec.jp/aboutalos_e.html (accessed 6 October 2009)

ALVIN WONG, BRUCE CHAPMAN, ANNIE RICHARDSON, ANTHONY FREEMAN, 1997, SIR-C EDucation CD#03 (SIRCED03-B), PC Special Edition, California Institute of Technology, Pasadena, California, USA. Available online at: http:/southport.jpl.nasa.gov/cdrom/sirced03/cdrom/DOCUMENT/HTML/TEACHERS/MODULE02/MOD2SECE.HTM (accessed 10 September 2009)

BUTLER, RHETT A., 2005, Nigeria has worst deforestation rate, FAO revises Figures. Available online at: Mongabay.com (accessed 14 September 2009).

DOBSON, CRAIG, M., 2000, Forest information from Synthetic Aperture Radar. *Journal of Forestry*, **98**, pp. 41-43.

DUONG, N.D., 1998, Total Reflected Radiance Index – An Index to Support Land Cover Classification. *Proceedings of the 19th Asian Conference on Remote Sensing*, Manila, Philippines, Nov. 2008, pp. H-7-1 to H-7-6.

DUONG, N.D., THOA, L.K., HOAN, N.T., BINH, C.T., 1999, Monitoring of Forest Cover Change in Tanh Linh District, Binh Thuan province, Vietnam by Multi-temporal Landsat. *Proceedings of the 20th Asian Conference on Remote Sensing*, Nov. 1999, Vol.1, pp. 260-265.

FAO, 2004, National Forest Inventory - Field Manual Template. Forestry Department,

FAO. Available online at: http:/www.fao.org/documents/pub_dett.asp?pub_id=191385&lang=en (accessed 29 August 2009).

FEILONG LING, ZENGYUAN LI, ERXUE CHEN, QUINMIN WANG, 2008, Forest mapping with multi-temporal dual polarization ALOS PALSAR data. *CD Proceedings of SPIE*, Vol. 7285, 728517.

FRANSSON, J.E.S., MAGNUSSON, M., OLSSON, H., ERIKSSON, L.E.B., SANDBERG, G., SMITH-JONFORSEN, G., ULANDER, L.M.H., 2007, Detection of forest changes using ALOS PALSAR satellite images. *CD Proceedings of International Geoscience and Remote Sensing Symposium (IGARSS 2007)*.

GDEM, 2009, ASTER Global Digital Elevation Model. Available online at: http:/www.ersdac.or.jp/GDEM/E/index.html (last accessed 06 October 2009)

GILES M. FOODY, DOREEN S. BOYD, MARK E.J. CUTLER, 2003, Predictive relations of tropical forest biomass from Landsat/ TM data and their transferability between regions. *Remote Sensing of Environment*, **85** (2003), pp. 463-474.

HELMER, E.H., BROWN, S. AND COHEN, W.B., 2000, Mapping montane tropical forest successional stage and land use with multi-date Landsat/ imagery. *International Journal of Remote Sensing*, **21**, pp. 2163-2183.

HOAN, N.T., DUONG, N.D., 2004, Proposing a Method to Establish Vietnam Forest Map by Using Multi-temporal GLI Images and Ecologic Models. *Proceedings Japan-Vietnam Geoinformatics Consortium Symposium*, Hanoi, Vietnam, CH1, pp. 457-463.

HOAN, N.T., DUONG, N.D., TATEISHI, R., 2005, Combination of ADEOS II – GLI and MODIS 250m Data for Land Cover Mapping of Indochina Peninsula. CD

Proceedings of the 26th Asian Conference on Remote Sensing (ACRS), Hanoi, Vietnam, Nov. 2005, LLC1-2.

HOAN, N.T., TATEISHI, R., 2008, Some techniques for preprocessing of ALOS/AVNIR-2 and ALOS/PALSAR data. *Proceedings of Japan Society of Remote Sensing Symposium*, Dec. 2008, pp.101-102.

HOAN, N.T., TATEISHI, R., 2009, Cloud Removal of Optical Image Using SAR Data for ALOS Applications - Experimenting on Simulated ALOS Data. *Journal of The Remote Sensing Society of Japan*, **29**, pp. 410-417.

IWAOA, K., YAMAMOTO, N., PATTONB, D., KODAMAA, S., NAKAMURAA, R., MATSUOKAA, M., TSUCHIDAA, SEKIGUCHIA, S., TSUKUDAA, E., 2008, Validating global digital elevation models with degree confluence project information and ASTER-DEM on GEO GRID. *Proceedings of the 21th Congress ISPRS*, Vol. XXXVII, Part B4, Beijing 2008, pp. 1847-1852.

JICA, 2008, Development Issues in Vietnam – JICA's Activities in Vietnam. Available online at: http:/www.jica.go.jp/vietnam/english/pdf/pamph_e01.pdf (accessed 03 October 2009)

JUHA HYYPPA, HANNU HYYPPA, MIKKO INKINEN, MARCUS ENGDAHL, SUSAN LINKO, YI-HONG ZHU, 2000, Accuracy comparison of various remote sensing data sources in the retrieval of forest and attributes. *Forest Ecology and Management*, **128** (2000), pp. 109-120.

KUPLICH, T.M., 2000, The study of ERS-1 SAR and Landsat/ TM synergism for land use classification. *International Journal of Remote Sensing*, **21**, pp. 2101-2111.

LIEW, S.C., 2001, *Principles of Remote Sensing* (digital book). Centre for Remote Imaging, Sensing and Processing, National University of Singapore.

LOPES, A., NEZRY, E., TOUZI, R., AND LAUR, H., 1993, Structure detection and statistical adaptive speckle filtering in SAR images. *International Journal of*

Remote Sensing, **14**, pp. 1735-1758.

MT&PK, 2009, Layers of a Rainforest. Learning about Rainforests. Available online at: http:/www.srl.caltech.edu/personnel/krubal/rainforest/Edit560s6/www/whlayers.html (Last accessed 14 October 2009).

MULJANTO NUGROHO, 2006, Integration of Multi Remotely Sensed Data and Geodatabases for Forestry Management in Indonesia. PhD thesis, Wageningen University, The Netherlands.

MURAI, S., 1996, *Remote Sensing Note.* Published by Japan Association on Remote Sensing, Tokyo, Japan, pp.18-19.

NAOKI ISHITSUKA, 2007, The scatter characteristic of rice paddy fields using L band multi polarimetric satellite SAR observation. *CD Proceedings of the first joint PI symposium of ALOS data nodes for ALOS science program* in Kyoto, JAXA, Nov. 2007.

PATRICK MEYFROIDT, ERIC F. LAMBIN, 2008, Forest transition in Vietnam and its environmental impacts. *Global Change Biology*, **14** (6), pp. 1319–1336.

RAHMAN, M.M., E. CSAPLOVICS, KOCH, B., 2005, An efficient regression strategy for extracting forest biomass information from satellite sensor data. *International Journal of Remote Sensing*, **26**, pp. 1511-1519.

SGRENZAROLI, M., DE GRANDI, G.F., EVA, H. AND ACHARD, F., 2002, Tropical forest cover monitoring estimates from the GRFM JERS-1 radar mosaics using wavelet zooming techniques and validation. *International Journal of Remote Sensing*, **23**, pp. 1329-1355.

SHANE CLOUDE, KARIN VIERGERVER, IAIN H WOODHOUSE, 2007, Forest Stucture Estimation using POLInSAR. *CD Proceedings of the first joint PI symposium of ALOS data nodes for ALOS science program* in Kyoto, JAXA, Nov. 2007

SRTM, 2006, Shuttle Radar Topography Mission (SRTM), Global Land Cover Facility. Available online at: http:/www.landcover.org/data/srtm/ (last accessed 06 October 2009)

TAKEUCHI, S., SUGA, Y., OGURO, Y., AND KONISHI, T., 2000, Monitoring of new plantation development in tropical rain forests using JERS-1 SAR data. A*dvances in Space Research*, **26**, pp. 1151-1154.

TAKEUCHI, W., 2008, Forest cover mapping in Vietnam with MODIS. On-the-Job training in Vietnam, Space Application For Environment (SAFE) program, 16-18 July 2008. Available online at: http:/www.safe.iis.u-tokyo.ac.jp/pdf/aprsaf20081210_Dat.pdf (accessed 10 Sep. 2009)

THUY LE TOAN, GHISLAIN PICARD, JEAN-MICHEL MARTINEZ, PIERRE MELON AND MALCOLM DAVIDSON, 2001, On the relationships between RADAR measurements and forest structure and biomass. *CD Proc. 3rd International Symposium, "Retrieval of Bio- and Geophysical Parameters from SAR Data for Land Applications"*, Sheffield, UK, Sep. 2001.

TOTTRUP, C., 2004, Improving tropical forest mapping using multi-date Landsat/ TM data and pre-classification image smoothing. *International Journal of Remote Sensing*, **25**, pp. 717-730.

UNESCO, 2009, Tentative lists - World Heritage Centre, 2009. Available online at: http:/whc.unesco.org/en/tentativelists/5070/ (accessed 20 September 2009).

VIETNAMESE, CHAN, L.M. AND DUNG, V.V., 1992, *Thực vật và thực vật đặc sản rừng*, N.T. Hoan (Vegetation and special vegetation of forest). Forestry University of Vietnam, Hanoi 1992, pp. 294-302.

VIETNAMESE, THAI VAN TRUNG, 1997, *Thảm thực vật rừng Việt Nam*, N.T. Hoan (The forest vegetation of Vietnam). Science and Techniques Publishing House,

Hanoi 1997, pp. 197-243.

ZHENGHAO, S. AND FUNG, K.B., 1994, A Comparison of Digital Speckle Filters. *Proceedings of International Geoscience and Remote Sensing Symposium (IGARSS 94)*, pp. 2129-2133.

YUJI SAKUNO, TISHIAKI KOZU, YOSHIAKI TSUZUKI, TSUNEO MATSUNAGA, 2007, Monitoring of water pollution and aquatic plants in the coastal lagoon environments using ALOS data. *CD Proceedings of the first joint PI symposium of ALOS data nodes for ALOS science program* in Kyoto, JAXA, Nov. 2007